Dissertation of the Degree of
Master of Landscape Architecture

Estimation of Water Availability in the Korean Peninsula Considering Climate Change

기후변화를 고려한 한반도의 가용 수자원 추정

February 2016

Graduate School of Seoul National University

Department of Landscape Architecture and
Rural System Engineering

So Hyun Yoo

Abstract

Estimation of Water Availability in the Korean Peninsula Considering Climate Change

Advising Professor : Dongkun Lee
Landscape Architecture and Rural Systems Engineering
Graduate School of Agriculture and Life Science
Seoul National University
Sohyun Yoo

Climate change is projected to have a direct impact on the water resources. In case of the Korean Peninsula, more than a half of the total rainfall amount is concentrated in summer. It has been always important issues that spatio-temporal variability of an available water resources in the Korean Peninsula. The water availability is projected to be influenced by climate change and it is expected to more intensify. Variations in water availability is related with the land use which is directly affected by water resources, such as agricultural area, urban area, and forests. Therefore, the changes in spatial variability along with the temporal changes of water availability should be investigated to establish an effective management plan and draw an implication for future spatial planning.

Available water resources can be defined in various ways, such as a storage of reservoir, and river discharge which can be used in a basin. This study defined water availability as a river discharge based on literature reviews. This study estimates water availability based on river discharge in the Korean Peninsula including North Korea, as the study area. In order to estimate water availability and draw a spatial implication considering climate change, HadGEM2-AO and RCP 8.5 scenario is applied as a future climate scenario, and grid-based hydrological model H08 is used. H08 was originally developed as a global hydrological model for the simulation of water availability in a spatial resolution of 1° × 1°. However, it is also applicable for a regional hydrological simulation in a spatial resolution of 5′ × 5′. Input meteorological data of GSWP2 is used for historical simulation, and RCP 8.5 scenario from HadGEM2-AO was used for future climate change simulation. A bias in air temperature and precipitation of GCM was validated by comparing with observed meteorological data in Korea. Parameters of H08 was calibrated and validated for historical simulation of 10 years from 1986 to 1995, then climate change simulation is carried out for the estimation of hydrological changes using validated H08.

In order to investigate hydrological characteristics and water availability in the Korean Peninsula, representative gauging stations was presented for Amnok, Duman, Chongchon, Taedong River basin in North Korea, and Han, Nakdong, Geum, Yeongsan River basin in South Korea. Quantitative hydrological characteristics were presented

for the representative 8 stations in the Korean Peninsula along with the meteorological aspects. Spatio-temporal variability was investigated for the hydrological attributes, such as evapotranspiration, runoff, as well as air temperature and precipitation. Estimated water availability based on RCP 8.5 scenario was spatially presented for the objective periods in order to derive spatial implication for the planning. However, there is uncertainties for future projection in the process of selecting future climate scenarios and hydrological model. This study assumed naturalized discharge which is not considering regulated flow due to the reservoir operation and artificial water supply capacity. This study estimated water availability on a grid basis using regionalized global hydrological model. The results of this study can be used as preliminary information for establishing spatial planning under climatic changes across the Korean Peninsula considering water availability.

□ Keywords: Water availability, Climate change, RCP scenario, GCM, Hydrological model, H08

□ Student number: 2014-20049

Table of contents

List of tables

List of figures

Ⅰ. Introduction

Water resources are directly related to human health and are essential for ecosystems, geophysical processes, and human activities (Milly et al., 2005). The availability of sufficient water at places where human activity takes place has always been an important issue (Alcamo et al., 1997). Strong evidences of climate change have appeared throughout the world over time (IPCC, 2014). Changing climate, observed since 1950, had no precedent in the past several hundred years. Moreover, extreme weather events, such as heavy rainfall and droughts, caused by changes in rainfall pattern occur with rising temperatures. Thus, it is likely to have an effect on the landscape where the responses to the changes occur. Accordingly, water availability will fall below the critical level because of climate change and would be a major issue across communities (Bates et al., 2008). The management of water availability is the principal challenge since changing water demands with increasing population will be difficult to manage with changing climate in the future. The changes in the available water resources over time are directly related to water use in landscapes such as forests and agricultural areas. Therefore, identifying the spatial variation of water availability is essential (Houghton-Carr et al., 2013). In response to the variability of water resources according to climate change, the information about how the water availability quantitatively and qualitatively changes with various spatial and temporal scale will be more important (UN, 2006). The estimation and assessment of the availability of water resources

affected by climate and socio-economic changes is needed (Vorosmarty et al., 2000).

In case of the Korean Peninsula, climate change is a major factor that exacerbates water resources problems caused by the seasonally biased distribution of available water resources (Ministry of Land, Infrastructure and Transport, 2013). The evaluation of the quantity of water resources and their spatial distribution is essential to establish a water supply plan (Martin and Giesen, 2009). It is expected that the spatial and temporal imbalance of water resources in the Korean Peninsula will be intensified depending on future climatic conditions. In order to effectively manage this problem, the quantitative evaluation of spatial and temporal variations of the available water resources is required.

Climate change research related to water availability is required for the determination of the impact on water resources in the Korean Peninsula. To derive the spatial implications of climate change on the water availability in the Korean Peninsula, the objectives of this study was set up as follows: ⅰ) Simulation of hydrological changes due to the climate change phenomenon in the Korean Peninsula, including North Korea, as the study area. ⅱ) Spatial distribution of water availability based on the hydrological cycle and expected climatic changes.

Ⅱ. Literature review

1. Climate change and water availability

1.1. Climate scenarios

Climate scenarios have been developed with various climate models to predict the impact of future climate change. The Intergovernmental Panel on Climate Change (IPCC) reports the projection of future climate around the world on a regular basis. The IPCC reports are based on the findings of peer reviewed reports, and climate change scenarios have been proposed for the future projections in this report. By inputting the anthropogenic factors on the global climate model (GCM), future greenhouse gas concentrations are calculated as a result of the impact of climate and projected future weather conditions. The Korea Meteorological Administration (KMA) introduced representative concentration pathways (RCP) as a greenhouse gas emission scenario in the IPCC Fifth Assessment Report in 2011 and has projects future climatic conditions based on the scenarios. In Table 1, the meaning of RCP scenarios[1)] has been described. The number assigned of RCP scenarios signifies the amount of energy absorbed additionally due to the greenhouse gas. The larger the number, the higher the greenhouse gas emissions. For active reduction of greenhouse gas emission, the RCP 2.6 scenario should be realized. RCP 4.5 is the scenario in which the greenhouse gas emission policy has been realized considerably.

1) http://sedac.ipcc-data.org/ddc/ar5_scenario_process/RCPs.html

The RCP 6.0 scenario assumes that the greenhouse gas reduction policies are barely applicable, and RCP 8.5 scenario is the business - as -usual scenario. Future climate projction and impact assessment based on the RCP scenarios reported in the IPCC Fifth Assessment Report.

Table 1 Description of RCP scenarios (Source: IPCC)

Scenario	Description
RCP 2.6	Peak in radiative forcing at ~ 3 W/m2 before 2100 and decline
RCP 4.5	Stabilization without overshoot pathway to 4.5 W/m2 at stabilization after 2100
RCP 6.0	Stabilization without overshoot pathway to 6 W/m2 at stabilization after 2100
RCP 8.5	Rising radiative forcing pathway leading to 8.5 W/m2 in 2100

Climate projections and scenarios are generated through the simulation process of GCM. GCM simulates climatic factors, such as temperature, humidity, radiation, precipitation, and air pressure, based on the laws of physics. GCM is one of the most effective tools to predict the future climate and is provided by various organizations and institutes all over the world (Table 2[2]). In order to estimate and assess the impact of future climate, a results from the various GCM climate simulations are widely used. Studies that project the future hydrological cycle are also progressing actively.

2) http://www.climate.go.kr/home/02_information/07_4.html

Table 2 Description of GCMs (Source: KMA)

GCM	Modeling center	Atmospheric resolution	Ocean resolution
BCC-CSM1.1	BCC	~2.8°, L26	0.3-1°, L40
CanESM2	CCCma	T63, L35	1.41°x0.94°, L40
GFDL-ESM2M	NOAA GFDL	2x2.5°, L24	1/3~1°, L63
HadGEM2-ES	MOHC	N96(~1.6°), L38	0.5~2°, L40
IPSL-CM5A-LR	IPSL	3.75x1.9, L39	0.5~2°, L31
MIROC-ESM	MIROC	T42, L80	0.5~1.7°, L43
MPI-ESM-LR	MPI-M	T63(~1.9°), L47	1.5°, L47
NorESM-ME	NCC	1.9x2.5°, L26	1°, L53

In case of regional climate change impact assessment, the spatial resolution of GCM is low because of a spatial scope of GCM is global. This is the reason why the process of downscaling of GCM is required. The regional climate model (RCM) is used in the downscaling process. In Korea, the KMA developed the RCM HadGEM3-RA based on HadGEM2-AO, which is developed by the Met Office Hadley Centre. KMA distributed the climate scenario, which has a spatial resolution of 12.5 km for the Korean Peninsula and 1 km for South Korea, and it has been used widely in the climate change research in Korea.

1.2. Concept of water availability

The meaning of water availability is the amount of available water resources. Water availability can be specifically defined in various ways. Cai and Rosegrant (2002) defined the available water resources as not only renewable water, such as surface water and groundwater

that can be supplied by natural hydrological circulation, but also artificial water transfer, desalinated water, and non-renewable groundwater. Vinay et al. (2013) defined the total water availability as the summation of river discharge of basin and stored water in aquifer and soil. Alcamo et al. (1997) defined the water availability of a basin as the amount of stored water in the reservoir of the basin. According to the Water Vision 2011-2020 of Water Resources Ministry of Land, Transport and Maritime Affairs, the total amount of water resources is obtained by multiplying the average annual precipitation and the land area. The total amount of water resources can be divided by the loss and runoff. Only runoff can be regarded as available water resources. The most available water resource is the runoff during floods. The remaining water resources, excluding the amount of water lost to the sea, and consisting of river water, water supplied by dams, and groundwater, is calculated as the actually available water resources (Ministry of Land, Transport and Maritime Affairs, 2011). Numerous studies have evaluated the available water resources by estimating the actually available water resources such as river discharge and the amount of stored groundwater (Lee et al., 2015). Many previous studies have assumed the water availability as the amount of discharge of the basin (Elliott et al., 2014; Hayashi et al., 2014; Collet et al., 2013; Oki et al., 2009; Haddeland et al., 2006; Alcamo et al., 2003; Doll et al., 1999). These studies on the estimation and evaluation of the water availability focus on estimating the river discharge and its changes with changing environmental conditions.

The estimation of water availability from on the grid-based hydrological model can provide an insight into the hydrological elements involved, such as surface runoff and available water resources, at all points of interest (Meigh et al., 1999). Therefore, many previous studies applied a grid-based model to estimate and evaluate of the hydrological impact and water availability. The available amount of surface water for a specific grid can be the river discharge of the grid (van Beek et al., 2011). Oki et al. (2009) presented the water availability of specific grid as shown in [Eq. 1] by accumulating the runoff from the upper grid cell. R refers to the runoff from a grid, and $\sum D_{up}$ is summation of the accumulated runoff from the upper grid, and α is the constant that represents factors such as water quality and water use affecting the amount of available water from the upper grid.

$$Q = R + \alpha \sum D_{up} \quad \text{[Eq. 1]}$$

When considering climate change, a variation in the flow regime of the river basin and sectoral water use of the basin can be constrained by a change in the water availability. Doll et al. (2003) projected vulnerable areas for water availability based on these future changes. In case of evaluating the water availability using the grid-based hydrological model for multiple catchments, the ratio between net water demand and available water in a grid can be an indicator of whether or not the amount of water can meet the net demand of the

grid (Wada et al., 2011; Falkenmark, 1989). Many previous studies have estimated the ratio of water demand and supply in order to determine the factors that can affect the amount of available water resource that the local community can directly use (Boulay et al., 2015). Reflecting a viewpoint in terms of water demand and supply balance, numerous studies have compared the ratio of water demand and supply (Hayashi et al., 2014; Collet et al., 2013; Hanasaki et al., 2013; Hanasaki et al., 2008; Alcamo et al., 2003). Lee et al. (2015) evaluated water availability in the Asian monsoon region by calculating the surface runoff and evapotranspiration, using a hydrological model. Elliott et al. (2014) considered only renewable surface water to evaluate water availability in terms of irrigation water supply. They regarded runoff from the grid as water availability by using a grid-based hydrological model.

2. Hydrological model studies in the Korean Peninsula considering climate change scenarios

A hydrological model is a mathematical description of physical processes in the natural hydrological cycle of the real world and is used to understand and predict the hydrological processes. It is an important tool widely used to plan and manage the water resources of basins. A hydrological model can be categorized by a simulation process, temporal and spatial structure, and method of solution. According to the simulation process, a hydrological model can be categorized as a lumped model or a distributed model. A lumped model considers the whole basin as a single system, and then analyzes the relationship between rainfall and runoff. A distributed model divides the basin into homogeneous elements, and then analyzes respective hydrological factors to quantify the hydrological characteristics of watershed (Jang, 2003). A distributed hydrological model can be further categorized by its basic calculation unit and spatial structure used into either a grid-based model or a catchment based model. A grid-based hydrological model has difficulty in calculation of larger basins. On the other hand, a subcatchment-based model has difficulties in calculating the overland flow simulation based on geographical elements and soil saturation (Jia et al., 2006). Preparing the input data for a distributed model is more difficult than the lumped model, but it is based on the physical theory and formula so it can reflect the spatial characteristics and circulation of hydrological elements (Jang et al, 2008). Moreover, a distributed model uses a digital elevation model

so the water balance elements can be calculated at any point of interest in a watershed. This indicates that the distributed hydrological model can calculate the spatial water balance and runoff reliably (Kim et al., 2010).

Water resources constitute an important sector that is expected to be directly affected by climate change and there are numerous studies on this. The analysis of the effect of climate change on water resources can be categorized by the approach to dealing with the climate data. The first approach is to analyze the trends using observation data. The second approach is divided into two methods, one using a climate model, and the second using a combination of a climate model and a deterministic hydrological model. Most of the previous studies have used GCM. Future climate scenarios generated from GCM can be inputted on the hydrological model to analyze the effects of climate change on water resources (Bae and Jeong, 2005). Changes in air temperature and precipitation cause changes in the hydrological elements, such as runoff and evapotranspiration, and water availability. A number of studies focusing on runoff changes have been undertaken in Korea since the climate change scenario were introduced. The majority of study sites for domestic research include watersheds in South Korea, which has provided for most of the runoff estimates of the basins. In addition, the evaluation of supply ability of available water resources by estimating the water flows of reservoirs and dams have also been conducted.

Previous studies related to the runoff estimation are described as

follows. Park et al. (2011) projected future discharge of Yongdam and Daecheong dam watersheds based on A1B scenario and SWAT hydrological model. Lee et al. (2012) evaluated the changes in runoff caused by climate change using SWAT model. Kim et al. (2010) considered the land use changes as well as climate change. They simulated the changes in water balance as well as the discharge of Han River basin using the SLURP model and land use change scenario based on the SRES A2 scenario and the CA-Markov Chain method. Park et al. (2010) simulated the water resources and hydrological changes in the Soyanggang basin considering climate change based on the A2, A1B, B1 scenarios and land use change using CA-Markov Chain method and regression equation considering the relationship between temperature and leaf area index (LAI). Many studies consider the uncertainty in climate change. Bae et al. (2011) assessed the impact of climate change on water resources by simulating the river discharge considering the uncertainties that may occur in a process of selecting GCM and the hydrological model. In order to take into account the uncertainty and present a range of uncertainty in the projected hydrological changes, they used the A2, A1B, B1 scenarios, and 13 GCMs, and 3 hydrological models named PRMS, SWAT, and SLURP.

Studies assessing the climate change impact of the actual amount of water supply capacity of the reservoirs have been actively conducted in recent years. Kim et al. (2010) simulated the river discharge using SLURP model and A2 scenario, and then analyzed the water scarcity

of Han River basin using the K-WEAP model based on the simulated discharge. Kim et al. (2013) analyzed the water scarcity in South Korea based on the water supply network using K-WEAP model for the simulated discharge using TANK model. Jeong et al. (2011) analyzed inflow, storage, and outflow of 5 reservoirs in Han River basin using a fuzzy inference mechanism based on the precipitation changes of A1B scenario. Nam et al. (2014) assessed the agricultural water availability at a local scale by using an irrigation vulnerability assessment model based on the simulated inflow using TANK model and the amount of water supply and demand of reservoirs under RCP scenarios.

3. Regional application of H08 in previous studies

H08 was originally developed as a global hydrological model with a spatial resolution of 1° × 1°. However, it is also applicable for the simulation of the hydrological cycle and river discharge at a regional scale. H08 can not only simulate natural hydrological processes, but also the impact of anthropogenic activities, such as reservoir operation and water withdrawal. The spatial resolution of H08 for global application can be 1° × 1° or 0.5° × 0.5°. In case of regional application of H08, 5′ × 5′ (approximately 9 km × 9 km) of the spatial resolution can be applicable (Hanasaki and Yamamoto, 2010).

Khajuria et al. (2013) applied H08 in India to estimate the present and future water availability on a spatial resolution of 0.5° × 0.5°. They used the land surface module and river routing module in the H08 model to simulate the annual flow and divided it with the total population, and then estimated the annual per capita water availability. Future water withdrawal and availability with changing climate and population was estimated for India.

Mateo et al. (2014) modeled the coupled H08 and CaMa-Flood model to assess the impact of reservoir operation on the inundation in the Chao Phraya River basin in Thailand. H08 was used to simulate land surface hydrological process and reservoir operation rules. Additionally, the applied spatial resolution of H08 was 5′ × 5′.

Okada et al. (2014) developed the CROVER model, which consists of H08 and crop model PRYSBI-2, to assess the integrated impact of

climate change on the hydrological processes and the crop yield in the Songhua River basin in China. H08 was used to simulate the runoff, evapotranspiration, and soil moisture.

Masood et al. (2014) used H08 to simulate the impact of climate change on the hydrological processes in the Ganges - Brahmaputra - Meghna (GBM) River basin in a spatial resolution of 5′ × 5′ based on the RCP scenarios.

Agricultural activities in the Upper Chao Phraya river basin is directly related to surface water and groundwater resources affected by flood and drought conditions. Pratoomchai et al. (2015) investigated the impact of drought and flood conditions on the agricultural productivity related to the surface water and groundwater. H08 was used to simulate changes in surface runoff, discharge, and evapotranspiration along with the soil moisture deficit method and Penman-Monteith method for calculating groundwater storage and crop water demand.

Table 3 presents previous studies on the regional application of H08 for regional impact assessment of environmental changes on the hydrological process and water availability. H08 has been successfully applied to a part of the catchment area spread over 100,000 km^2. Therefore, it is considered that H08 is appropriate for application in a scale of the Korean Peninsula.

Table 3 Study sites and spatial resolution of previous studies for regional application of H08

Author	Year	Study site	Area(km^2)	Spatial resolution
Khajuria et al.	2013	India	3,287,263	0.5°×0.5°
Mateo et al.	2014	Chao Phraya river basin, Thailand	160,400	5′×5′
Masood et al.	2014	Ganges-Brahmaputra-Meghna(GBM) river basin	1,712,700	5′×5′
Okada et al.	2014	Songhua river basin, Northeast China	212,000	5′×5′
Pratoomchai et al.	2015	Upper Chao Phraya river basin, Thailand	109,973	5′×5′

Ⅲ. Methodology

1. Scope of the study

Since water resources are widely involved in fields such as natural hydrology, energy circulation, and human activity, it is necessary to limit the scope of the study. Especially, a study to assess the impact of future conditions on water resources along with climate change, water use changes, and human activities should also be considered. In order to assess the impacts of climate change, socio-economic changes were excluded from the scope of this study. Thus, the estimation of water availability in future has been studied for climate change impact assessment. Climate change leads to changes in land use and in the distribution of crop species. However, this study does not cover the impact of land use changes or crop species changes on water resources. Therefore, this study only estimates water balance and river discharge on land surfaces caused by climatic phenomena.

The location of this study is the Korean Peninsula. However, major rivers are located near in the national border with China, which were included in the simulation. To limit the spatial scope to latitudinal and longitudinal extents for convenience in simulation, the areas within the Korean Peninsula (124°E - 131°E, 33°N - 44°N) was included in the simulation.

The period for model calibration and validation was set to 10 years (from 1986 to 1995). For the first 5 years, the model was calibrated;

then the model was validated for the next 5 years. After the completion of model validation, a reference period and objective periods were set to assess the impact of climate change as shown in Table 4.

Table 4 Temporal scope of this study

Classification	Period
Calibration, validation period	1986-1995
Reference(baseline) period	1971-2000
Objective period 1 (2020s)	2010-2039
Objective period 2 (2050s)	2040-2069
Objective period 3 (2080s)	2070-2099

2. Materials and method

2.1. Study flow

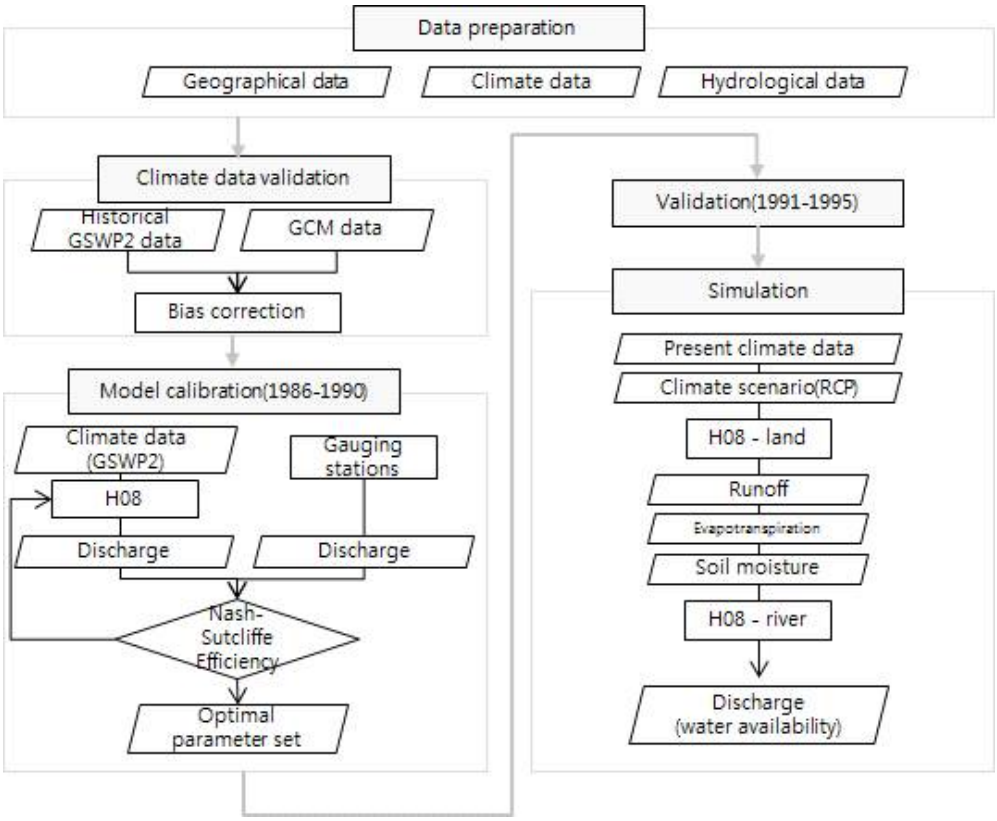

Figure 1 Flow chart of this study

Figure 1 presents the flow chart of this study. First of all, an input data for model simulation including meteorological data, geographical data and hydrological data was prepared. Then a process of verifying the input climate data by comparing with the observed climate data is required to correct the bias of the climate data for model simulation. The bias-corrected meteorological data is used as the input data for

hydrological simulation for calibration period in order to optimize the model parameters to Korean Peninsula. The model calibration is carried out by tuning the parameters based on NSE value, which can evaluate the model performance on the river discharge simulation compared with the observed discharge. After the calibration, validation is carried out to evaluate the adaptability of the model. After the validation of the model, climate change impact assessment simulation is carried out. Finally, the simulated river discharge is regarded as water availability.

2.2. Introduction to hydrological model H08

H08 was developed by Hanasaki et al. (2008) to estimate water availability in a global scale. This model can simulate representative anthropogenic activities that affect the hydrological cycle such as reservoir operation, water withdrawal, crop growth as well as natural hydrological process (Hanasaki et al., 2008). H08 model is consisted with 6 modules – Land surface hydrology module, river routing module, crop growth module, reservoir operation module, water withdrawal module, environmental flow module.

Land surface module of H08 can be classified as land surface model (LSM) that can solve both the surface energy and water balances (Haddeland et al., 2011).

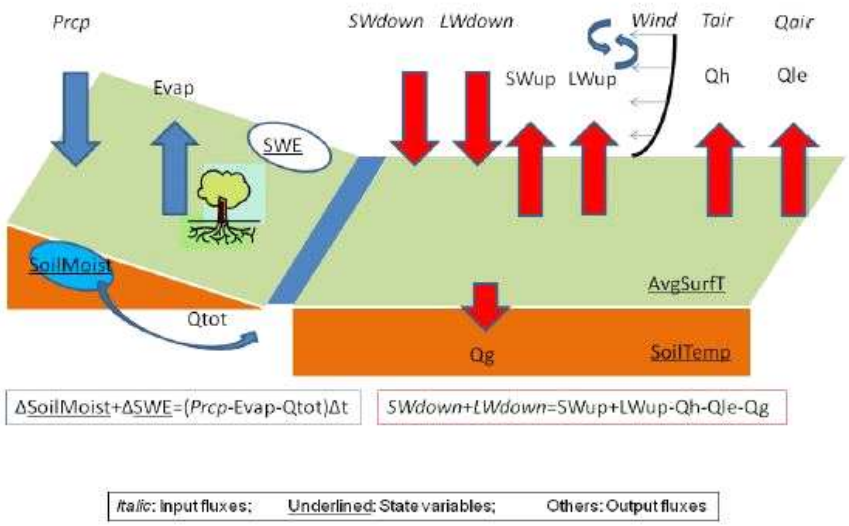

Figure 2 Schematic diagram of land surface process module of H08 (Hanasaki and Yamamoto, 2010)

FIgure 2 shows schematic diagram of land surface process in H08. Land surface module calculates water and energy balance based on bucket model (Manabe, 1969). In H08, one grid is conceptually one bucket. When the bucket is empty, the soil moisture of bucket is at wilting point. When the bucket is full, soil moisture is at field capacity. The definition of field capacity is maximum capacity of soil water contents that can be exist against the gravity force. Evapotranspiration is expressed as a function of potential evapotranspiration and soil moisture. In the original bucket model, runoff is generated only when the bucket is full. But H08 applied leaky bucket (Robock et al., 1995) so that subsurface runoff is calculated. Total runoff can be divided into surface runoff and subsurface runoff.

LSMs have differences in their choice of evapotranspiration and runoff schemes. There are many formulas for calculating evapotranspiration, such as Penman-Monteith, Pristley-Taylor, and Hamon. In this leaky bucket model, evapotranspiration is estimated by using bulk formula which uses bulk transfer coefficient to calculate turbulent heat fluxes. Potential evapotranspiration $E_P[kg/m^2/s]$ can be estimated by [Eq. 2].

$$E_P(T_S) = \rho C_D U(q_{SAT}(T_S) - q_a) \quad \text{[Eq. 2]}$$

$\rho[kg/m^3]$ is density of air, C_D is bulk transfer coefficient, $U[m/s]$ is wind speed, $q_{SAT}(T_S)[kg/kg]$ is saturated specific humidity of a given surface temperature. Actual evapotranspiration can be calculated by [Eq.3] by multiplying a function of soil moisture W to potential evapotranspiration.

$$E = \beta E_P(T_S) \quad \text{[Eq. 3]}$$

$$\beta = \begin{cases} 1 & 0.75\,W_f \leq W \\ W/0.75\,W_f & W < 0.75\,W_f \end{cases} \quad \text{[Eq. 4]}$$

$W[kg/m^2]$is soil moisture, W_f is fixed with $150kg/m^2$ as a soil moisture at field capacity. Actual evapotranspiration is proportional to the soil moisture W.

Water balance equation of soil is represented as [Eq. 5]

$$\frac{dW}{dt} = Rainf + Q_{sm} - E - Q_s - Q_{sb} \quad \text{[Eq. 5]}$$

$Q_s[kg/m^2/s]$is surface runoff, $Q_{sm}[kg/m^2/s]$is snow melt rate, Q_{sb} $[kg/m^2/s]$is subsurface runoff. surface runoff Q_s take place based on [Eq. 6]. Runoff scheme of this model is based on saturation excess and beta function which defines runoff as a nonlinear function of soil moisture (Haddeland et al., 2011). Surface runoff is generated if the soil water content exceeded the field capacity.

$$Q_s = \begin{cases} W - W_f & W_f < W \\ 0 & W \leq W_f \end{cases} \quad \text{[Eq. 6]}$$

In case of subsurface runoff Q_{sb}, it is newly added scheme for leaky bucket module compared with original bucket model. Subsurface runoff is generated based on [Eq. 7]. τ and γ are globally uniform as a constant parameter.

$$Q_{sb} = \frac{W_f}{\tau}\left(\frac{W}{W_f}\right)^{\gamma} \quad \text{[Eq. 7]}$$

River routing module of H08 is based on TRIP (Total Runoff Integrating Pathways) model (Oki and Sud, 1998). Land surface module calculates runoff on every grid, and then river routing module calculate river discharge accumulating runoff from upper grid based on flow direction.

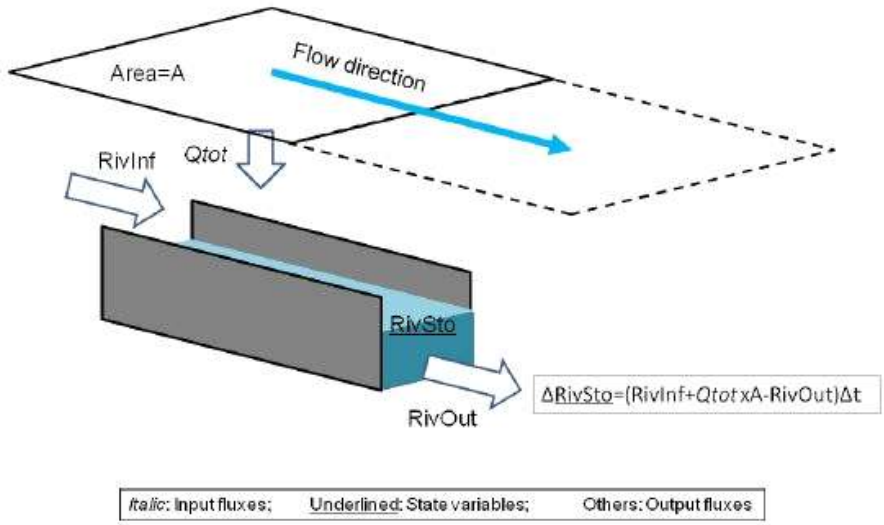

Figure 3 Schematic diagram of the river module of H08 (Hanasaki and Yamamoto, 2010)

There were two reasons for the selection of the H08 model in this study. First, this model can include multiple basins in one simulation to estimate water availability in the Korean Peninsula for the present and future climatic conditions. Second, the simulation results representing the water availability can be shown on a grid for spatial implications as a result, since H08 is a grid-based hydrological model. In this study, the land surface module and river routing module of H08 is applied.

For regional application of the global hydrological model H08, the applicable spatial resolution is 5′ × 5′ (approximately 9 km × 9 km) owing to the model structure. In case of Korean Peninsula, the spatial domain for simulation was set to be 124°E - 131°E, 33°N - 44°N.

Accordingly, in this mode, the Korean peninsula is configured by 84 grids on the horizontal axis, 123 grids on the vertical axis. It consists of a total number of 11088 grids.

2.3. Meteorological data

Eight meteorological variables (albedo, surface pressure, rainfall rate, wind speed, longwave downward radiation, specific humidity, shortwave downward radiation, air temperature) for H08 simulation is presented in Table 5. The input data for the past time period is provided by the Second Global Soil Wetness Project (GSWP2). In order to model surface - atmosphere system and provide the soil wetness data as a critically important component of the global energy and water balance (Dirmeyer et al., 2006), Global Soil Wetness Project (GSWP) was suggested. GSWP2 distributed the 3-hourly hydro-meteorological data, such as soil moisture, air temperature, water equivalent, and land surface fluxes. Some studies have carried out the validation of GSWP2 based on observed climate data (Hanasaki et al., 2008). The GSWP2 meteorological data can be easily obtained from the server of the H08 meteorological data[3].

3) http://h08.nies.go.jp/ddc/

Table 5 Meteorological variables

Meteorological variables	Unit
Albedo	-
Surface pressure	Pa
Rainfall rate	mm/s
Wind speed	m/s
Longwave downward radiation	W/m^2
Specific humidity	kg/kg
Shortwave downward radiation	W/m^2
Air temperature	K

H08 simulates the energy balance of the land surface as well as the water balance. The most principle meteorological variables to simulate hydrological process are air temperature and precipitation. Therefore, these 2 variables should be validated by comparing with the observed data from the Korea Meteorological Administration. The period of the available data of GSWP2 is 10 years (from 1986 to 1995). The model calibration and validation period was defined to be same as the period of the GSWP2 data.

Various GCMs generate future climate scenarios to assess the impact of climate change. The HadGEM2-AO model was downscaled by Korea Meteorological Administration to a spatial resolution of 1 km in South Korea. In Korean Peninsula, the spatial resolution of the downscaled HadGEM2-AO is 12.5 km. In this study, HadGEM2-AO was selected for climate change impact assessment on the water availability in Korean Peninsula because of its adaptability proved in many previous studies in Korea. HadGEM is known for its excellent performance, especially for East Asia and the Pacific Rim (Korea

Meteorological Administration, 2012). The RCP 8.5 scenario, which assumed current trends for future greenhouse gas emissions, is applied in this study. The climate change impacts based on the monthly climate data were estimated for the same period as Table 4. The climate scenario from the selected GCM is also obtained from the H08 meteorological data server.

Table 6 Classification of the climate data

Classification	Period	Source	Climate model
Observed	1961-1995	KMA (Korea Meteorological Administration)	Observed data
Calibration, validation	1986-1995	GSWP2 (Global Soil Wetness Project 2)	Observed data
Baseline	1971-2000	RCP 8.5 scenario	HadGEM2-AO
2020s	2010-2039		
2050s	2040-2069		
2080s	2070-2099		

The meteorological variables for future periods are same as the variables presented in Table 5. There are various methodologies for the projection and application of future scenarios to the hydrological models. In this study, the “shifting” and “scaling” methods (Lehner et al., 2006) were selected to apply to the future climate variables. This method is relatively simplified by adding, subtracting, or multiplying the amount that is expected to change in the future if present climatic conditions persist, and thus, predicts the impact of future climate change (Hanasaki et al., 2013). Meteorological variables to predict

changes in climate impacts are shown in Table 7. Variables for the future periods include rainfall, air temperature, and longwave downward radiation data. The remaining climate variables are fixed at the present condition.

Table 7 Meteorological variables and elements of the climate change scenario

Variables	Future projection method
Rainfall[$kg/m^2/s$]	Scaling
Air temperature[K]	Shifting
Longwave downward radiation[W/m^2]	Shifting
Shortwave downward radiation[W/m^2]	Fixed
Relative humidity[%]	Fixed
Wind speed[m/s]	Fixed
Air pressure[Pa]	Fixed

2.4. Geographical data

DEM data is provided by hydroSHEDS[4] and is resampled on ArcGIS to adjust the spatial resolution of 5′ × 5′. DEM is the principal geographical data input for the calculation of river discharge, since the flow direction map can be derived from the DEM data. Flow direction has a major influence on the hydrograph of the watershed by determining the length of flow from the starting point of the river to the observation point (Oki and Sud, 1998). The flow direction as a map data input of H08 is presented in Figure 4. Every grid has a specific number, which means the flow direction that is represented by the numbers from 0 to 9. Numbers from 1 to 8 represent various flow

4) http://hydrosheds.cr.usgs.gov/index.php

directions(Figure 4), 0 represents the sea, and 9 means the river outlet.

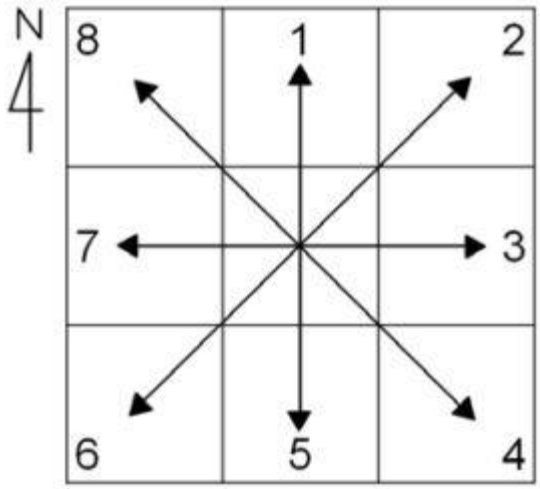

Figure 4 Flow direction for each cell (Hanasaki and Yamamoto(2010))

There are various methods to determine whether the modified flow direction can represent the true conditions. It is necessary to make a manual correction of points in the map (Oki and Sud, 1998), so that the catchment area delineated by the flow direction map could be matched with the actual catchment area. In this study, the comparison of the flow direction map of a spatial resolution of 9 km and the detailed flow direction map was carried out so that the original flow direction map can delineate the relevant catchment area when compared with the actual catchment area by manual correction of the flow direction map. Table 8 presents the catchment area delineated from the corrected flow direction map.

Table 8 Observed and simulated catchment area of the gauging stations from the corrected flow direction map

Watershed	Station	Location		Catchment area(km^2)		
		Lon.	Lat.	Observed	Simulated	Error(%)
Amnok	Supung reservoir	124.96	40.46	52,912	46,291	-14.3
	Unbong reseroir	126.51	41.38	24,168	19,911	-21.38
Taedong	Seohaegabmun reservoir	125.19	38.68	15,714	17,040	7.78
Han	Yeoju	127.65	37.3	11,095	8,673	-21.83
	Jingwan	127.15	37.65	202	203	0.5
	Hangang	126.96	37.52	24,753	21,470	-13.26
Geum	Gongju	127.14	36.46	7,150	7,180	0.42
	Gyuam	126.89	36.28	8,253	7,940	-3.79
Nakdong	Waegwan	128.39	36.18	11,074	11,309	2.12
	Goryeong	128.39	35.75	14,034	14,643	4.34
	Jeokpo	128.36	35.53	16,450	16,665	1.31
	Samrangjin	128.83	35.38	22,892	22,114	-3.4
Yeongsan	Naju	126.73	35.04	2,059	2,101	2.04

2.5. Hydrological data

Hydrological data is essentially required to calibrate and validate simulation results of the hydrological model and to evaluate the model performances. In case of South Korea, the Water Resources Management Information System (WAMIS)[5] provides the historical hydrological data. The observational hydrological data before 1995 can be obtained in terms of water level; so the confirmation and adjustment of the rating curve is required. In case of North Korea, the

5) www.wamis.go.kr

data distributed from the Global Runoff Distribution Center (GRDC)[6] was used. GRDC provides global river discharge data for the historical periods. It is reliable because it is widely used in a variety of previous studies and it is well validated with actual observational discharge data with the stations of the Korean Peninsula (Son et al., 2013). Therefore, the stations in North Korea can be calibrated and validated using the GRDC monthly average data. The stations in Korean Peninsula from the GRDC data are listed in Table 9.

Table 9 Information of stations in the Korean Peninsula from GRDC

Country [7]	Watershed	Station	Location		Area[km^2]
			Lon.	Lat	
KP	Duman	Yenam	128.83	41.73	720
KP	Amnok	Jonchon	126.45	40.67	2192
KP		Kumchang	127.13	41.53	18245
KP	Taedong	Mirim	125.78	39.02	12175
KP		Dokchon	126.3	39.75	3300
KP		Songchon	126.22	39.27	1878
KP		Samdung	126.18	38.98	2727
KR	Han	Indogyo	126.97	37.52	25046
KR		Yeoju	127.648	37.2961	11104.4
KR	Geum	Gongju	127.126	36.4636	7149.5
KR	Yeongsan	Naju	126.734	35.0333	2058.7
KR	Seomjin	Sing Jeon	127.57	35.18	4480
KR	Nakdong	Waegwan	128.394	36.0003	11074.4
KR		Jindong	128.48	35.38	20403
KR		Samrangjin	128.85	35.4	22916

The objective of this study is to estimate the impact of changes in the hydrological status and future water availability across the entire

6) http://www.bafg.de/GRDC/EN/03_dtprdcts/32_LTMM/longtermmonthly_node.html
7) KP : North Korea(Democratic People's Republic of Korea), KR : South Korea(Republic of Korea)

peninsula. Therefore, it is necessary to represent the simulation results for the main river basins in the peninsula. In case of North Korea, Amnok, Duman, Chongchon, and Taedong river basins were selected based on the major gauging stations. In case of South Korea, Han, Nakdong, Geum, and Yeongsan river basins were selected based on the major gauging stations. Table 10 provides the basic information on the major river basins and stations in Korean Peninsula.

Table 10 Observation period and references of hydrological data

Watershed	Station	Data period	Reference
Amnok	Kumchang	1976-1984	Global Runoff Data Center[8]
Duman	Yenam	1976-1979	
	Khasan	-	-
Chongchon	Pugwon	1923-1927	Lautensach, 1988
	Puksongri	1923-1927	
Taedong	Mirim	1976-1982	Global Runoff Data Center
	Dokchon	1976-1981	
Han	Yeoju	1986-1995, 1976-2009	Korea Water Resources Corporation[9], Global Runoff Data Center
	Hangang	1986-1995, 1947-1979	
Geum	Gongju	1986-1995, 1976-2009	
	Gyuam	1986-1995	
Nakdong	Waegwan	1986-1995, 1976-2009	
	Jeokpo	1986-1995	
	Samrangjin	1986-1995, 1953-1972	
Yeongsan	Naju	1986-1995, 1976-2009	

8) http://www.bafg.de/GRDC/EN/03_dtprdcts/32_LTMM/longtermmonthly_node.html
9) www.wamis.or.kr

Ⅳ. Results and discussion

1. Validation of meteorological data

1.1. Validation and bias correction of GSWP2 data

Meteorological data of GSWP2 is used for the period of model calibration and validation due to the accessibility of historical climate data for H08 simulation. The period of the data is 10 years from 1986 to 1995. Verification of the data is carried out by comparing observed 30-year climatological normals from 1981 to 2010 distributed by Korea Meteorological Administration[10]. Analyzed meteorological variables are air temperature and precipitation. Major weather stations used for validation of GSWP2 historical data are suggested on Table 11.

Table 11 Meteorological stations in the Korean peninsula

Watershed	Station	Location	
		Longitude	Latitude
Duman river	Sonbong	130.4	42.32
Amnok river	Hyesan	128.17	41.4
	Sinuiju	124.38	40.1
Chongchon river	Anju	125.65	39.62
Taedong river	Pyongyang	125.78	39.03
Ryesong river	Kaesong	126.57	37.97
Han river	Seoul	126.97	37.57
	Chuncheon	127.74	37.9
Geum river	Daejeon	127.39	36.37
Nakdong river	Busan	129.03	35.02
Yeongsan river	Gwangju	126.89	35.17
Seomjin river	Namwon	127.39	35.4

10) http://www.kma.go.kr/weather/climate/average_north.jsp

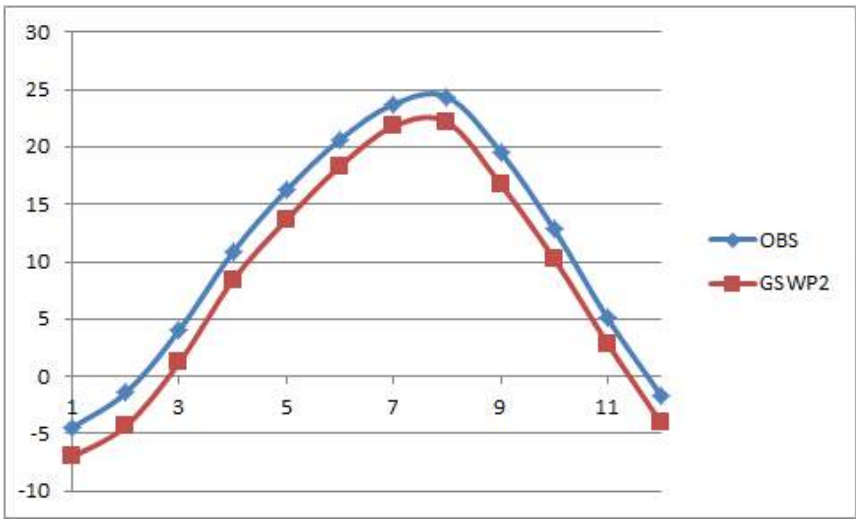

Figure 5 Comparison of monthly average temperature[℃] between observation and GSWP2

Figure 5 shows comparison of mean monthly air temperature of GSWP2 and observed data of the stations presented in Table 11. Mean monthly air temperature of GSWP2 is lower than observed value in a certain amount for the simulated period constantly. The original spatial resolution of GSWP2 meteorological data is 1 degree × 1 degree, so it is interpolated to a spatial resolution of 5 minutes × 5 minutes which was same as H08 simulation. In order to correct meteorological bias between observed data and simulated data, a ratio between observed value and simulated value can be defined as a bias correction factor (Bao et al., 2012). The bias of simulated GSWP2 meteorological data was corrected by multiplying monthly correction factor. Mean monthly temperature for observed data, GSWP2 data, and their correction factor are suggested on Table 12. As a result, calculated R^2 of corrected

GSWP2 mean annual temperature data and observed data for 10 years is 0.8879 (Figure 6).

Table 12 Comparison of observation and GSWP2 monthly temperature and correction factor

Month	OBS[℃]	GSWP2[℃]	Correction factor
1	-4.45	-7.02538	0.633418
2	-1.425	-4.32852	0.329212
3	4.05	1.225806	3.303948
4	10.84167	8.385971	1.292834
5	16.23333	13.65018	1.18924
6	20.64167	18.31283	1.12717
7	23.725	21.79436	1.088585
8	24.35833	22.16645	1.098883
9	19.55833	16.73821	1.168484
10	12.83333	10.24916	1.252136
11	5.058333	2.856155	1.771029
12	-1.68333	-4.07071	0.413523
average	10.81181	8.329541	

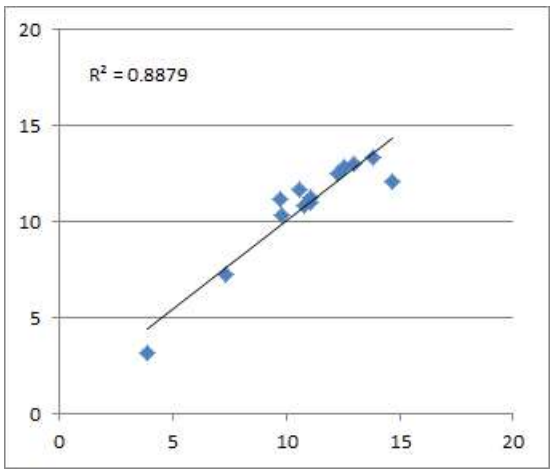

Figure 6 Comparison of annual average temperature[℃] between observation and GSWP2

Comparison of mean monthly precipitation between observation and GSWP2 data is also presented in Figure 7. In case of precipitation, GSWP2 data appeared similar to the observed data except for the small differences in winter period (Table 13).

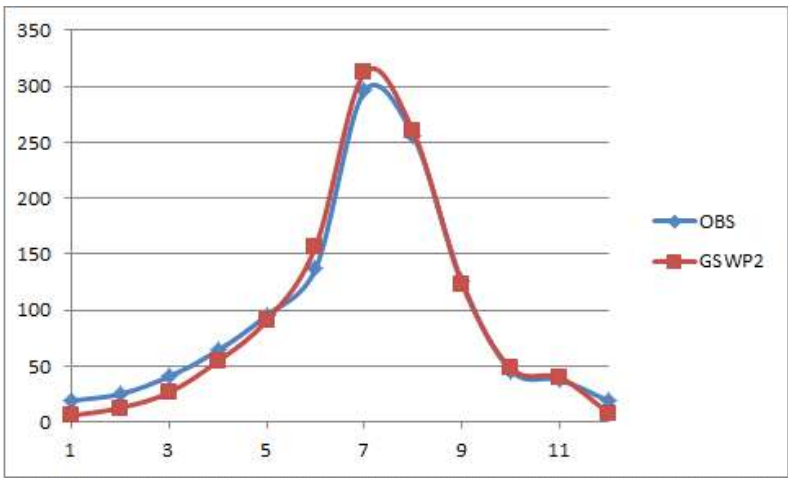

Figure 7 Comparison of monthly average precipitation[mm] between observation and GSWP2

Corrected mean annual precipitation data of GSWP2 compared with observed data for 10 years from 1986 to 1995 and calculated R^2 is presented in Figure 8.

As a result of bias correction of GSWP2 data, Figure 9 shows spatial variability of meteorological variables of GSWP2 used in this study for model calibration and validation period.

Table 13 Comparison of observation and GSWP2 monthly precipitation and correction factor

Month	OBS[mm]	GSWP2[mm]	Correction factor
1	19.01667	5.690204	3.342001
2	24.85833	12.46111	1.994874
3	40.45833	26.31819	1.537276
4	63.78333	54.21428	1.176504
5	95.41667	90.70703	1.051921
6	136.9	156.74	0.873421
7	295.7417	311.9215	0.948129
8	255.75	259.5222	0.985465
9	125.2917	123.2059	1.016929
10	45.83333	47.76976	0.959463
11	37.73333	39.66203	0.951372
12	18.85	7.829944	2.407425
sum	1159.633	1136.042	

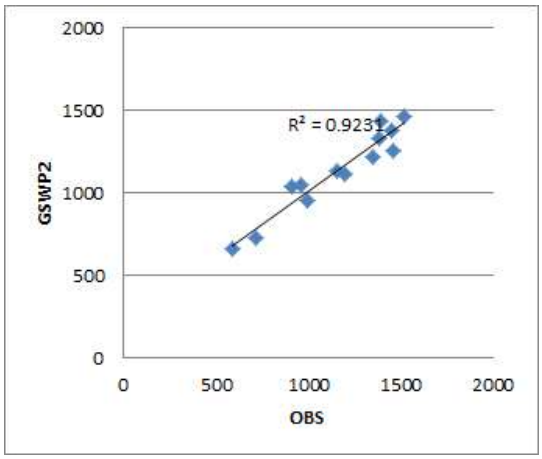

Figure 8 Comparison of annual precipitation[mm] between observation and GSWP2

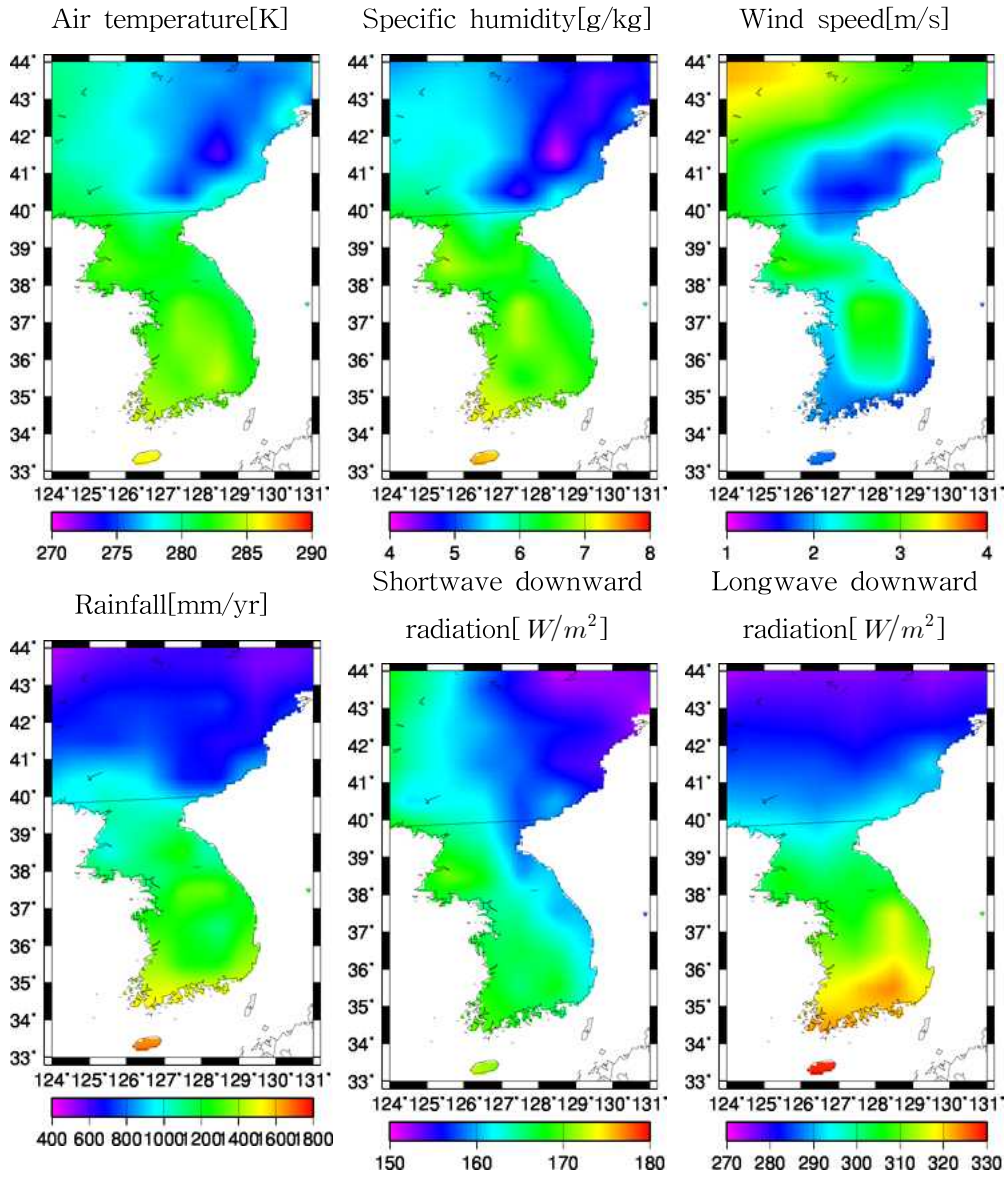

Figure 9 Meterological data from GSWP2 (average value from 1986 to 1995)

1.2. Validation and bias correction of GCM historical data

HadGEM2-AO is selected for climate change simulation as GCM in this study because most of previous studies in Korea selected this model for climate change impact assessment due to its adaptability to East Asia and the Pacific Rim (Korea Meteorological Administration, 2012). The validation and bias correction of air temperature and precipitation derived from the GCM is also carried out by using same method as the process of GSWP2 data based on 30-year climatological normals from 1981 to 2010.

Simulated mean monthly air temperature from the GCM is presented in Figure 10 compared with observed data. Same methodology used in the bias correction of GSWP2 data was applied for bias correction of climate data from GCM. Correction factor was defined as changed ratio from observed value to simulated value on a monthly basis (Table 14). Corrected temperature data of GCM on a annual basis is presented in Figure 11 compared with observed data for 10 years from 1986 to 1995.

Table 14 Comparison of observation and HadGEM2-AO monthly temperature and correction factor

Month	OBS[℃]	HadGEM2-AO[℃]	Correction factor
1	-4.45	-6.34092	0.701791
2	-1.425	-3.63876	0.391617
3	4.05	2.74544	1.475174
4	10.84167	9.510232	1.14
5	16.23333	15.05778	1.078069
6	20.64167	19.20608	1.074747
7	23.725	22.01859	1.077499
8	24.35833	22.39392	1.087721
9	19.55833	18.34633	1.066063
10	12.83333	12.13416	1.05762
11	5.058333	3.947176	1.281507
12	-1.68333	-2.95247	0.570144
average	10.81181	9.368963	

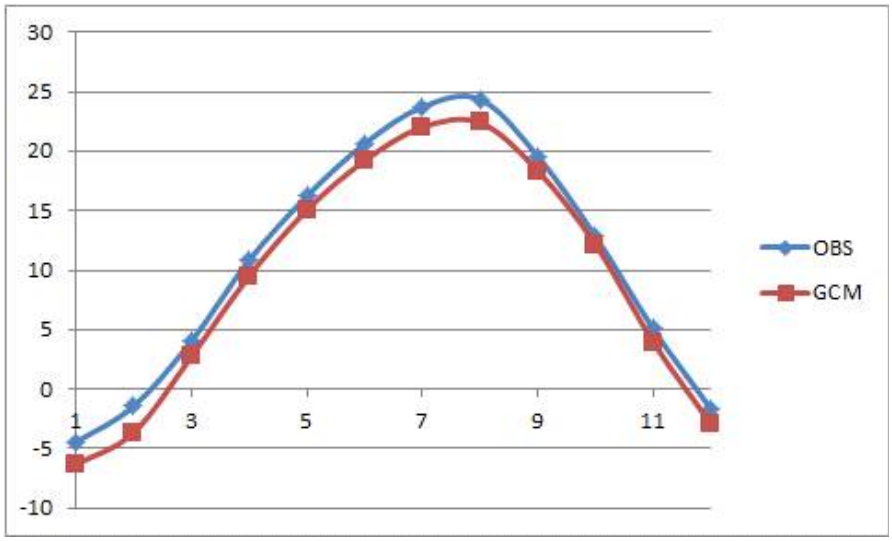

Figure 10 Comparison of monthly average temperature[℃] between observation and HadGEM2-AO

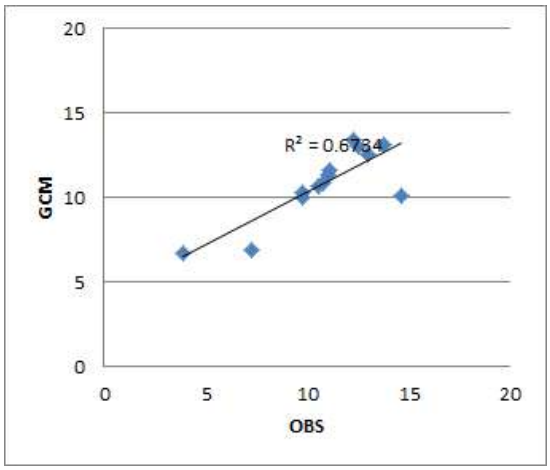

Figure 11 Comparison of annual temperature[℃] between observation and HadGEM2-AO

Figure 12 shows precipitation of GCM and observation. In case of precipitation data, GCM was evaluated that most GCMs could not simulate the peak rainfall events in summer so that the amount of summer rainfall is smaller than observed precipitation data. This is because GCM has low ability on simulating storm in summer and local rainfall events (Moon et al., 2013). Therefore, bias correction process was carried out in a same way as described above which is multiplying monthly correction factor. Figure 12 shows mean monthly precipitation of GCM and observation, and the value of correction factor is also presented in Table 15.

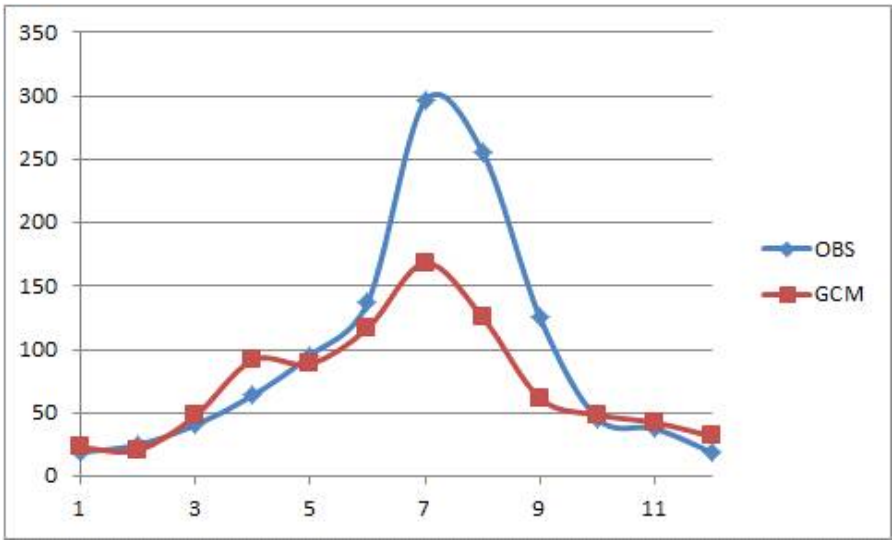

Figure 12 Comparison of monthly average precipitation[mm] between observation and HadGEM2-AO

Table 15 Comparison of observation and HadGEM2-AO monthly precipitation and correction factor

Month	OBS[mm]	HadGEM2-AO[mm]	Correction factor
1	19.01667	22.92972	0.829346
2	24.85833	20.69282	1.201302
3	40.45833	47.71821	0.847859
4	63.78333	91.64412	0.695989
5	95.41667	88.79413	1.074583
6	136.9	116.8833	1.171254
7	295.7417	168.1376	1.758926
8	255.75	125.4675	2.038376
9	125.2917	61.65168	2.032251
10	45.83333	48.55482	0.94395
11	37.73333	42.38216	0.890312
12	18.85	31.59677	0.59658
sum	1159.633	866.4529	

Corrected annual precipitation and observed data are plotted in Figure 13. Figure 14 and 15 present monthly precipitation of the stations

before versus after the bias correction of GCM. In case of North Korea, the precipitation is relatively low compared with regions of South Korea. The precipitation in northern region is slightly increased and southern region is slightly decreased in the process of multiplying uniform correction factor across the whole Korean Peninsula. It is because the amount of mean annual rainfall in southern region is larger than the northern region as shown in Figure 9

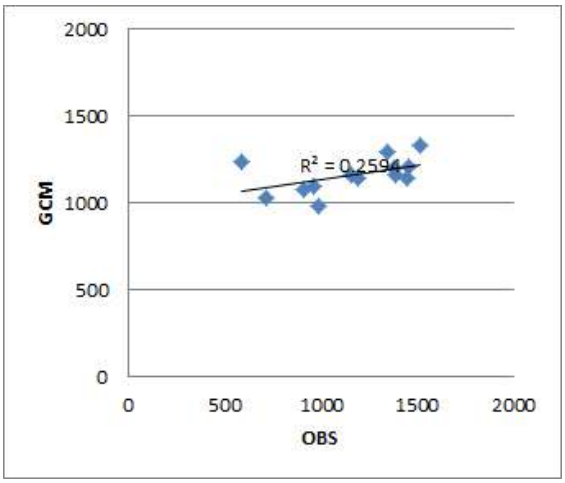

Figure 13 Comparison of annual precipitation[mm] between observation and HadGEM2-AO

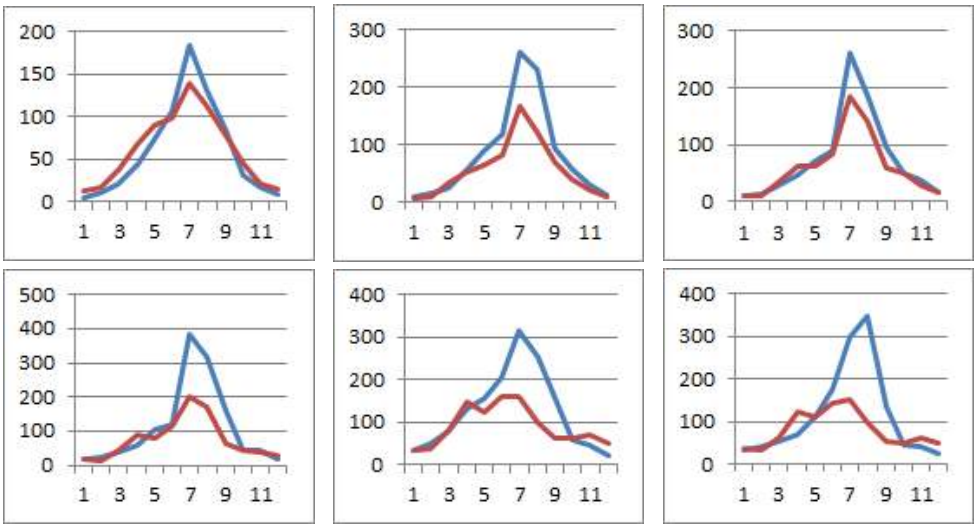

Figure 14 Monthly average precipitation from HadGEM2-AO for representative stations in Korean Peninsula before bias correction (from the top left: Sonbong, Sinuiju, Pyongyang, Chuncheon, Busan, Namwon).
Blue line : OBS, red line : HadGEM2-AO

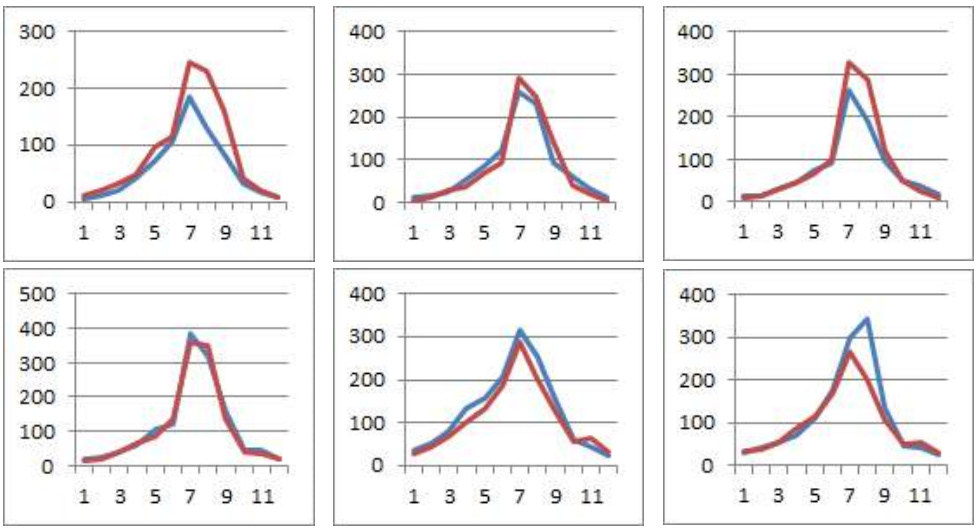

Figure 15 Monthly average precipitation from HadGEM2-AO for representative stations in Korean Peninsula after bias correction (from the top left: Sonbong, Sinuiju, Pyongyang, Chuncheon, Busan, Namwon)
Blue line : OBS, red line : HadGEM2-AO

2. Calibration and validation of H08

2.1. Parameter sensitivity analysis

The most sensitive parameters in H08 are soil depth SD, bulk transfer coefficient C_D that affects potential evapotranspiration, time constant τ that determines daily maximum subsurface runoff, and shape parameter γ related with a relationship between subsurface runoff and soil moisture (Masood et al., 2015; Hanasaki et al., 2014). Therefore, it is necessary to investigate the effects of these 4 variables on runoff hydrograph through a sensitivity analysis of the parameters.

Default values of 4 parameters in H08 are as follows: SD is 1m, C_D is 0.003, τ is 100, γ is 2. These default values were decided as a standard value for the turing of parameters. A lower bound of parameter is decided as a half of default value and an upper bound is decided as doubled default value (Table 16). The sensitivity analysis was carried out for 10 years from 1986 to 1995 which was set to the period of model calibration and validation for Hangang gauging station.

Table 16 Tested parameters for calibration

	SD	C_D	γ	τ
Lower bound	0.5	0.0015	1.0	50
H08 default value	1.0	0.003	2.0	100
Upper bound	2.0	0.006	4.0	200

In case of parameter SD, runoff hydrograph became gradual as the

soil depth increases (Figure 16) based on [Eq. 6] which calculates surface runoff from land surface module.

$$Q_s = \begin{cases} W - W_f & W_f < W \\ 0 & W \leq W_f \end{cases} \quad \text{[Eq. 6]}$$

Surface runoff Q_s is generated when the soil moisture W exceeds field capacity W_f. Figure 16 shows that runoff generation is delayed fluctuation of runoff hydrograph is decrease as SD increases because maximum capacity of soil moisture increases with soil depth. In a spring and winter season which recorded relatively low precipitation, generated runoff from the case of high value in SD is bigger than the case of low SD. On the other hand, it is simulated that generated runoff of high SD is smaller than the case of low SD.

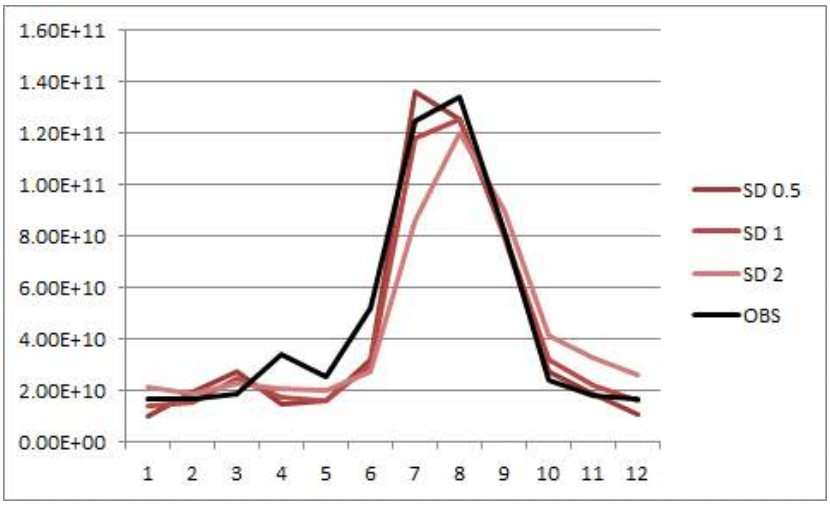

Figure 16 Discharge of Han River according to the changes in SD [mm/day]

Bulk transfer coefficient C_D is a parameter that directly affects to potential evapotranspiration E_P based on [Eq. 2].

$$E_P(T_S) = \rho C_D U(q_{SAT}(T_S) - q_a) \quad \text{[Eq. 2]}$$

When C_D increases, potential evapotranspiration increases according to [Eq. 2] and runoff decreases based on the water balance equation [Eq. 5]. Figure 17 presents the tendency of runoff generation according to the variation of C_D.

$$\frac{dW}{dt} = Rainf + Q_{sm} - E - Q_s - Q_{sb} \quad \text{[Eq. 5]}$$

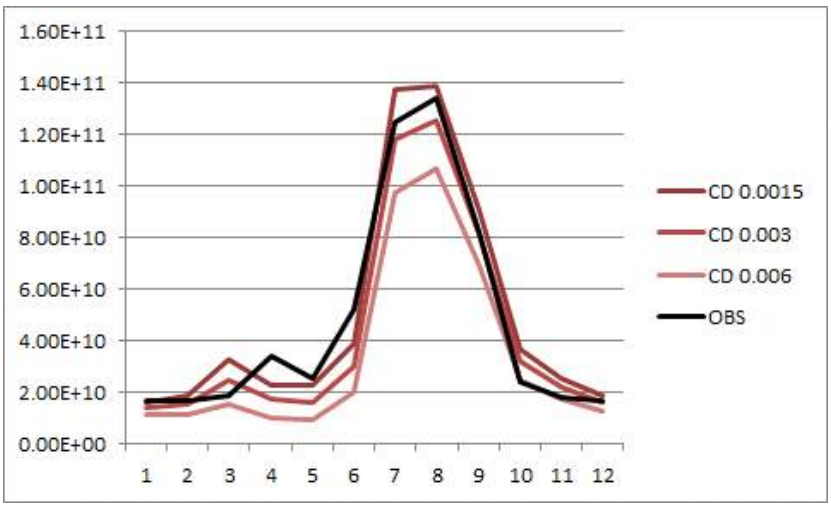

Figure 17 Discharge of Han River according to the changes in CD [mm/day]

Subsurface runoff Q_{sb} is calculated by [Eq. 7] that determines a relationship between soil moisture W and field capacity W_f.

$$Q_{sb} = \frac{W_f}{\tau}(\frac{W}{W_f})^{\gamma} \quad \text{[Eq. 7]}$$

As shown in Figure 18, runoff decreases with increasing γ except for summer that rainfall is concentrated. When the rainfall is concentrated, soil moisture increases to the field capacity, and then W/W_f approaches to 1. It means that the influence of γ on a runoff hydrograph decreases with increasing precipitation. The value of W/W_f is below 1 except for summer. Therefore, when γ increases, subsurface runoff Q_{sb} decreases and surface runoff Q_s increases based on a water balance equation [Eq. 3] under the condition precipitation and evapotranspiration is constant. τ is time constant which determines daily maximum subsurface runoff. When τ increases, subsurface runoff Q_{sb} decreases, and surface runoff Q_s increased based on [Eq. 7]. The parameter γ and τ affects the sensitivity of variation in Q_{sb} and Q_s. It should be noted that the sensitivity of these parameters to total runoff hydrograph which can be divided into a subsurface and surface runoff should be investigated (Mateo, 2012). In case of the parameter γ and τ, total runoff decrease with increasing values of the 2 parameters respectively (Figure 18, 19).

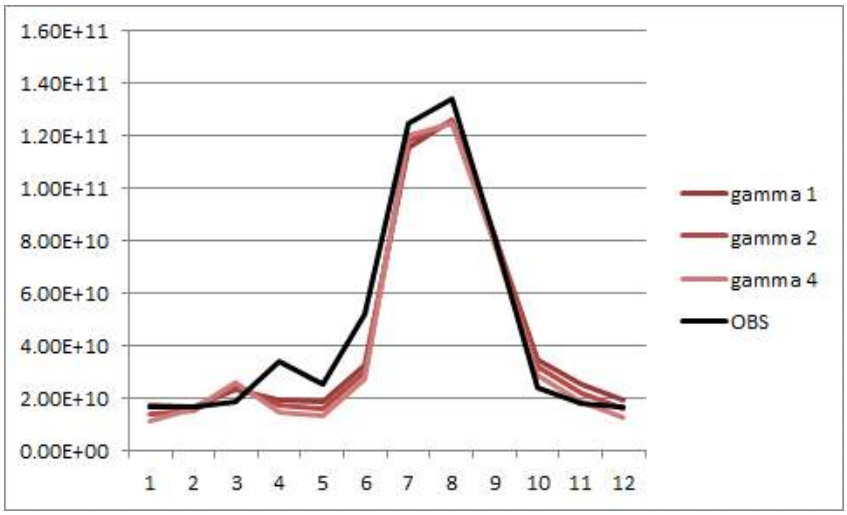

Figure 18 Discharge of Han River according to the changes in γ [mm/day]

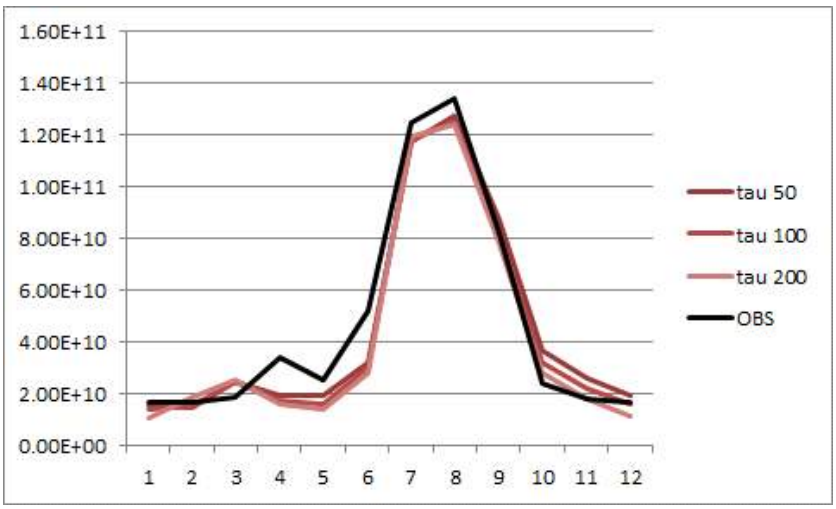

Figure 19 Discharge of Han River basin according to the changes in τ [mm/day]

2.2. Calibration of parameters

Model calibration and validation is carried out based on the GSWP2 meteorological data for 10 years of the period from 1986 to 1995. The

parameters were tuned for the first 5 years, and then simulated results based on the tuned parameters are validated for the last 5 years. Table 17 describes the list of gauging stations in the Korean Peninsula and types of available data used for calibration and validation. The code of the stations are temporarily assigned for convenience in the simulation process (Table 17). The observed discharge data of the GRDC which was used to calibrate the simulation results of the North Korea, only monthly data was available so that the interannual variations of simulated discharge did not considered for the calibration. In case of South Korea, WAMIS provide the interannual variability of river discharge as well as monthly discharge.

Table 17 Code of discharge stations and available types of observation data in this study

Watershed	Station	Code	Available OBS data[11)]
Amnok	Supung reservoir	N1	-
	Unbong reservoir	N2	-
	Kumchang	N3	M
Duman	Khasan	N4	-
	Yenam	N5	M
Chongchon	Puksongri	N6	-
Taedong	Seohaegabmun	N7	-
	Mirim	N8	M
	Dokchon	N9	M
Han	Yeoju	S1	M, Y
	Hangang	S2	M, Y
Geum	Gongju	S3	M, Y
	Gyuam	S4	M, Y
Nakdong	Waegwan	S5	M, Y
	Jeokpo	S6	M, Y
	Samrangjin	S7	M, Y
Yeongsan	Naju	S8	M, Y

The range of the parameters for calibration is same as shown in Table 16, and then the simulation was carried out for 81(=3^4) times for possible all the combinations of parameter set based on Table 16.

In order to derive optimal parameter set that can represent the hydrological process similar to real world, Nash-Sutcliffe model efficiency coefficient (NSE) is decided as an index to evaluate the applicability of model. NSE can be calculated by [Eq. 8]. Q_o^t is observed value at time t, $\overline{Q_o}$ is average total observed value, and Q_m^t is simulated value at time t (Nash and Sutcliffe, 1970). NSE has a value of range from $-\infty$ to 1. If the observed value and the simulated value is exactly same, NSE is represented to 1. Therefore, a simulated parameter set which has a value of NSE close to 1 is evaluated as a optimal parameter set that can simulates the real hydrologic phenomena reliably.

$$NSE = 1 - \frac{\sum_{t=1}^{T}(Q_o^t - Q_m^t)^2}{\sum_{t=1}^{T}(Q_o^t - \overline{Q_o})^2} \quad \text{[Eq. 8]}$$

Calculated NSE value is presented in Figure 20 based on simulated monthly discharge. Parameter sets are presented in Table 18 according to the value of NSE in highest order for the stations in Table 17

11) M : Only monthly average data for years of table10 is available, Y : Monthly average data and its interannual variation for years of table 10 is available

which have observed data for the simulated period, and then the parameter set which has the highest value of NSE is selected as an optimal parameter set that can represent the Korean Peninsula.

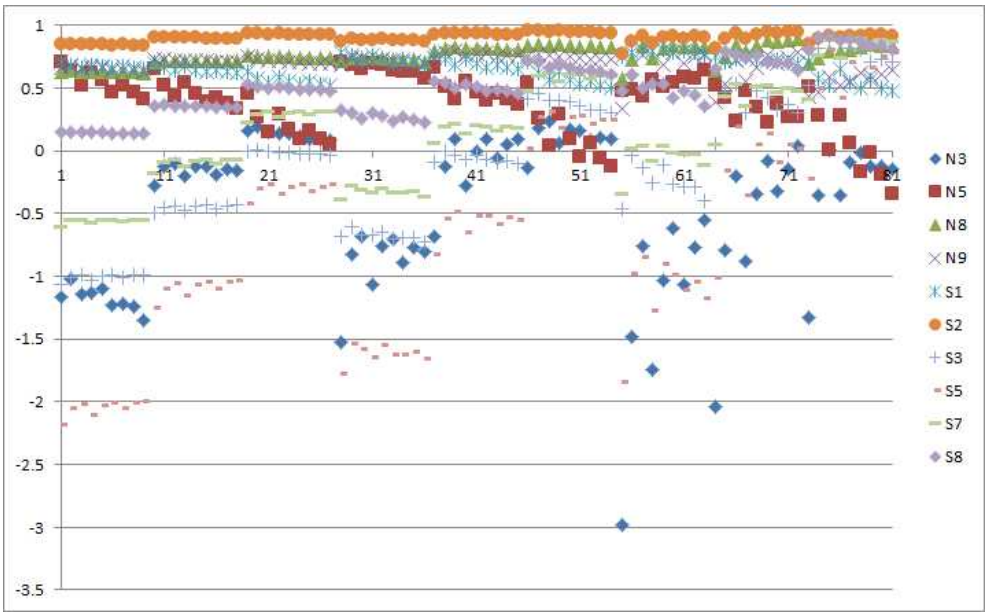

Figure 20 81 combinations of parameters and NSE for Kumchang, Yenam, Mirim, Dokchon, Yeoju, Hangang, Gongju, Waegwan, Samrangjin, Naju station for calibration period

Figure 20 shows all values of NSE based on the possible combinations of parameters. It is investigated that applicability of the parameter set which is represented as NSE value of the stations located in the South Korea is higher than the stations located in North Korea. Especially Kumchang station showed a lowest applicability with the low value of NSE. It is because the historical data of stations in South Korea is obtained in a same period with simulated period unlike

the stations located in North Korea. Table 18 shows 5 parameter sets which have the highest NSE value based on the simulated monthly discharge for 10 stations of the Korean Peninsula.

Table 18 Selected parameter set according to average NSE value

	SD	CD	γ	τ
Set 1	1.0	0.006	1.0	50
Set 2	1.0	0.006	1.0	100
Set 3	2.0	0.003	2.0	200
Set 4	2.0	0.003	4.0	200
Set 5	1.0	0.006	1.0	200

It was presented that top 5 combinations of parameters which have highest value of NSE among the 81 combinations in Table 19. The set 2 in Table 19 has the highest value in average NSE for the representative stations. Therefore, combination of parameters of set 2 is decided as an optimal parameter set for the Korean Peninsula.

Table 19 Order of parameter set according to ranking of respective NSE value of the stations and average NSE value of stations

Station	NSE				
	Set 1	Set 2	Set 3	Set 4	Set 5
N3	-0.1390209	0.1868466	-0.0760563	0.0377594	0.2333258
N5	0.5405963	0.2584994	0.2225441	0.2720746	0.0420492
N8	0.8434685	0.8494597	0.8846761	0.8932102	0.8424649
N9	0.7534607	0.7690814	0.7657216	0.7879039	0.7641413
S1	0.7064974	0.6210934	0.7216428	0.698029	0.5612036
S2	0.9601957	0.9593224	0.9471908	0.9496881	0.9508327
S3	0.4154237	0.4575716	0.4233243	0.3028412	0.4020997
S5	0.0143175	0.2668974	0.1356563	0.0198941	0.3088179
S7	0.473001	0.5987461	0.5199958	0.4737668	0.6193086
S8	0.7214605	0.7058833	0.7111296	0.6414967	0.6668549
average	0.52894	0.56734	0.525583	0.507666	0.53911

2.3. Validation of simulated discharge

A performance of the calibrated model was validated for the validation period based on the tuned parameters through the estimation of river discharge for major rivers in Korean Peninsula. An indicator for the evaluation of applicability of the calibrated model is NSE value which was used in the calibration process. Long-term historical discharge data for the calibration and validation period is obtained only for the stations in South Korea, such as Yeoju, Hangang station in Han River basin, Gongju, Gyuam station in Geum River basin, Waegwan, Jeokpo, Samrangjin station in Nakdong River basin, Naju station in Yeongsan River basin. The value of NSE derived from the river discharge simulation for the 10 years is presented in Table 20 based on the calibrated model. Simulated and observed hydrograph can be found in Figure 21 based on the calculated NSE in Table 20.

Table 20 NSE of calibrated H08 simulation result for calibration and validation period

Watershed	Station	NSE	
		Calibration period (1986-1990)	Validation period (1991-1995)
Han	Yeoju(S1)	0.279	0.643
	Hangang(S2)	0.756	0.732
Geum	Gongju(S3)	0.847	0.37
	Gyuam(S4)	0.852	0.806
Nakdong	Waegwan(S5)	0.702	0.397
	Jeokpo(S6)	0.848	0.777
	Samrangjin(S7)	0.56	0.725
Yeongsan	Naju(S8)	0.262	0.37

Yeoju station in Han River basin showed low applicability based on the selected parameter set for the calibration period, whereas the applicability for validation period is good. It is because a trend of the observed and simulated discharge appears to be different for the earlier period of calibration. Naju station in Yeongsan River basin also has low applicability due to the hydrologic phenomena in 1990 and missing data in 1992. In the year 1990, a trend of the hydrograph of all stations showed similar tendency except for observed data of Naju station. Simulated discharge of Naju in the year 1990 and 1992 has a similar tendency with other stations in Table 20. It is seemed that a regional hydro-meteorological phenomenon is not reflected in this model as shown in the hydrograph of the Figure 21(h).

Figure 22 shows mean monthly discharge of all the simulated and observed period for the stations. Kumchang station in Amnok River basin showed the strongest discrepancy between the observed and

simulated data. Thus the applicability based on NSE value of Kumchang station is evaluated as relatively poor. An applicability of the model for Taedong River basin is evaluated as appropriate based on NSE value over 0.7 for the correspondence of overall tendency of hydrograph despite the discrepancy of summer discharge for Mirim and Dokchon station located in a downstream area of Taedong River basin (Table 20). In case of the stations in South Korea, applicability of the calibrated model is evaluated as high based on the NSE value over 0.5 for the most part of the stations with similar tendency of simulated and observed discharge because of the consensus of the simulated and observed period.

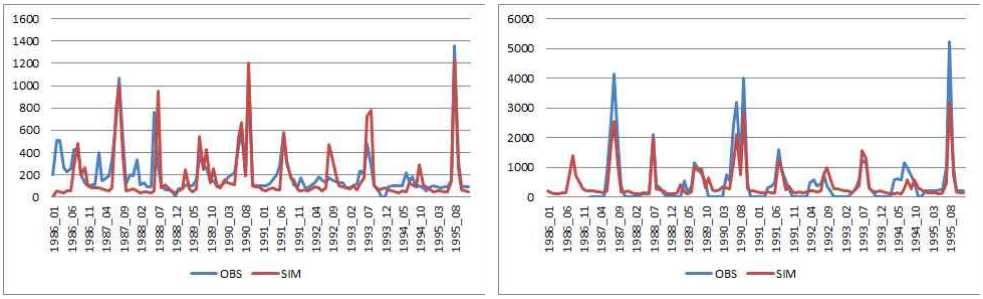

(a)

(b)

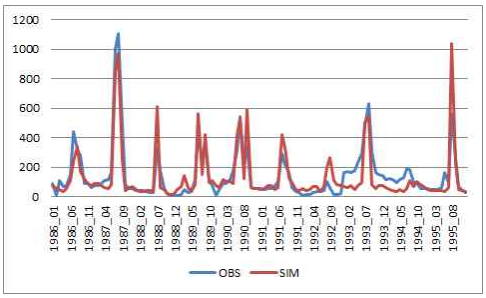

(c)

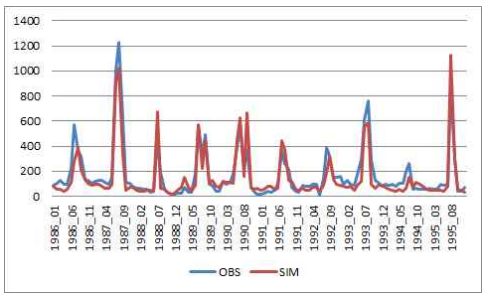

(d)

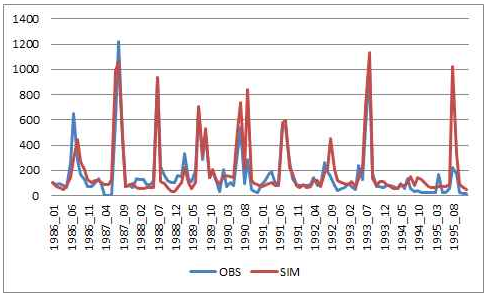

(e)

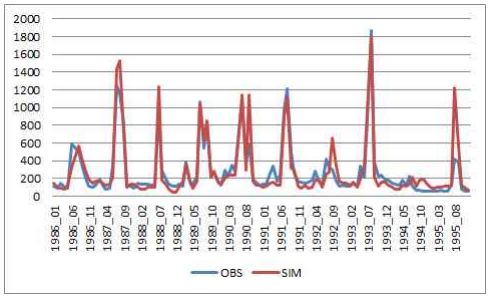

(f)

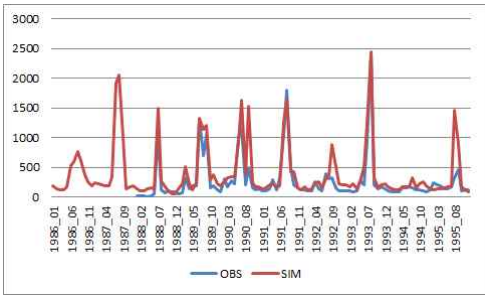

(g)

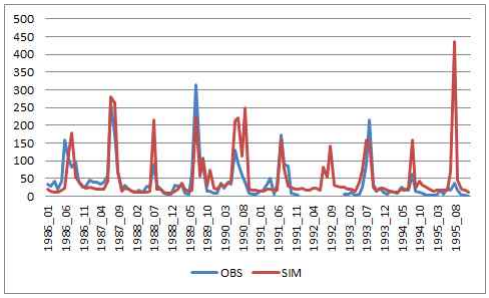

(h)

Figure 21 Observed and simulated discharge[m^3/s] for (a)Yeoju (b)Hangang (c)Gongju (d)Gyuam (e)Waegwan (f)Jeokpo (g)Samrangjin (h)Naju station

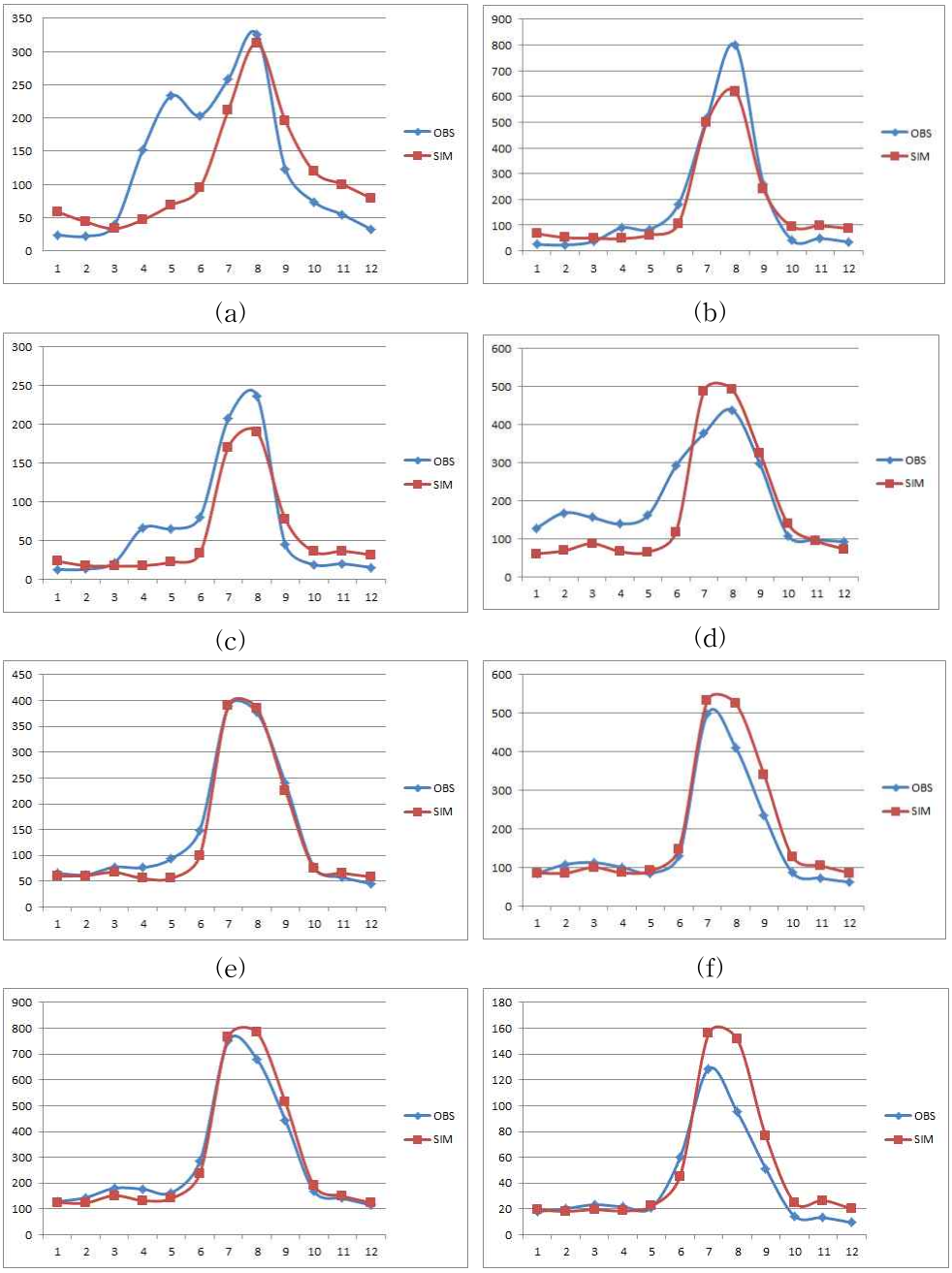

Figure 22 Observed and simulated average monthly discharge[m^3/s] for (a)Kumchang (b)Mirim (c)Dokchon (d)Yeoju (e)Gongju (f)Waegwan (g)Jeokpo (h)Naju station

3. Hydro-meteorological simulation

3.1. Meteorological characteristics and changes

In order to estimate the impact of climate change on water availability in the Korean Peninsula, it is investigated the spatial distribution of expected scenario-based meteorological changes across the Korean Peninsula. Air temperature and precipitation are the most important meteorological elements to assess the impact of climate change on water availability. Thus, it is necessary to investigate the spatio-temporal changes in air temperature and precipitation in advance of estimation of water availability.

3.1.1. Air temperature

Figure 23 shows spatial distribution of air temperature for the baseline period and its expected changes to the future period. Rising temperature with changing climate has investigated in numerous previous studies. The same trend was found in the climate change scenario used in this study. Projected changed ratio from the baseline period to the objective periods (2020s, 2050s and 2080s) is presented in Figure 24 along with its spatial distribution. Air temperature is projected to be increased by 1℃ in 2020s, 3℃ in 2050s, and 5~6℃ in 2080s. The rate of rising temperature in the northern region is larger than the southern region.

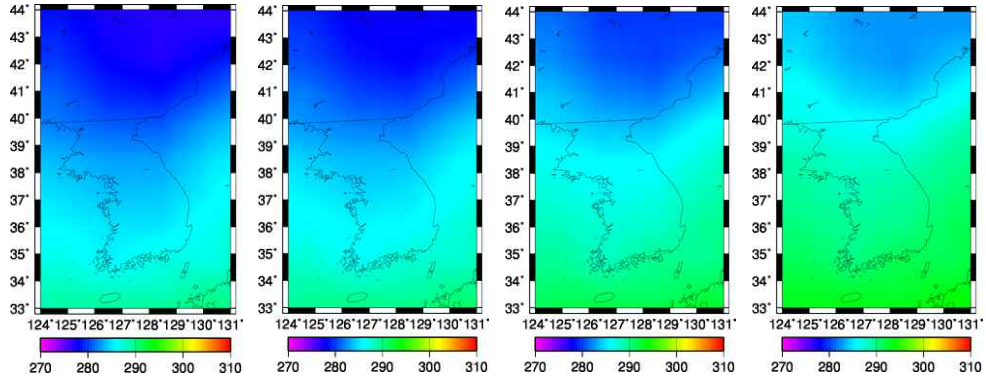

Figure 23 Spatial distribution of mean annual temperature[K] by climate change scenario for (a)baseline period, (b)2020s, (c)2050s, (d)2080s

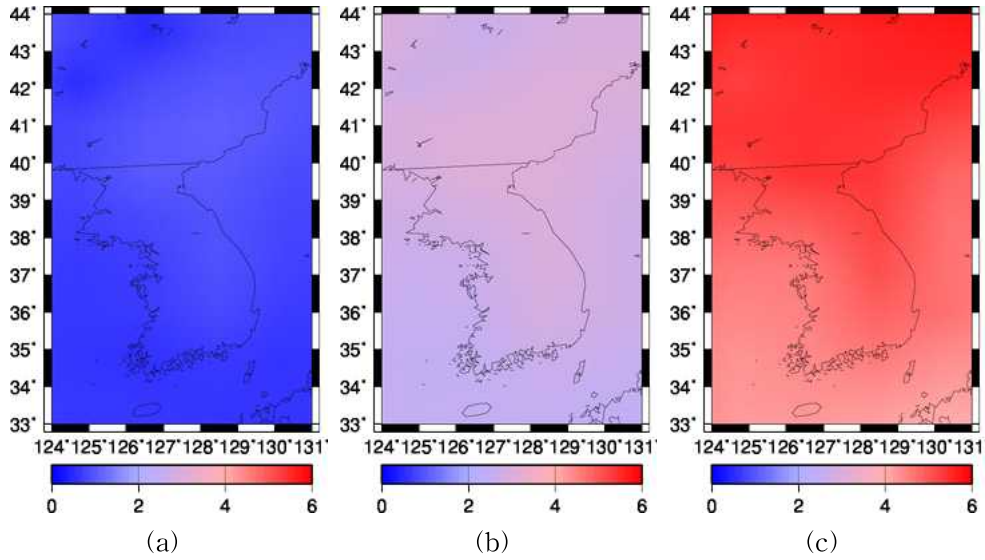

Figure 24 Spatial pattern of change of mean annual temperature[K] from the baseline period to (a)2020s, (b)2050s, (c)2080s

Air temperature of the reference and objective period is presented in Table 21 for the major gauging stations. There is slightly large

increase in temperature of some stations, such as Amnok, Duman, Chongchon in northern area which is located in the region under the impact of the continental climate compared with southern area as shown in Figure 24 (c). Mean annual temperature of baseline period was 11.127℃ across the Korean Peninsula. It is projected that the temperature will increase to 11.92℃ in 2020s, 13.92℃ in 2050s, and 16℃ in 2080s. Mean monthly air temperature of the stations for the baseline and objective periods is presented in Figure 25.

Table 21 Projected changes in average annual temperature [℃] in the Korean Peninsula

Watershed	Station	Period			
		Baseline	2020s	2050s	2080s
Amnok	Supung	9.663442	10.53238	12.63576	14.94317
Duman	Khasan	6.467678	7.442479	9.485969	11.98383
Chongchon	Puksongri	10.2459	11.12511	13.17418	15.40647
Taedong	Seohaegabmun	11.17551	11.96752	13.96217	16.11439
Han	Hangang	11.57132	12.35659	14.30385	16.29932
Geum	Gyuam	12.48789	13.21069	15.12924	17.07188
Nakdong	Samrangjin	14.26202	14.99234	17.00286	18.92391
Yeongsan	Naju	13.14125	13.76179	15.67227	17.60266
Average		11.12688	11.92361	13.92079	16.0432

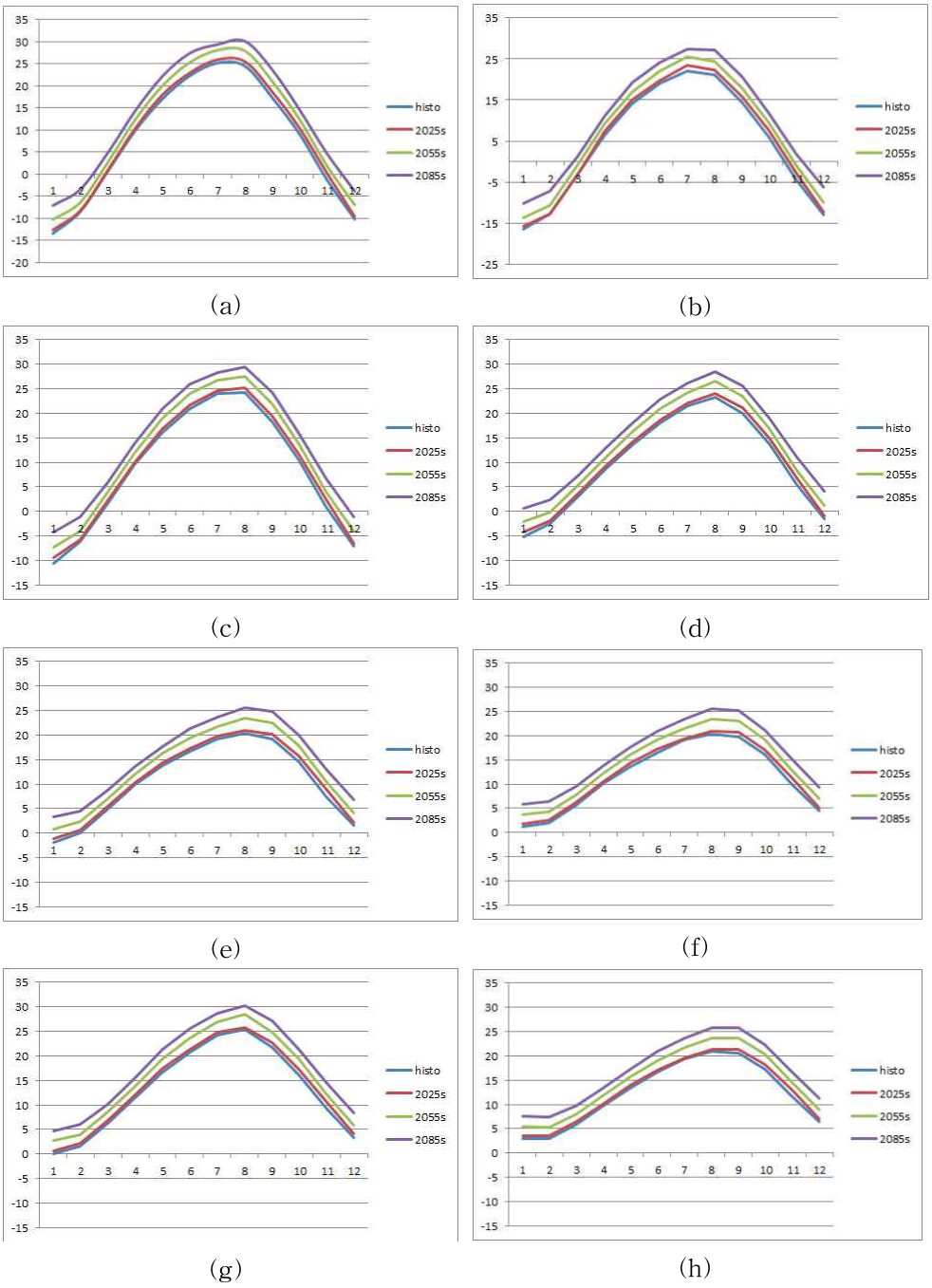

Figure 25 Monthly average temperature[℃] of baseline and future period by climate change scenario for (a)Supung, (b)Khasan, (c)Puksongri, (d)Seohaegabmun, (e)Hangang, (f)Gyuam, (g)Samrangjin, (h)Naju station

3.1.2. Precipitation

Precipitation is projected to be increased in the future as shown in Figure 26 and 27. In case of precipitation, increased ratio is calculated from the baseline period to the objective periods. Changed ratio of precipitation is different depending on the region. The tendency of larger increase in precipitation is presented in the middle and northwestern region of the peninsula and Nakdong River basin in the southeast area. The precipitation of these regions is gradually increased to 2020s, 2050s, and 2080s. Relatively small increases in precipitation is projected for the regions of south coast in South Korea and northeastern region which downstream of Duman river basin is located in North Korea. The difference of changed ratio in precipitation is projected to increase gradually for the objective periods.

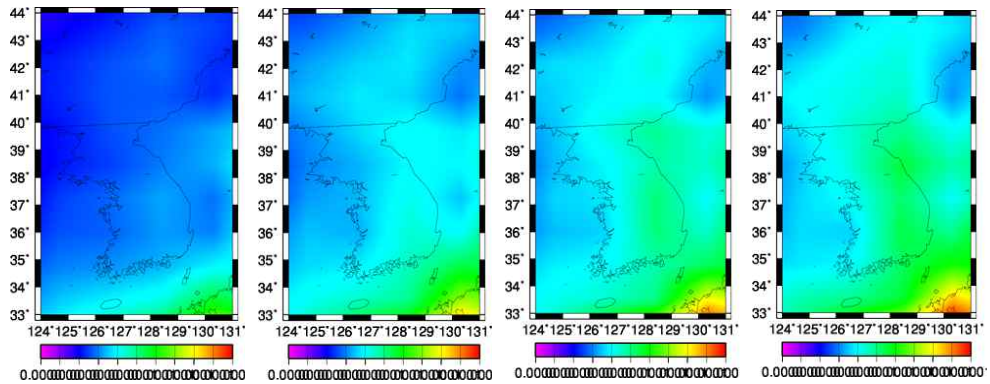

Figure 26 Spatial distribution of annual precipitation[mm/s] by climate change scenario for (a)baseline period, (b)2020s, (c)2050s, (d)2080s

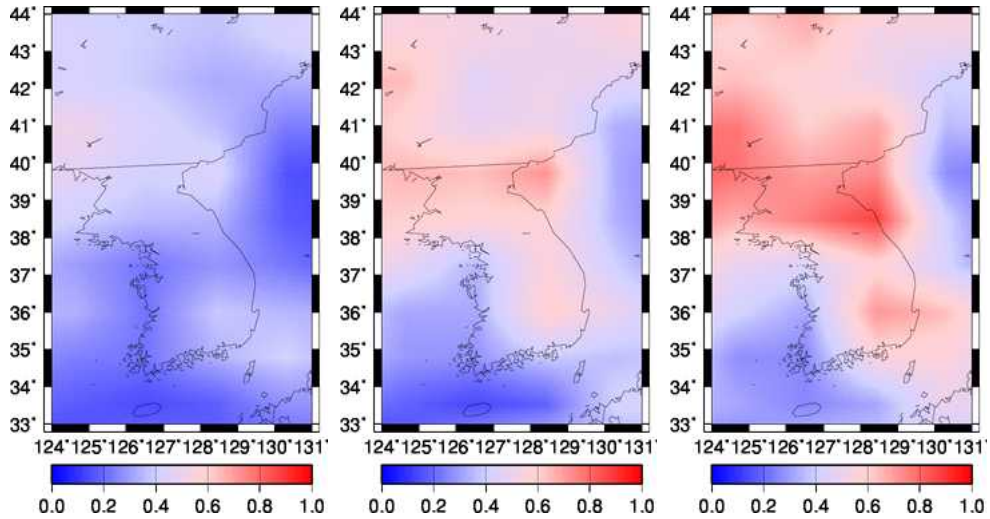

(a) (b) (c)

Figure 27 Spatial pattern of changed ratio of annual precipitation from the baseline period to (a)2020s, (b)2050s, (c)2080s

Precipitation of the major stations for the baseline and objective periods is presented in Table 22. The precipitation in 2020s is projected to be decreased at the stations in downstream of Duman, Chongchon, Taedong, Geum, and Han River basin. Average precipitation in the Korean Peninsula in 2020s is projected to be decreased from 1126.876 mm in baseline to 1124.744 mm. In some regions, the highest precipitation is projected in the 2050s amongst all the objective periods at the stations in Han, Geum, Nakdong, Yeongsan River basin. However, precipitation is projected to be increased in most regions as shown in Figure 28 based on the general trend in the late 21th century gradually after 2050s. Precipitation is projected to be increased to 15.78% as the average increased rate across the whole study area (Table 22). According to the report of

National Institute of Meteorological Research (NIMR), precipitation of Korea is going to be increased to 20.4% by the end of 21th century based on the RCP 8.5 scenario in spite of regional differences (NIMR, 2011). As shown in Table 22, increased ratio of the stations in North Korea is bigger than the stations in South Korea. When considering the uncertainties in GCMs, average projected increased ratio of precipitation using multiple GCM is 6.1% for the Korean Peninsula, and 18% for the North Korea (Shin and Jung, 2015).

Table 22 Projected changes in annual precipitation [mm/yr] in the Korean Peninsula

Watershed	Station	Period			
		Baseline	2020s	2050s	2080s
Amnok	Supung	1068.456	1074.358	1153.34	1267.566
Duman	Khasan	1063.463	1041.608	1128.536	1103.78
Chongchon	Puksongri	1056.035	1033.257	1184.475	1256.932
Taedong	Seohaegabmun	1011.831	991.6913	1142.399	1215.514
Han	Hangang	1209.04	1115.15	1264.637	1358.807
Geum	Gyuam	1126.187	1113.919	1229.364	1258.923
Nakdong	Samrangjin	1314.133	1433.001	1537.259	1702.797
Yeongsan	Naju	1165.865	1194.965	1265.829	1273.505
Average		1126.876	1124.744	1238.23	1304.728

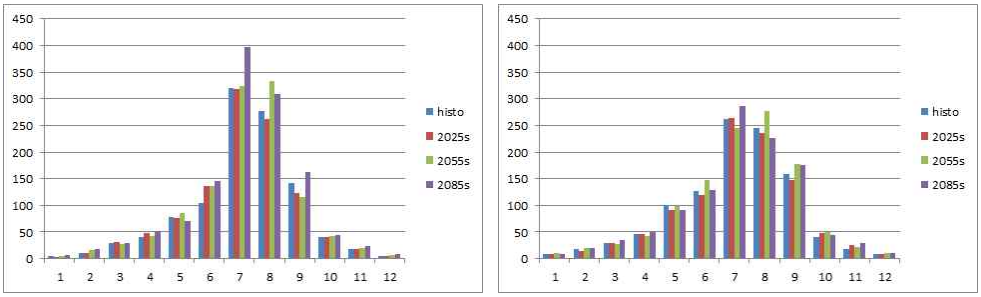

(a)

(b)

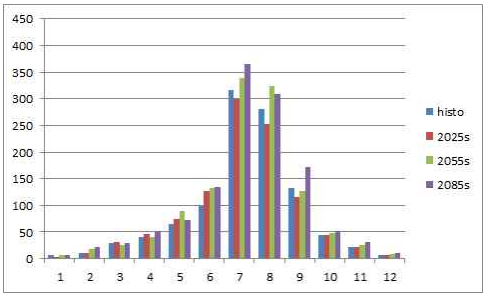

(c)

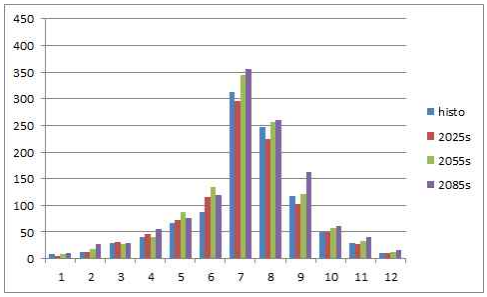

(d)

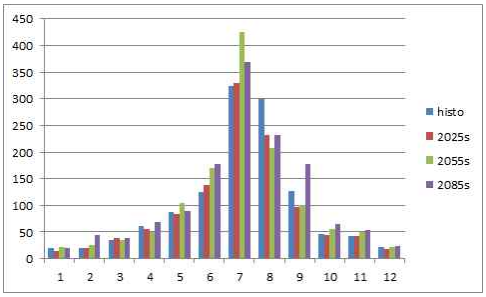

(e)

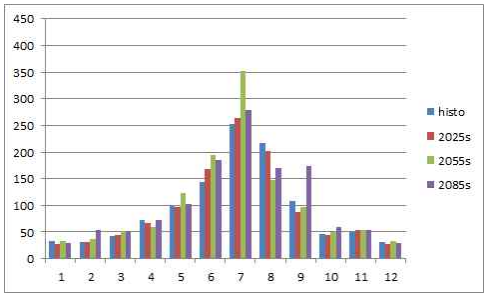

(f)

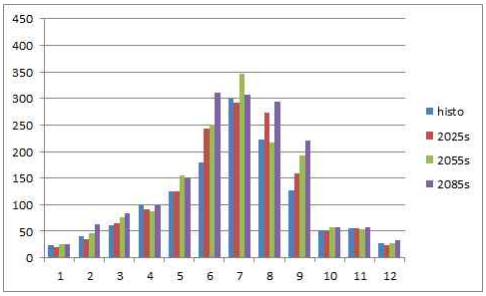

(g)

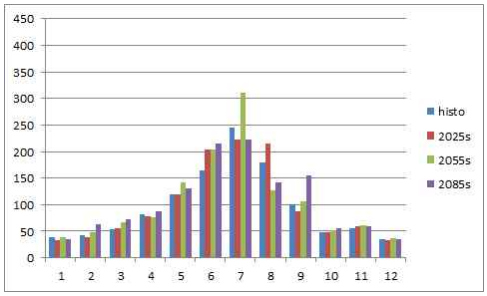

(h)

Figure 28 Monthly precipitation[mm] of baseline and future period by climate change scenario for (a)Supung, (b)Khasan, (c)Puksongri, (d)Seohaegabmun, (e)Hangang, (f)Gyuam, (g)Samrangjin, (h)Naju station

3.2. Hydrological characteristics and changes

In order to estimate the impact of scenario of climate change on water availability in the Korean Peninsula, it is necessary to investigate the regional variability of hydrological elements affected by air temperature and precipitation. H08 can simulate water balance as well as energy balance. However, this study considered only hydrological attributes because it directly affects to the concept of water availability defined above. The hydrological elements simulated in H08 are potential evapotranspiration, actual evapotranspiration, surface runoff, subsurface runoff, and total runoff. These attributes contributes to assess the water availability based on river discharge. Water availability is affected by spatio-temporal variability of hydrological attributes, and it is required to investigate its spatial distribution, as well as climatic variables across varying time series.

In order to investigate hydrological characteristics of the major river basins, historical simulation was carried out for the baseline period on the preferential basis. Simulated hydrological elements are evapotranspiration, subsurface, surface and total runoff, as well as precipitation on a monthly basis (Figure 29). The changes in hydrological attributes as described in Figure 29 are presented in Table 23 for the objective periods.

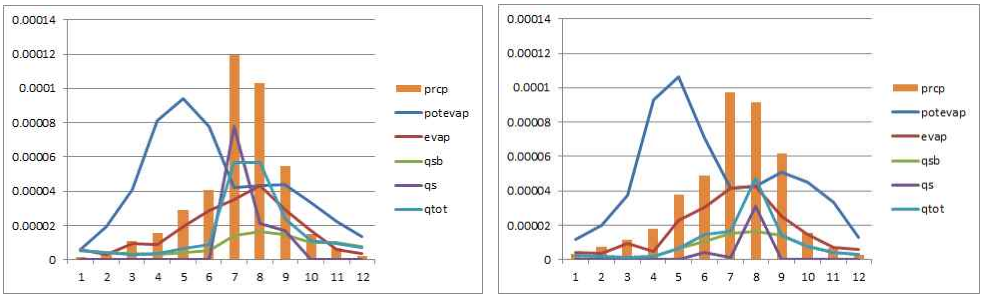

(a) Supung (b) Khasan

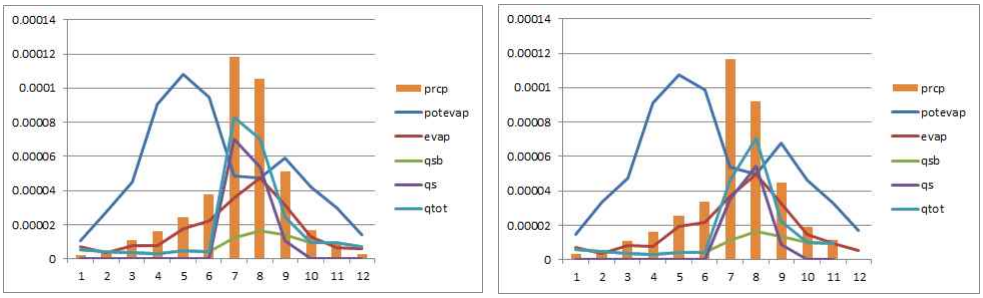

(c) Puksongri (d) Seohaegabmun

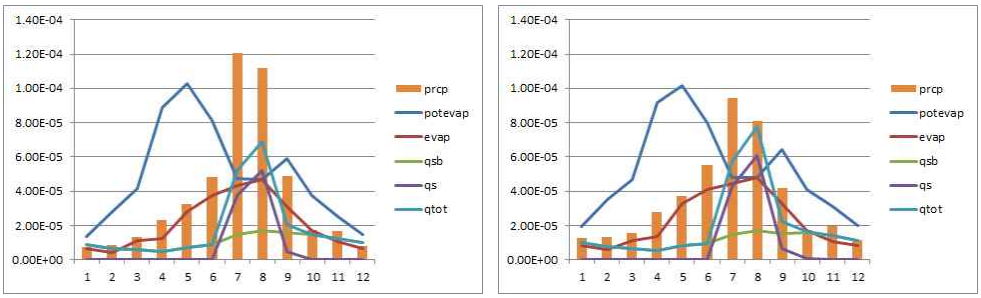

(e) Hangang (f) Gyuam

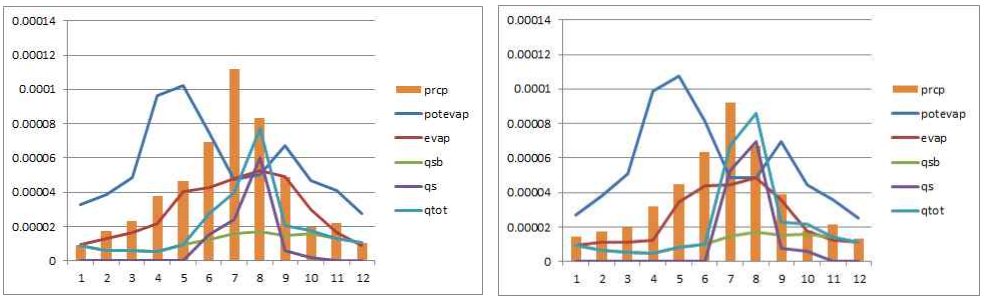

(g) Samrangjin (h) Naju

Figure 29 Monthly average hydrological elements in historical period for major stations (prcp : precipitation, potevap : potential evapotranspiration, evap : evapotranspiration, qsb : subsurface runoff, qs : surface runoff, qtot : total runoff [mm/s])

Table 23 Projected hydrological changes for the baseline and future period

Watershed	Station	Period	Hydrological variables[12]			
			PotEvap	Evap	Qtot	SoilMois
Amnok	Supung	baseline	1358.8	554.5	569.4	828.5
		2020s	1292.8	649.6	600.9	941.1
		2050s	1393.3	639.04	566.9	735.9
		2080s	1506.2	696.5	952.3	738.8
Duman	Khasan	baseline	1490.7	558.7	323.4	753.5
		2020s	1329.3	642.6	344.06	856.6
		2050s	1419.9	636.9	304.3	635.9
		2080s	1560.9	656.4	238.4	629.2
Chongchon	Puksongri	baseline	1623.4	543.3	606.9	790.2
		2020s	1418.5	663.06	577.3	840.3
		2050s	1508.7	654.7	627.9	660.8
		2080s	1610.6	703.3	645.8	653.7
Taedong	Seohaegabmun	baseline	1734.4	571.8	510.8	806.7
		2020s	1512.8	684.5	484.3	840.6
		2050s	1594.1	703.5	514.1	685.05
		2080s	1706.4	756.4	531.3	692.4
Han	Hangang	baseline	1540.1	672.8	585.2	1060.8
		2020s	1353.9	764.2	498.6	980.2
		2050s	1432.3	807.2	526.4	873.3
		2080s	1509.7	896.6	533.9	939.3
Geum	Gyuam	baseline	1647	720.7	650.1	1126.7
		2020s	1428.5	834.06	606.8	1002.5
		2050s	1505.7	882.3	602.5	895.3
		2080s	1589.9	945.9	575.2	917.6
Nakdong	Samrangjin	baseline	1770.1	770.8	639.04	1122.02
		2020s	1535.4	918.5	749.9	1030.7
		2050s	1639.06	965.6	692.7	933.5
		2080s	1723.7	1036.8	842.4	911.1
Yeongsan	Naju	baseline	1772.6	771.2	708.2	1091.2
		2020s	1526.6	909.4	709.1	1000.4
		2050s	1598.2	949.8	614.4	894.1
		2080s	1691.3	1012.5	555.9	910.5

12) PotEvap : potentail evapotranspiration[mm/yr], Evap : evapotranspiration[mm/yr], Qtot : total runoff[mm/yr], SoilMois : soil moisture[mm]

3.2.1. Evapotranspiration

Amount of evapotranspiration is affected by various reasons, such as differences in elevation, amounts of surface water to evaporate, air temperature, wind, and solar radiance (Masood et al., 2015). Potential evapotranspiration is affected by bulk transfer coefficient, wind speed, and a difference between specific humidity and saturated specific humidity based on [Eq. 2].

Bulk transfer coefficient C_D was calibrated because it is a principal parameter that affects runoff hydrograph. Wind speed is low in coastal areas in South Korea and plateau area in North Korea as shown in Figure 9. This can be the reason of spatial distribution of wind speed value in Figure 30. Potential evapotranspiration in 2020s is projected to be decreased compared with baseline period and gradually increased to 2080s. The potential evapotranspiration is going to be increased in 2080s while the amount of 2020s and 2050s is smaller than the baseline period. The increased amount of potential evapotranspiration in northern plateau region is larger than other areas.

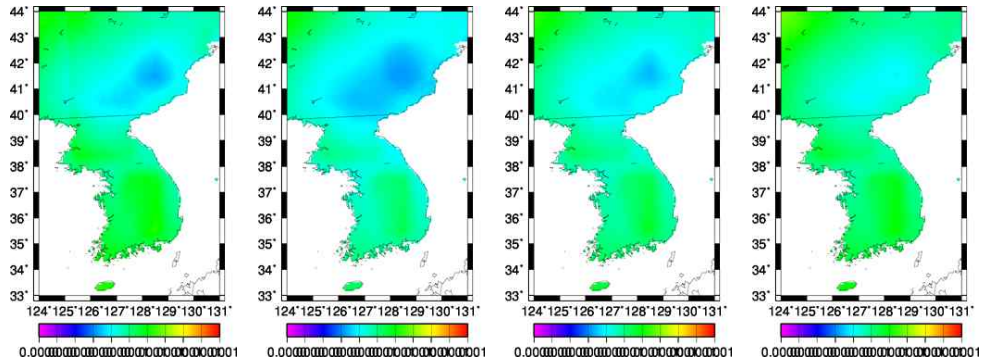

Figure 30 Spatial distribution of potential evapotranspiration[mm/s] by climate change scenario for (a)baseline period, (b)2020s, (c)2050s, (d)2080s

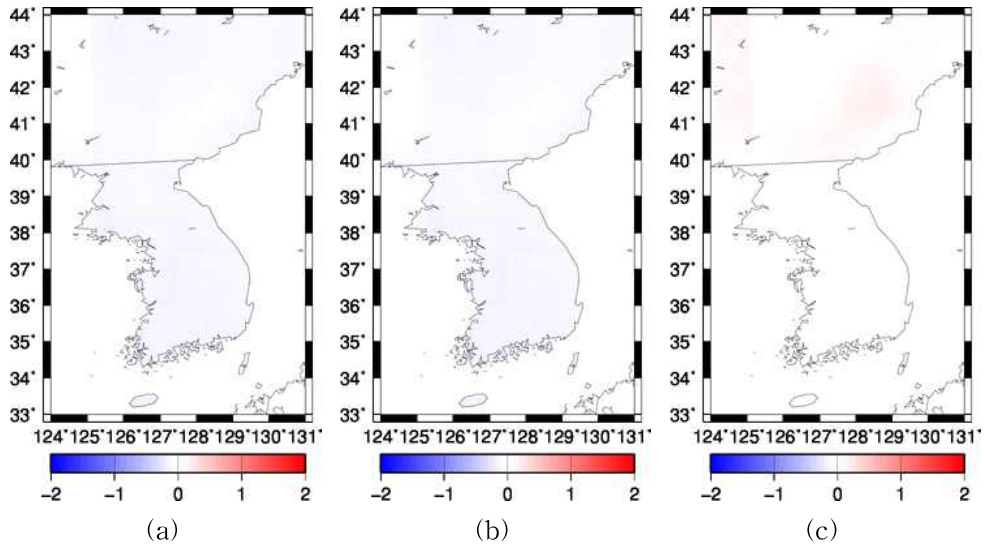

Figure 31 Spatial pattern of changed ratio(%) of potential evapotranspiration from the baseline period to (a)2020s, (b)2050s, (c)2080s

Actual evapotranspiration can be estimated by [Eq. 3] and [Eq. 4] by multiplying a function of soil moisture to potential evapotranspiration. It is projected to be continuously increased for all the objective periods. The amount of evapotranspiration increases as precipitation

increases because soil become saturated with increasing rainfall according to [Eq. 3]. Potential evapotranspiration is same with actual evapotranspiration when the soil moisture is larger than 75% of field capacity based on [Eq. 4].

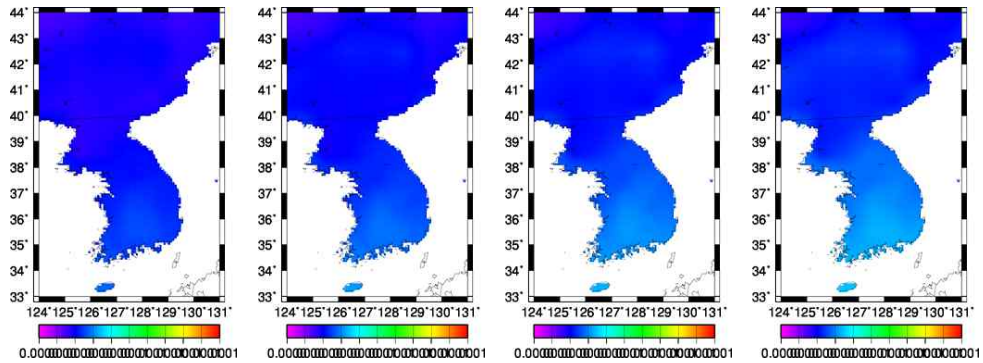

(a) (b) (c) (d)

Figure 32 Spatial distribution of evapotranspiration[mm/s] by climate change scenario for (a)baseline period, (b)2020s, (c)2050s, (d)2080s

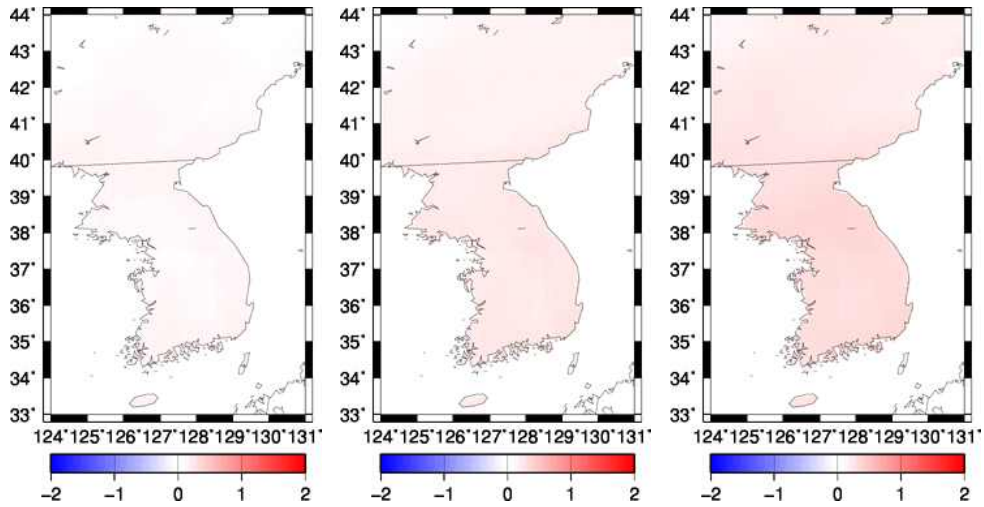

(a) (b) (c)

Figure 33 Spatial pattern of changed ratio(%) of evapotranspiration from the baseline period to (a)2020s, (b)2050s, (c)2080s

3.2.2. Runoff

Total runoff can be divided into surface runoff and subsurface runoff based on water balance equation [Eq. 6] in H08. Surface runoff occurs if the soil moisture exceed the field capacity, and does not occur if the soil moisture is smaller than the field capacity. Subsurface runoff is generated in proportion to the ratio between soil moisture and field capacity and is affected by the parameter τ and γ according to [Eq. 7] which was calibrated.

Subsurface runoff is a function of field capacity and soil moisture which tends to be maintained at a constant value throughout the year without significant change as shown in Figure 29. It is less sensitive to precipitation change than the surface runoff, as well as its spatial pattern of its distribution (Figure 34). Subsurface runoff is decreased in the period of 2020s compared with baseline period and projected to be slightly increased by 2080s (Figure 35).

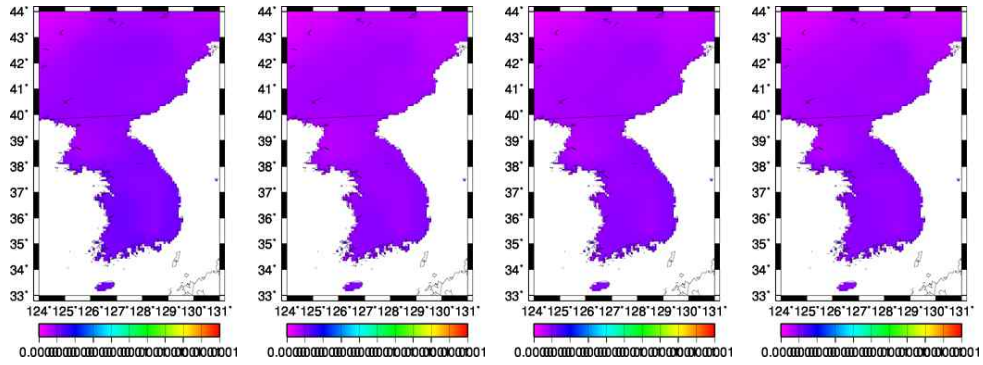

Figure 34 Spatial distribution of subsurface runoff[mm/s] by climate change scenario for (a)baseline period, (b)2020s, (c)2050s, (d)2080s

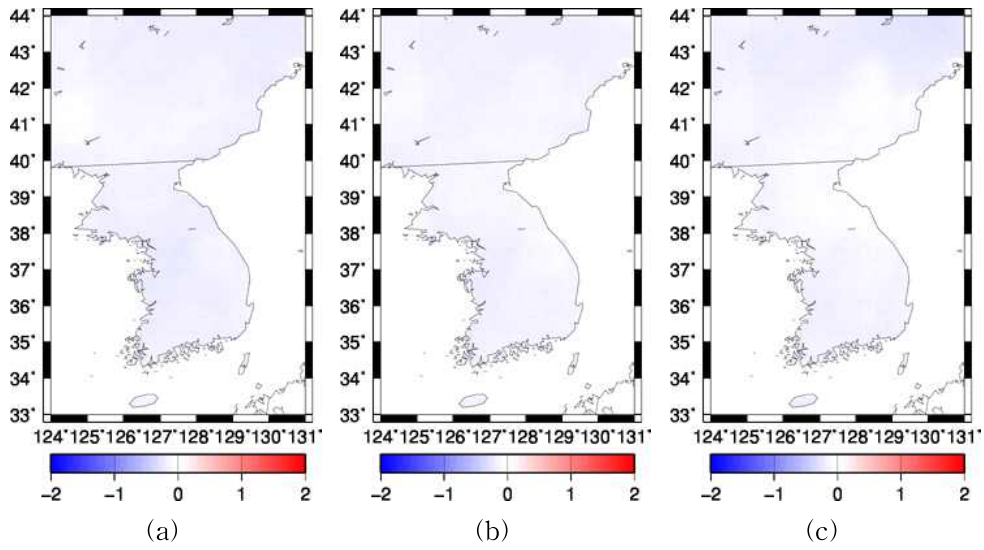

Figure 35 Spatial pattern of changed ratio(%) of subsurface runoff from the baseline period to (a)2020s, (b)2050s, (c)2080s

Surface runoff is generated due to the increase in soil moisture which is sensitive to changes in precipitation. Spatial pattern of surface runoff is presented in Figure 36. When it comes to changes in

precipitation based on climate scenario, spatial changes of surface runoff and precipitation is appeared similar. Surface runoff is decreased in 2020s in most parts of the country except for southern area, especially where the Nakdong River basin is located. Surface runoff is projected to be increased gradually by the 2080s in most parts of the Korean Peninsula. As shown in Figure 37, Nakdong River basin showed a significant increase in surface runoff compared with other areas. On the other hand, it is projected to be decreased compared with baseline period in northeast area where the Duman River basin located. The spatial pattern of changes in surface runoff is similar with the pattern of changes in precipitation.

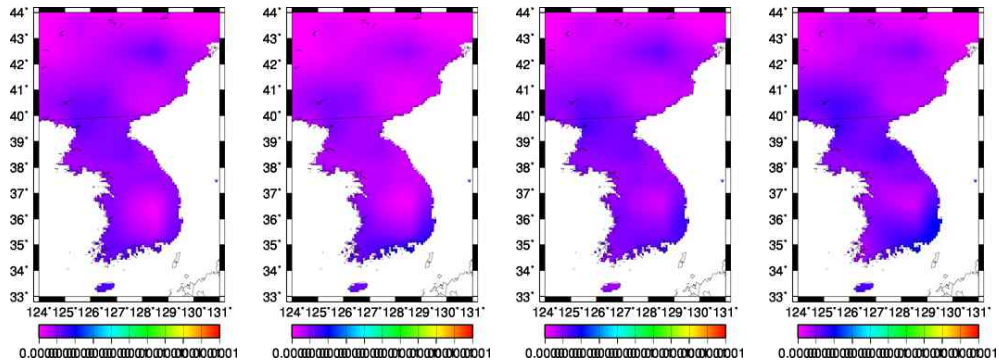

Figure 36 Spatial distribution of surface runoff[mm/s] by climate change scenario for (a)baseline period, (b)2020s, (c)2050s, (d)2080s

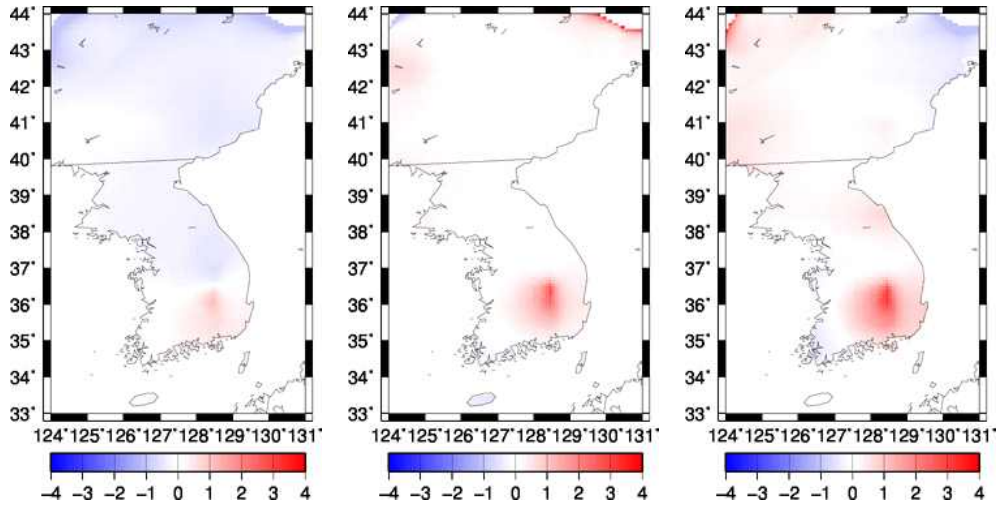

Figure 37 Spatial pattern of changed ratio of surface runoff from the baseline period to (a)2020s, (b)2050s, (c)2080s

Total runoff is sum of surface and subsurface runoff. However, sensitivity of runoff hydrograph to subsurface and surface runoff is different from each other according to Figure 29. Figure 38 shows spatial distribution of total runoff for the baseline and objective periods. Changed ratio from the baseline period to objective periods is presented in Figure 39. An overall tendency of spatial distribution and changed ratio of total runoff is similar to the trends of variability of changes in precipitation.

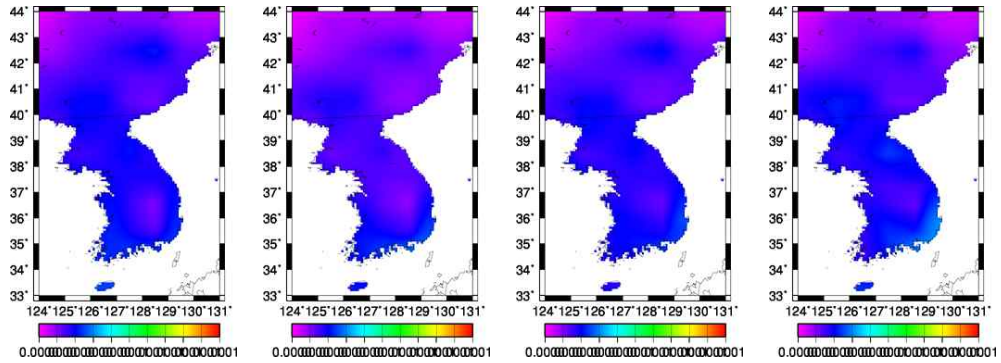

(a) (b) (c) (d)

Figure 38 Spatial distribution of total runoff[mm/s] by climate change scenario for (a)baseline period, (b)2020s, (c)2050s, (d)2080s

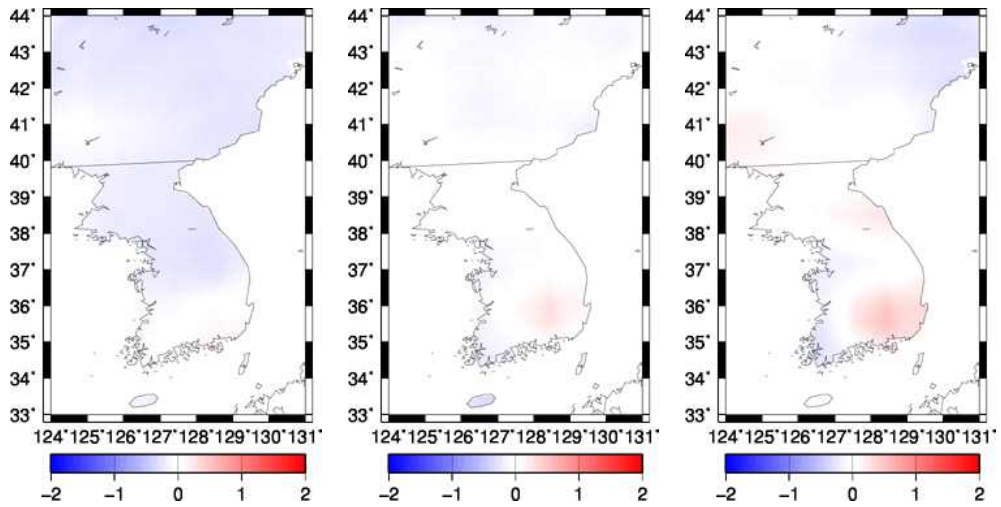

(a) (b) (c)

Figure 39 Spatial pattern of changed ratio of total runoff from the baseline period to (a)2020s, (b)2050s, (c)2080s

Figure 40 presents spatio-temporal variability of hydrological elements of the stations in major river basins in the Korean Peninsula for the baseline and objective periods based on Table 23. Potential

evapotranspiration of all stations is projected to be decreased in 2020s, and then gradually increased by the 2080s. Evapotranspiration is projected to be continuously increased by the 2080s in most parts of the region. The tendency of variations in total runoff is different from region to region. The amount of total runoff of each stations not equal to the river discharge. Simulated amount of runoff can represent one component of water balance of the region. Runoff is projected to be continuously decreased in Khasan, Gyuam, Naju station, and increased in Supung, Puksongri, Samrangjin station. Amount of the elements of water balance is related with the tendency of rainfall pattern, especially evapotranspiration and runoff which is directly affected by the amount of available water on surfaces. Thus, runoff, soil moisture, and evapotranspiration is large at the stations located in southern Korea, such as Hangang in Han River basin, Gyuam in Geum River basin, Samrangjin in Nakdong River basin, and Naju station in Yeongsan River basin.

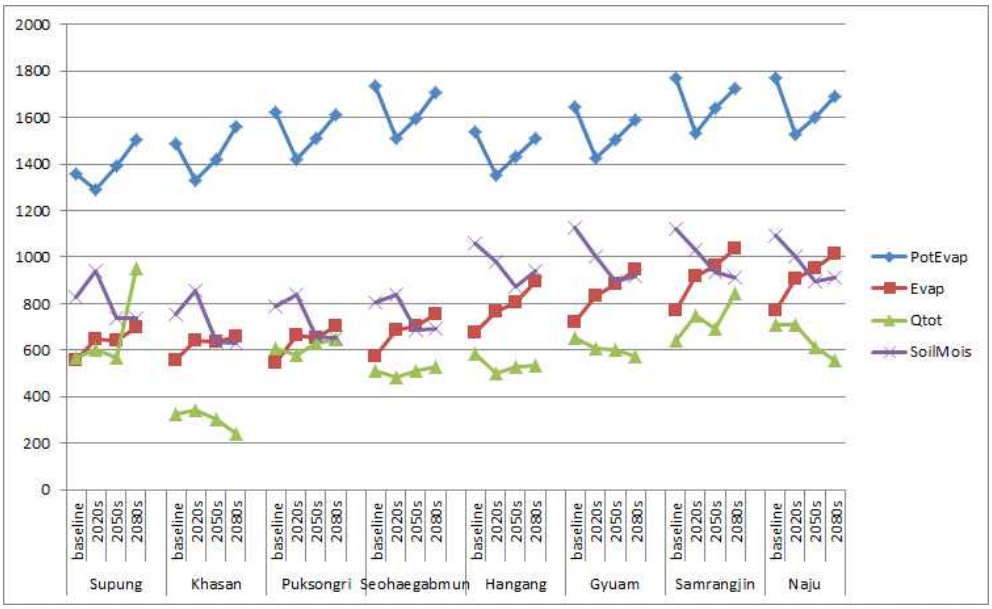

Figure 40 Comparison of simulated potential evapotranspiration[mm/yr], evapotranspiration[mm/yr], total runoff[mm/yr], soil moisture[mm]

3.3. Estimation of water availability

In this study, water availability is defined as a river discharge. River discharge of one grid is affected by various components from the meteorological variables to hydrological attributes investigated above. Water availability for major river basins is estimated based on changes in climate and hydrology. In order to estimate spatio-temporal variability in water availability, river discharge is projected and spatially presented for baseline and objective periods of Amnok, Duman, Chongchon, Taedong River in North Korea and Han, Nakdong, Geum, Yeongsan River in South Korea.

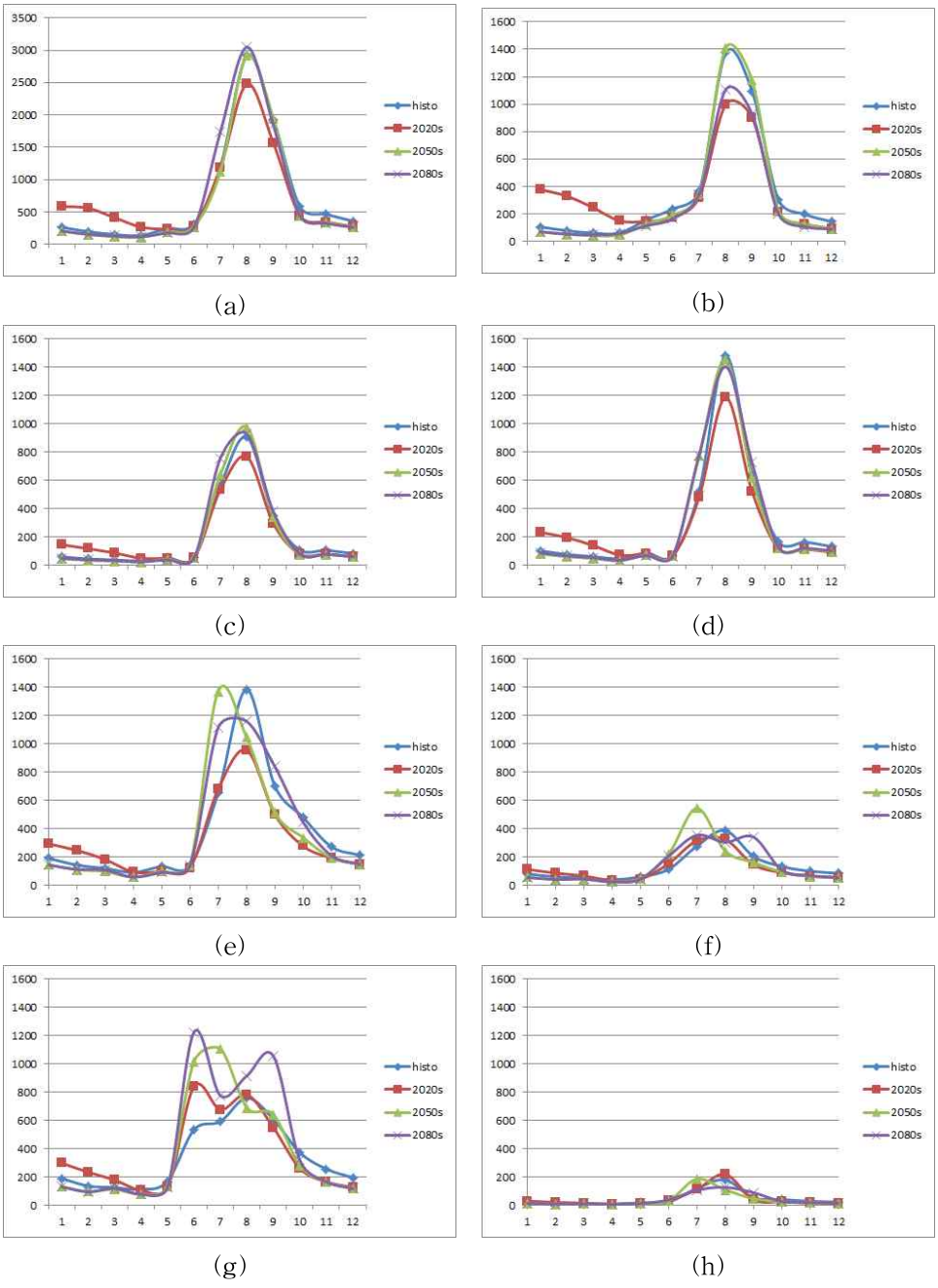

Figure 41 Monthly discharge[m^3/s] of baseline and future period by climate change scenario for (a)Supung, (b)Khasan, (c)Puksongri, (d)Seohaegabmun, (e)Hangang, (f)Gyuam, (g)Samrangjin, (h)Naju station

Simulated monthly river discharge is presented in Figure 41 for the principal 8 river basins. The majority of the stations are located in downstream region of the rivers. Amnok River basin where the Supung station located is the biggest river basin in the Korean Peninsula. This is the reason why a range of the value of y-axis of Supung station is different from other stations Figure 41 (a). In case of the basins in North Korea, month of peak discharge is same across all the objective periods. Mostly, discharge in 2020s is the lowest amongst all the periods, and tends to have a similar tendency of monthly discharge in the 2050s and 2080s. In case of the basins in South Korea, monthly variation in discharge is different from each objective period. River discharge of 2020s is decreased in Han River and Geum River, and increased in Nakdong River and Yeongsan River. In 2050s, month of peak discharge of all the basins changed to an earlier month. River discharge in 2080s of the stations in South Korea decreased for most stations and month of peak discharge is also changed in Han, Geum, Yeongsan River to the months similar with simulated results in the baseline and 2020s except for Samrangjin in Nakdong River basin. In case of Samrangjin station, total amount of discharge is projected to be increased with the course of time in climate scenario. However, monthly variation in discharge became intense as shown in Figure 41 (g).

Table 24 Projected mean annual discharge [m^3/s] in the Korean Peninsula

Watershed	Station	Period			
		Baseline	2020s	2050s	2080s
Amnok	Supung	728.508	719.1678	670.3311	724.4784
Duman	Khasan	369.451	335.8808	346.8199	290.9473
Chongchon	Puksongri	199.722	192.6889	199.6968	209.8714
Taedong	Seohaegabmun	295.8921	274.5976	294.7237	302.822
Han	Hangang	377.1458	316.1815	355.4432	381.3324
Geum	Gyuam	132.8693	124.2232	133.0489	137.3105
Nakdong	Samrangjin	338.3875	362.3996	381.9661	427.396
Yeongsan	Naju	45.78367	46.25489	41.15759	39.96073

Table 24 describes total annual amount of river discharge for the baseline and objective periods as shown in Figure 42. Discharge of Supung station in Amnok River basin is projected to be decreased in 2050s, and then increased by 2080s. Discharge of Khasan station in Duman River basin is projected to be decreased continuously for all the objective periods by the 2080s. Discharge of Puksongri station in Chongchon River basin is projected to be decreased in 2020s, and then increased by the end of 21th century. Mean annual discharge of Seohaegabmun of Taedong River basin in 2020s is decreased and gradually increased by the 2080s similar with the tendency of changes in discharge of Chongchon River basin. Variability of discharge of Hangang station has also similar tendency with Chongchon River basin and Taedong River basin which shows decreased discharge in 2020s and increased discharge in 2050s and 2080s, as well as Gyuam station in Geum River basin. Only discharge of Samrangjin station in Nakdong River basin is continuously increased from the baseline to 2080s. Naju station in Yeongsan river basin shows increased discharge

in 2020s, and then continuously decreased by the 2080s.

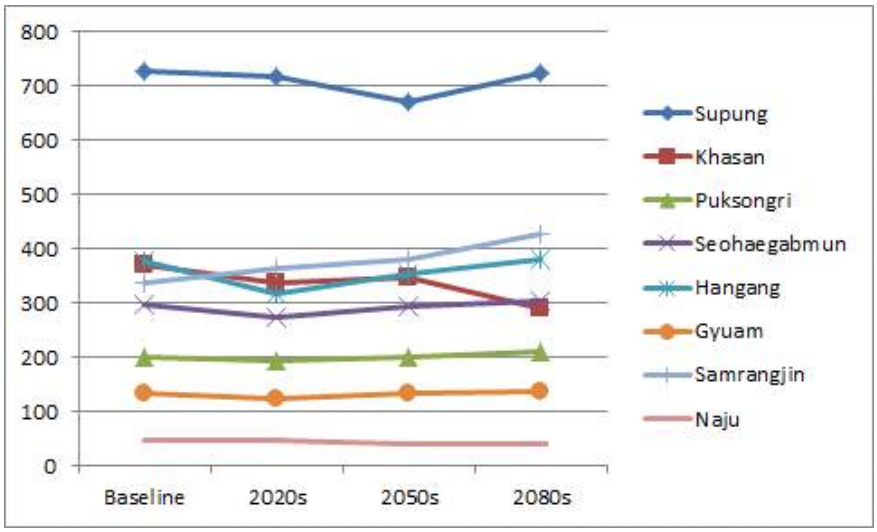

Figure 42 Mean annual discharge [m^3/s] of the stations

Simulated discharge for major river basins is regarded as water availability. When it comes to considering temporal variability of water availability, investigation of its seasonal variation is also required because rainfall is seasonally biased and concentrated in summer, especially in the Korean Peninsula. Mean seasonal discharge in spring and winter is projected to be increased in 2020s, while the discharge in summer and autumn is decreased at the same period (Figure 43). In 2050, discharge in spring and winter is going to be decreased below the amount of baseline, and then discharge in summer and autumn is increased. There is regional bias on the river discharge in 2080s. Summer discharge of Amnok, Han, Geum, and Nakdong River is projected to be increased, and autumn discharge of Taedong, Han,

Geum, and Nakdong River is going to be increased. In case of spring and winter discharge, temporal variation from baseline to 2080s is simulated to have a low variability except for 2020s. On the other hand, summer and autumn discharge have different spatial variability depending on a regional characteristics.

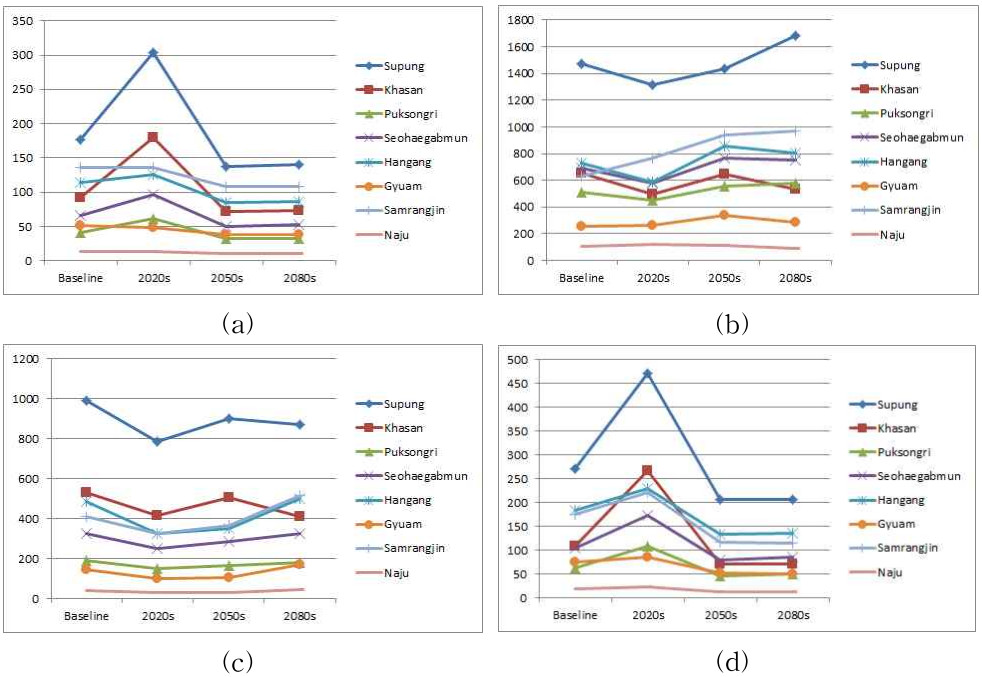

FIgure 43 Mean seasonal discharge[m^3/s] of the stations for (a)spring(MAM), (b)summer(JJA), (c)autumn(SON), (d)winter(JJA)

Spatial distribution and variations of the simulated river discharge is presented in Figure 44. Spatial variability of water availability based on river discharge also can be represented spatially from baseline to the objective periods. Water availability defined as river discharge of a

grid is affected by hydrological attributes, such as runoff and evapotranspiration which was investigated above. Water availability of white colored region is same with baseline period. Blue colored region and Red colored region has decrease and increase in water availability, respectively. Spatial variation of water availability tends to be similar with spatial distribution of total runoff and precipitation. Because river discharge is accumulated runoff from upper grid based on flow direction.

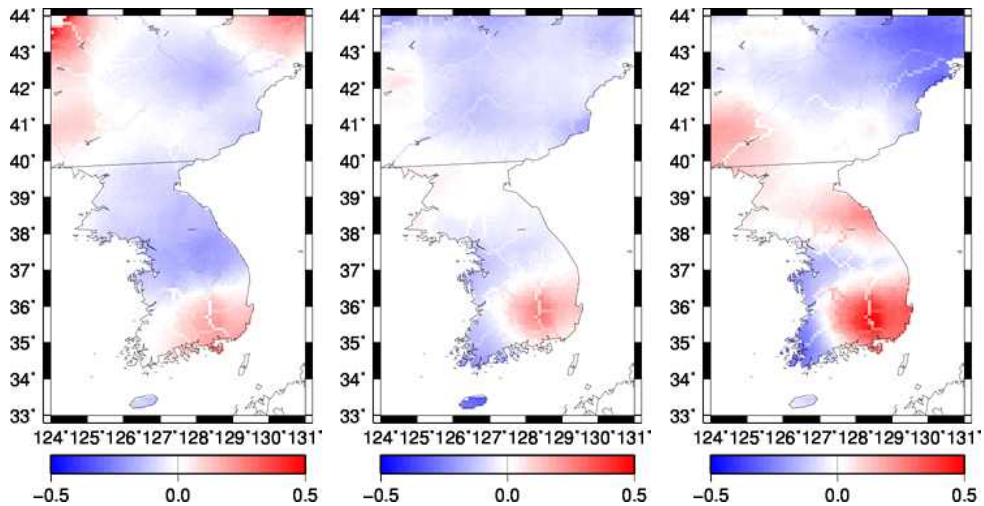

(a) (b) (c)

Figure 44 Spatial pattern of changed ratio(%) of water availability from the baseline period to (a)2020s, (b)2050s, (c)2080s

4. Implication for spatial planning

Water resources and its availability of region are being considered as an essential component to establish a spatial plan such as land use planning in consideration of its spatio-temporal variability. This study applied grid-based hydrological model to estimate a water availability by calculating water balance and river discharge under changing climate in the future. Input data of the model for calculation is also grid-based. One grid of hydrological simulation can represent geographical characteristics, climate condition, water balance, and river discharge. The regional characteristics as a input of hydrological model in this study focused on geographical aspects, such as flow direction derived from DEM. Therefore, regional implication of this study is focused on geographical and meteorological characteristics, as well as hydrological characteristics in order to estimate and assess the impact of climate change on water availability.

Figure 45 shows spatial pattern of changed ratio of water availability in Amnok River outlet region from the baseline to the objective periods. In case of Amnok River basin, water availability is projected to be increased in 2020s, and decreased in 2050s especially main river stream. River stream also can be represented on this simulated results because the river stream is representation of accumulated runoff from upper grid. Discharge of downstream of Amnok River is decreased on 2050s compared with baseline. However, overall river discharge of downstream area in Amnok River is going to be increased while the

accumulated river discharge of Amnok River is projected to be decreased. One example of spatial application of the simulation result can be introduction of facilities related with water resources management such as reservoir. There will be a region projected to be in the conditions of decrease in water availability while river discharge of main stream is going to be increased compared with nearby areas. In this case, reservoir can be introduced in this river to enhance the water availability in the projected future hydrological condition of the region.

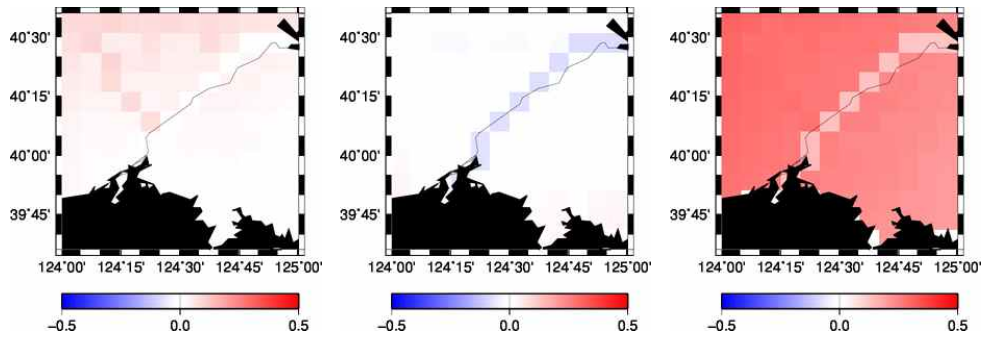

Figure 45 Spatial pattern of changed ratio(%) of water availability in Amnok River outlet region from the baseline period to (a)2020s, (b)2050s, (c)2080s

In case of the downstream region of Duman River, the discharge is projected to be decreased continuously by the 2080s. On the other hand, river discharge of nearby northeast area will be increased on 2020s. However, water availability of this region generally tends to be decreased. Decreased ratio of 2080s in nearby region is much larger than main stream of Duman River (Figure 46). In this case, reservoir

or weir can be installed in the main stream of the river to enhance the water availability of the region against to the expected changes in water availability. Spatio-temporal variation of water availability of nearby area of river junction of Namhan and Bukhan River is presented in Figure 47 and Nakdong River outlet region is presented in Figure 48.

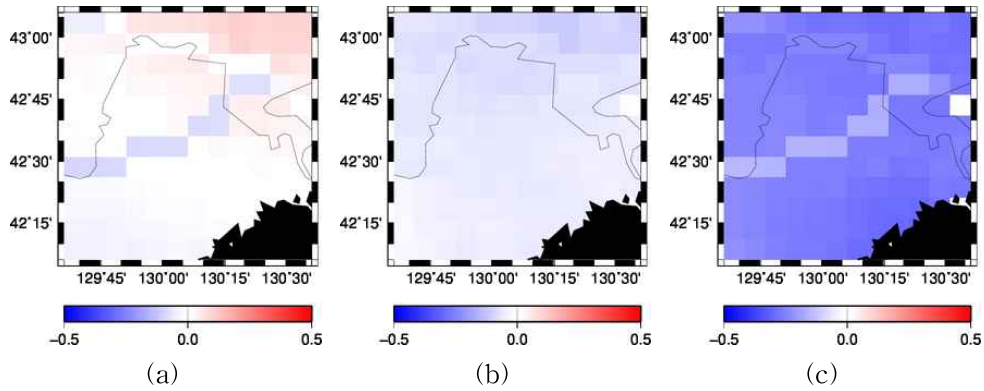

Figure 46 Spatial pattern of changed ratio(%) of water availability in Duman River outlet region from the baseline period to (a)2020s, (b)2050s, (c)2080s

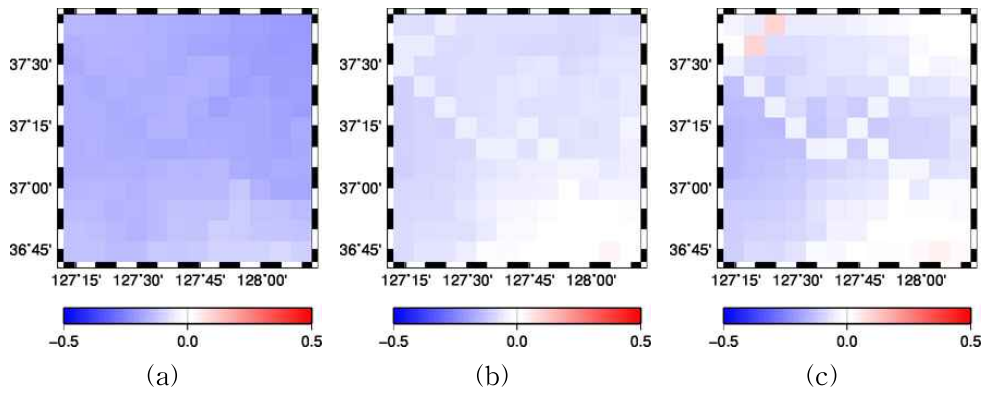

Figure 47 Spatial pattern of changed ratio(%) of water availability in Han River basin region from the baseline period to (a)2020s, (b)2050s, (c)2080s

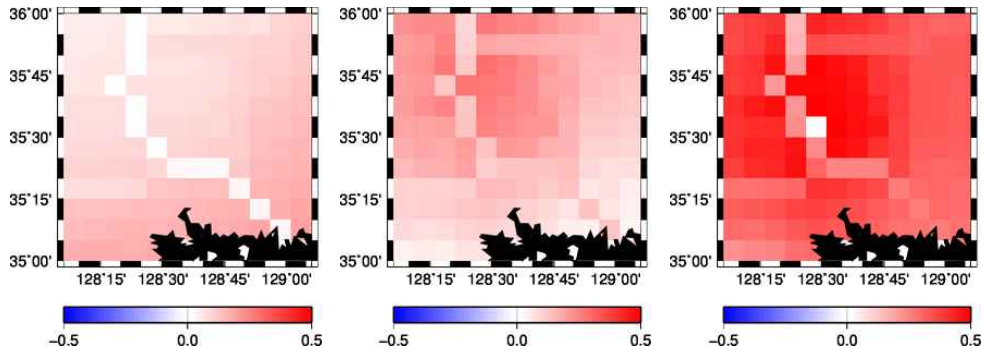

Figure 48 Spatial pattern of changed ratio(%) of water availability in Nakdong River outlet region from the baseline period to (a)2020s, (b)2050s, (c)2080s

Ⅴ. Conclusion

Amount of available water resources of region has been important issues for establishing various land management plan in dealing with climate change. It is necessary to estimate and assess an impact of climate change on water availability to establish an effective management plan and draw an implication for future spatial planning, global hydrological model H08 is regionally applied for simulating hydrological cycle and water availability in this study. The model was calibrated and validated based on 10-year data of GSWP2 from 1986 to 1995. Input meteorological data for the hydrological simulation was also validated. In order to estimate future water availability, future climate scenario from the GCM is used after the correction of bias in air temperature and precipitation. Model calibration was conducted by tuning 4 parameters based on historical discharge data for major river basins in the Korean Peninsula. There were many differences in changes of meteorological and hydrological characteristics as well as river discharge defined as water availability from region to region.

Naturalized flow is assumed for the simulation of river discharge in this study. However, major rivers in the Korean Peninsula has various reservoirs, so that assuming naturalized flow is only reliable in the stations located in upstream area. This study did not considered reservoir operation rules and water supply capacity of the reservoirs. As a result, this study projected water availability based on the naturalized river discharge in the Korean Peninsula on a macroscale using regionalized global hydrological model. When considering climate

change scenario generated from the GCM and future hydrological simulation, an uncertainty of the process of selecting GCM and hydrological model should be considered. Limitation of this study in terms of future projection is mainly caused by this process. This study considered one climate change scenario, which is based on the HadGEM2-AO and RCP 8.5. Hydrological simulation results also should be compared with performance of other models which is successfully applied in the Korean Peninsula.

This study estimated water availability based on projection of river discharge and water balance simulation and derived spatial implication introducing a hydraulic structure such as reservoir for effective management of available water resources against climate change in a scale of the Korean Peninsula and this results could be used as a preliminary information for establishing spatial planning under climatic changes across the Korean Peninsula considering water availability.

Ⅵ. References

Alcamo, J., Döll, P., Henrichs, T., Kaspar, F., Lehner, B., Rösch, T., & Siebert, S. (2003). Development and testing of the WaterGAP 2 global model of water use and availability. Hydrological Sciences Journal, 48(3), 317 – 337. doi:10.1623/hysj.48.3.317.45290

Alcamo, J., Döll, P., Henrichs, T., Kaspar, F., Lehner, B., Rösch, T., & Siebert, S. (2003). Global estimates of water withdrawals and availability under current and future "business-as-usual" conditions. Hydrological Sciences Journal, 48(3), 339 – 348. doi:10.1623/hysj.48.3.339.45278

Alcamo, J., Doll, P., Kaspar, F., Siebert, S. (1997). Global change and global scenarios of water use and availability : An application of WaterGAP1.0. Report A9701, Center for Environmental Systems Research, University of Kassel, Germany

Bae, D.-H. & Jeong, I.-W. (2005). Impact assessment of climate change on water resources, Disaster Prevention Review, 21, 16-22

Bae, D.-H., Jeong, I.-W., Lee, B.-J., & Lee, M.-H. (2011). Future Korean water resources projection considering uncertainty of GCMs and hydrological models, Journal of Korea Water Resources Association, 44(5), 389-406

Bao, Z., Fu, G., Wang, G., Jin, J., He, R., Yan, X., & Liu, C. (2012). Hydrological projection for the Miyun Reservoir basin with the impact of climate change and human activity. Quaternary International, 282, 96 – 103. doi:10.1016/j.quaint.2012.07.012

Bates, B.C., Z.W. Kundzewicz, S. Wu and J.P. Palutikof, Eds. (2008). Climate Change and Water. Technical Paper of the Intergovernmental Panel on Climate Change, IPCC Secretariat, Geneva, 210 pp.

Boulay, A.-M., Bare, J., De Camillis, C., Döll, P., Gassert, F., Gerten, D., … Pfister, S. (2015). Consensus building on the development of a stress-based indicator for LCA-based impact assessment of water consumption: outcome of the expert workshops. The International Journal of Life Cycle Assessment, 577 - 583. doi:10.1007/s11367-015-0869-8

Cai, X., & Rosegrant, M. W. (2002). Global Water Demand and Supply Projections. Water International, 27(2), 159 - 169. doi:10.1080/02508060208686989

Collet, L., Ruelland, D., Borrell-Estupina, V., Dezetter, A., & Servat, E. (2013). Integrated modelling to assess long-term water supply capacity of a meso-scale Mediterranean catchment. Science of the Total Environment, 461-462, 528 - 540. doi:10.1016/j.scitotenv.2013.05.036

Dirmeyer, P. a., Gao, X., Zhao, M., Guo, Z., Oki, T., & Hanasaki, N. (2006). GSWP-2: Multimodel analysis and implications for our perception of the land surface. Bulletin of the American Meteorological Society, 87(10), 1381 - 1397. doi:10.1175/BAMS-87-10-1381

Döll P, Kaspar F, Alcamo J. (1999). Computation of global water availability and water use at the scale of large drainage basins.

Math Geol 4:111 – 118

Döll, P., Kaspar, F., & Lehner, B. (2003). A global hydrological model for deriving water availability indicators: Model tuning and validation. Journal of Hydrology, 270(1-2), 105 – 134. doi:10.1016/S0022-1694(02)00283-4

Elliott, J., Deryng, D., Müller, C., Frieler, K., Konzmann, M., Gerten, D., … Wisser, D. (2014). Constraints and potentials of future irrigation water availability on agricultural production under climate change. Proceedings of the National Academy of Sciences of the United States of America, 111(9), 3239 – 44. doi:10.1073/pnas.1222474110

Falkenmark, M. (1989). The massive water scarcity now threatening Africa-why isn't it being addressed?, Ambio, 18, 112 – 118

GRDC, (2015), Long-Term Mean Monthly Discharges and Annual Characteristics of GRDC Stations / Online provided by the Global Runoff Data Centre of WMO. 2015 ed. Koblenz: Federal Institute of Hydrology (BfG)

Haddeland, I., Clark, D. B., Franssen, W., Ludwig, F., Voß, F., Arnell, N. W., … Yeh, P. (2011). Multimodel estimate of the global terrestrial water balance: setup and first results, 869 – 884. doi:10.1175/2011JHM1324.1

Haddeland, I., Lettenmaier, D. P., & Skaugen, T. (2006). Effects of irrigation on the water and energy balances of the Colorado and Mekong river basins. Journal of Hydrology, 324(1-4), 210 – 223. doi:10.1016/j.jhydrol.2005.09.028

Hanasaki, N. & Yamamoto, T. (2010) H08 User's Manual, H08 Documentation.

Hanasaki, N., Fujimori, S., Yamamoto, T., Yoshikawa, S., Masaki, Y., Hijioka, Y., … Kanae, S. (2013). A global water scarcity assessment under Shared Socio-economic Pathways – Part 2: Water availability and scarcity. Hydrology and Earth System Sciences, 17(7), 2393 – 2413. doi:10.5194/hess-17-2393-2013

Hanasaki, N., Kanae, S., Oki, T., Masuda, K., Motoya, K., Shirakawa, N., … Tanaka, K. (2008). An integrated model for the assessment of global water resources – Part 1 : Model description and input meteorological forcing. Hydrol. Earth Syst. Sci., 12, 1007 – 1025. doi:10.5194/hess-12-1027-2008

Hanasaki, N., Kanae, S., Oki, T., Masuda, K., Motoya, K., Shirakawa, N., … Tanaka, K. (2008). An integrated model for the assessment of global water resources – Part 2: Applications and assessments. Hydrology and Earth System Sciences, 12(4), 1027 – 1037. doi:10.5194/hess-12-1027-2008

Hanasaki, N., Saito, Y., Chaiyasaen, C., Champathong, A., Ekkawatpanit, C., Saphaokham, S., … Thongduang, J. (2014). A quasi-real-time hydrological simulation of the Chao Phraya River using meteorological data from the Thai Meteorological Department Automatic Weather Stations. Hydrological Research Letters, 8(1), 9 – 14. doi:10.3178/hrl.8.9

Hayashi, A., Akimoto, K., Homma, T., Wada, K., & Tomoda, T. (2014). Change in the Annual Water Withdrawal-to-Availability Ratio

and Its Major Causes: An Evaluation for Asian River Basins Under Socioeconomic Development and Climate Change Scenarios. Energy and Environment Research, 4(2). doi:10.5539/eer.v4n2p34

Houghton-Carr, H.A., Boorman, D.B and Heuser, K. (2013). Land use, climate change and water availability: Phase 2a. Rapid Evidence Assessment: Results and synthesis. Centre for Ecology & Hydrology, Wallingford, UK.

IPCC. (2014). Summary for policymakers. In: Climate Change 2014: Impacts, Adaptation, and Vulnerability. Part A: Global and Sectoral Aspects. Contribution of Working Group II to the Fifth Assessment Report of the Intergovernmental Panel on Climate Change [Field, C.B., V.R. Barros, D.J. Dokken, K.J. Mach, M.D. Mastrandrea, T.E. Bilir, M. Chatterjee, K.L. Ebi, Y.O. Estrada, R.C. Genova, B. Girma, E.S. Kissel, A.N. Levy, S. MacCracken, P.R. Mastrandrea, and L.L.White (eds.)]. Cambridge University Press, Cambridge, United Kingdom and New York, NY, USA, pp. 1-32.

Jang, C.-H., Kim, H.-J., Noh, S.-J., & Kim, C.-G. (2008). Analysis of the hydrologic cycle in Pangyo watershed using distributed hydrologic model, Journal of Korea Water Resources Association, 1315-1319 pp.

Jang, J.-S. (2003). Introduction of hydrologic models and parameters, Korean National Committee on Irrigation and Drainage, 10:1, 99-102

Jeong, G.-H., Jeon, M.-H., Kim, H.-S., & Kim, T.-W. (2011). Adaptation capability of reservoirs considering climate change in the Han river basin, South Korea, Journal of the Korean Society of Civil Engineers, 31(5B), 439-447

Jia, Y., Wang, H., Zhou, Z., Qiu, Y., Luo, X., Wang, J., Yan, D. & Qin, D. (2006). Development of the WEP-L distributed hydrological model and dynamic assessment of water resources in the Yellow River basin, Journal of Hydrology, 331, 606-629

Khajuria, A., Yoshikawa, S., & Kanae, S. (2013). Estimation and prediction of water availability and water withdrawal in India. Journal of Japan Society of Civil Engineers, 69(4), 145 - 150.

Kim, B.-S., Kim, S.-J., Kim, H.-S., & Jun, H.-D. (2010). An impact assessment of climate and landuse change on water resources in the Han river, Journal of Korea Water Resources Association, 43(3), 309-323

Kim, B.-S., Yoon, S.-G., Yang, D.-M., & Kwon, H.-H. (2010). Development of grid-based conceptual hydrologic model, Journal of Korea Water Resources Association, 43:7, 667-679

Kim, C.-R., Kim, Y.-O., Seo, S.-B., & Choi, S.-W. (2013). Water balance projection using climate change scenarios in the Korean Peninsula, Journal of Korea Water Resources Association, 46(8), 807-819

Kim, S.-J., Kim, B.-S., Jun, H.-D., & Kim, H.-S. (2010). The evaluation of climate change impacts on the water scarcity of the Han river basin in South Korea using high resolution RCM

data, Journal of Korea Water Resources Association, 43(3), 295-308

Kondo, J. (1994). Meteorology of Hydrological Environment, Asakura Shoten, Tokyo, Japan, 368 pp.

Korea Meteorological Administration. (2012). Climate change projection report in Korea, pp. 19

Lautensach, H. (1988). Korea: A geography based on the author's travels and literature, Springer-Verlag.

Lee, J.-M., Kim, Y.-D., Kang, B.-S., & Lee, H.-S. (2012). Impact of climate change on runoff in Namgang dam watershed, Journal of Korea Water Resources Association, 45(6), 517-529.

Lee, M.-H. & Bae, D.-H. (2015). Climate Change Impact Assessment on Green and Blue Water over Asian Monsoon Region. Water Resources Management, 29(7), 2407 - 2427. doi:10.1007/s11269-015-0949-3

Lehner, B., P. Doll, J. Alcamo, T. Henrichs, and F. Kaspar. (2006). Estimating the Impact of Global Change on Flood and Drought Risks in Europe: A Continental, Integrated Analysis, Climatic Change, 75, 273-299

Manabe, S. (1969). Climate and the ocean circulation - 1: The atmospheric circulation and the hydrology of the Earth's surface, Mon.Weather Rev., 97, 739 - 774.

Martin, N. and Giesen, N. (2009). Spatial distribution of groundwater production and development potential in the Volta River basin of Ghana and Burkina Faso, Water International, 30:2, 239-249.

Masood, M., Yeh, P. J.-F., Hanasaki, N., & Takeuchi, K. (2014). Model study of the impacts of future climate change on the hydrology of Ganges – Brahmaputra – Meghna (GBM) basin. Hydrology and Earth System Sciences Discussions, 11(6), 5747 – 5791. doi:10.5194/hessd-11-5747-2014

Mateo, C. M. (2012) Hydrological modeling with reservoir operation in the Chao Phraya River Basin for flood mitigation, Master's thesis documentation, Graduate School of Engineering, the University of Tokyo.

Mateo, C. M., Hanasaki, N., Komori, D., Tanaka, K., Kiguchi, M., Champathong, a., … Oki, T. (2014). Assessing the impacts of reservoir operation to floodplain inundation by combining hydrological, reservoirmanagement, and hydrodynamicmodels, 7245 – 7266. doi:10.1002/2013WR014845.

Meigh, J., McKenzie, A., & Sene, K. (1999). A grid-based approach to water scarcity estimates for eastern and southern Africa. Water Resources Management, (13), 85 – 115.

Milly, P.C.D., Dunne, K.A., Vecchia, A.V. (2005). Global pattern of trends in streamflow and water availability in a changing climate, Nature, 148, 347-350.

Ministry of Land, Infrastructure and Transport. (2013). Water and sustainable development 2015 – Water for the future, 22 pp.

Ministry of Land, Transport and Maritime Affairs. (2011). Water Vision 2020.

Moon, S.-J., Kim, J.-J., & Kang, B.-S. (2013). Bias correction fof

GCM long-term prediction using nonstationary quantile mapping, Journal of Korea Water Resources Association, 46:8, 833-842.

Nam, W.-H., Hong, E.-M., Kim, T.-G., & Choi, J.-Y. (2014). Projection of future water supply sustainability in agricultural reservoirs under RCP climate change scenarios, Journal of the Korean Society of Agricultural Engineers, 56(4), 59 - 68.

Nash, J. E. and J. V. Sutcliffe. (1970). River flow forecasting through conceptual models part I — A discussion of principles, Journal of Hydrology, 10 (3), 282 - 290.

NIMR. (2011). Climate change scenario report 2011 to respond to the IPCC 5th Assessment Report. National Institute of Meteorological Research, Korea

Okada, M., Iizumi, T., Sakurai, G., Hanasaki, N., Sakai, T., Okamoto, K., & Yokozawa, M. (2014). Modeling irrigation based climate change adaptation in agriculture: Model development and evaluation in Northeast China. Journal of Advances in Modeling Earth Systems, 6, 513 - 526. doi:10.1002/2013MS000282.

Oki, T. and Sud, Y. C. (1998). Design of Total Runoff Integrating Pathways (TRIP)-A Global River Channel Network, Earth Inter., 2, EI013.

Oki, T., Agata, Y., Kanae, S., Saruhashi, T., Yang, D., & Musiake, K. (2001). Global assessment of current water resources using total runoff integrating pathways. Hydrological Sciences Journal, 46(6), 983 - 995. doi:10.1080/02626660109492890

Park, J.-H., Kwon, H.-H., & Noh, S.-H. (2011). Outlook of discharge

for Daecheong and Yongdam dam watershed using A1B climate change scenario based RCM and SWAT model, Journal of Korea Water Resources Association, 44(12), 929-940.

Park, M.-J., Shin, H.-J., Park, G.-A., & Kim, S.-J. (2010). Assessment of future hydrological behavior of Soyanggang Dam watershed using SWAT, Journal of the Korean Society of Civil Engineers, 30(4B), 337-346.

Pratoomchai, W., Kazama, S., Ekkawatpanit, C., & Komori, D. (2015). Opportunities and constraints in adapting to flood and drought conditions in the Upper Chao Phraya River basin in Thailand. International Journal of River Basin Management, (April), 1 - 15. doi:10.1080/15715124.2015.1013036

Robock, A., K. Vinnikov, C. Schlosser, N. Speranskaya, & Y. Xue. (1995). Use of midlatitude soil moisture and meteoro- logical observations to validate soil moisture simulations with biosphere and bucket models. J. Climate, 8, 15 - 35.

Shin, Y. & Jung, H. (2015). Assessing uncertainty in future climate change in Northeast Asia using multiple CMIP5 GCMs with four RCP scenarios, Journal of Environmental Impact Assessment, 24(3), 205-216.

Son, K.-H., Lee, M.-H., & Bae, D.-H. (2012). Runoff analysis and assessment using land surface model on East Asia, Journal of Korea Water Resources Association, 15(2), 165-178.

UN World Water Assessment Programme(UN-Water WWAP). (2006). The United Nations World Water Development Report

Van Beek, L. P. H., Wada, Y., & Bierkens, M. F. P. (2011). Global monthly water stress: 1. Water balance and water availability. Water Resources Research, 47(7). doi:10.1029/2010WR009791

Vinay, S., Bharath, S., Bharath, H. A., & Ramachandra, T. V. (2013). Hydrologic model with landscape dynamics for drought monitoring, Joint International Workshop of ISPRS VIII/1 and WG IV/4 on Geospatial Data for Disaster and Risk Reduction, 67 - 72.

Vorosmarth, C.J., Green, P., Salisbury, J., Lammers, R.B. (2000). Global water resources: Vulnerability from climate change and population growth, Science 289:5477, 284-288.

Wada, Y., van Beek, L. P. H. (2011). and Bierkens, M. F. P.: Modelling global water stress of the recent past: on the relative importance of trends in water demand and climate variability, Hydrol. Earth Syst. Sci., 15, 3785-3808, doi:10.5194/hess-15-3785-2011

국문초록

기후변화를 고려한 한반도의 가용 수자원 추정

지도교수 : 이 동 근
서울대학교 대학원
조경·지역지스템공학부 생태조경학 전공
유 소 현

기온과 강수량의 변화로 나타나는 기후변화 현상은 전 지구적으로 일어나고 있으며 이는 가용 수자원에 직접적으로 영향을 끼칠 것으로 예측되고 있다. 한반도 지역의 경우, 강우가 여름철에 집중되므로 가용 수자원의 시간적, 공간적 편중이 주요하게 다루어져 왔다. 기후변화로 인하여 이러한 한반도 가용수자원의 시·공간적 편중이 심화될 것으로 예상되며 이는 수자원 안정성의 문제를 악화시키는 요인이 될 것으로 예상되고 있다. 가용 수자원의 변동은 도시지역, 작물 재배지, 산림 등 수자원을 직접적으로 이용하게 되는 토지이용과도 밀접하게 관련되어 있기 때문에 그 공간적 변동에 대한 파악은 필수적이다.

가용 수자원은 유역 내에서 사용할 수 있는 물의 양을 의미하며, 연구 범위에 따라서 댐의 저수량, 하천 유량 등 다양하게 정의될 수 있다. 본 연구에서는 문헌 고찰을 통해 가용 수자원을 하천의 유량으로 정의하였다. 이에 근거하여 기후변화 영향에 따른 한반도 가용 수자원의 변동을 추정하기 위해 북한을 포함한 한반도 전 지역을 연구 대상지로 하여 RCP 기후변화 시나리오를 입력 자료로 하여 수문 모형을 활용하여 모의된 유

량을 가용 수자원으로 추정하였다. 향후 공간 계획적 시사점을 제공하기 위하여 격자 기반의 수문 모형 중 한반도 스케일에서 적용하기 적합한 모형으로 H08 모형을 선정하였다. H08은 1° × 1° 해상도의 전 지구적인 수자원 가용성을 평가하기 위해 개발된 모형으로 5′ × 5′ 해상도로 지역적으로도 적용이 가능하다. 입력자료로 과거 기간에 대해서는 GSWP2에서 제공하는 기상자료를 활용하였으며 기후변화 시뮬레이션을 위해서 HadGEM2-AO 모형에서 생산되는 RCP 8.5 시나리오를 사용하였다. GCM으로부터 제공되는 미래 기온, 강수량 자료는 과거 관측 자료에 근거하여 편차를 보정하였다. 과거 기간의 기후자료를 바탕으로 모형의 매개변수를 검·보정하여 적용성을 검증하였으며, 보정된 모형에 기후변화 시나리오를 적용하여 한반도의 미래 수문 변동 및 가용 수자원의 변화를 추정하였다.

한반도의 가용 수자원과 수문 변동을 파악하기 위하여 한반도 전 범위를 대상으로 각 요소들의 시·공간적 변동을 표현하는 동시에 대표적인 관측소 지점을 선정하여 정량적인 모의를 진행하였다. 북한 지역의 경우는 압록강, 두만강, 청천강, 대동강 유역, 남한 지역의 경우는 한강, 낙동강, 금강, 영산강 유역의 관측소를 선정하여 총 8개 관측소에 대해 기온, 강수량의 기후 요소와 더불어 유출량, 증발산량의 수문 요소의 변동을 파악하였으며 최종적으로 유량을 추정하여 RCP 8.5시나리오에 근거한 한반도의 수문 요소 및 유량 변동을 추정하였다. 수문 모의 결과를 공간적으로 제시하여 최종적으로 이를 공간 계획적으로 활용할 수 있는 시사점을 제공하였다. 하지만 미래 현상을 모의하는 과정에 있어서 1가지 GCM만을 적용하여 미래 기후 시나리오가 가지는 불확실성을 고려하지 못하였다는 점과, 댐의 유량 조절 효과와 시설물의 물 공급 능력을 반영하지 못했다는 한계점을 지니고 있다. 본 연구는 전 지구적 수문 모형을 한반도를 대상

으로 지역적으로 적용하여 격자 단위로 주요 하천 유량에 근거하여 가용 수자원을 전망하였으며 본 연구의 결과는 향후 미래 전망 기간에 유황 변동에 대비한 시설물 도입 등의 공간 계획 시 기초자료로 활용될 수 있을 것이다.

▫ 주요어: 수자원 가용성, 기후변화, RCP 시나리오, GCM, 수문 모형, H08

▫ 학번: 2014-20049

Dissertation of the Degree of
Master of Landscape Architecture

Estimation of Water Availability in the Korean Peninsula Considering Climate Change

기후변화를 고려한 한반도의 가용 수자원 추정

February 2016

Graduate School of Seoul National University

Department of Landscape Architecture and
Rural System Engineering

So Hyun Yoo

Abstract

Estimation of Water Availability in the Korean Peninsula Considering Climate Change

Advising Professor : Dongkun Lee
Landscape Architecture and Rural Systems Engineering
Graduate School of Agriculture and Life Science
Seoul National University
Sohyun Yoo

Climate change is projected to have a direct impact on the water resources. In case of the Korean Peninsula, more than a half of the total rainfall amount is concentrated in summer. It has been always important issues that spatio-temporal variability of an available water resources in the Korean Peninsula. The water availability is projected to be influenced by climate change and it is expected to more intensify. Variations in water availability is related with the land use which is directly affected by water resources, such as agricultural area, urban area, and forests. Therefore, the changes in spatial variability along with the temporal changes of water availability should be investigated to establish an effective management plan and draw an implication for future spatial planning.

Available water resources can be defined in various ways, such as a storage of reservoir, and river discharge which can be used in a basin. This study defined water availability as a river discharge based on literature reviews. This study estimates water availability based on river discharge in the Korean Peninsula including North Korea, as the study area. In order to estimate water availability and draw a spatial implication considering climate change, HadGEM2-AO and RCP 8.5 scenario is applied as a future climate scenario, and grid-based hydrological model H08 is used. H08 was originally developed as a global hydrological model for the simulation of water availability in a spatial resolution of 1° × 1°. However, it is also applicable for a regional hydrological simulation in a spatial resolution of 5′ × 5′. Input meteorological data of GSWP2 is used for historical simulation, and RCP 8.5 scenario from HadGEM2-AO was used for future climate change simulation. A bias in air temperature and precipitation of GCM was validated by comparing with observed meteorological data in Korea. Parameters of H08 was calibrated and validated for historical simulation of 10 years from 1986 to 1995, then climate change simulation is carried out for the estimation of hydrological changes using validated H08.

In order to investigate hydrological characteristics and water availability in the Korean Peninsula, representative gauging stations was presented for Amnok, Duman, Chongchon, Taedong River basin in North Korea, and Han, Nakdong, Geum, Yeongsan River basin in South Korea. Quantitative hydrological characteristics were presented

for the representative 8 stations in the Korean Peninsula along with the meteorological aspects. Spatio-temporal variability was investigated for the hydrological attributes, such as evapotranspiration, runoff, as well as air temperature and precipitation. Estimated water availability based on RCP 8.5 scenario was spatially presented for the objective periods in order to derive spatial implication for the planning. However, there is uncertainties for future projection in the process of selecting future climate scenarios and hydrological model. This study assumed naturalized discharge which is not considering regulated flow due to the reservoir operation and artificial water supply capacity. This study estimated water availability on a grid basis using regionalized global hydrological model. The results of this study can be used as preliminary information for establishing spatial planning under climatic changes across the Korean Peninsula considering water availability.

□ Keywords: Water availability, Climate change, RCP scenario, GCM, Hydrological model, H08

□ Student number: 2014-20049

Table of contents

List of tables

List of figures

Ⅰ. Introduction

Water resources are directly related to human health and are essential for ecosystems, geophysical processes, and human activities (Milly et al., 2005). The availability of sufficient water at places where human activity takes place has always been an important issue (Alcamo et al., 1997). Strong evidences of climate change have appeared throughout the world over time (IPCC, 2014). Changing climate, observed since 1950, had no precedent in the past several hundred years. Moreover, extreme weather events, such as heavy rainfall and droughts, caused by changes in rainfall pattern occur with rising temperatures. Thus, it is likely to have an effect on the landscape where the responses to the changes occur. Accordingly, water availability will fall below the critical level because of climate change and would be a major issue across communities (Bates et al., 2008). The management of water availability is the principal challenge since changing water demands with increasing population will be difficult to manage with changing climate in the future. The changes in the available water resources over time are directly related to water use in landscapes such as forests and agricultural areas. Therefore, identifying the spatial variation of water availability is essential (Houghton-Carr et al., 2013). In response to the variability of water resources according to climate change, the information about how the water availability quantitatively and qualitatively changes with various spatial and temporal scale will be more important (UN, 2006). The estimation and assessment of the availability of water resources

affected by climate and socio-economic changes is needed (Vorosmarty et al., 2000).

In case of the Korean Peninsula, climate change is a major factor that exacerbates water resources problems caused by the seasonally biased distribution of available water resources (Ministry of Land, Infrastructure and Transport, 2013). The evaluation of the quantity of water resources and their spatial distribution is essential to establish a water supply plan (Martin and Giesen, 2009). It is expected that the spatial and temporal imbalance of water resources in the Korean Peninsula will be intensified depending on future climatic conditions. In order to effectively manage this problem, the quantitative evaluation of spatial and temporal variations of the available water resources is required.

Climate change research related to water availability is required for the determination of the impact on water resources in the Korean Peninsula. To derive the spatial implications of climate change on the water availability in the Korean Peninsula, the objectives of this study was set up as follows: ⅰ) Simulation of hydrological changes due to the climate change phenomenon in the Korean Peninsula, including North Korea, as the study area. ⅱ) Spatial distribution of water availability based on the hydrological cycle and expected climatic changes.

Ⅱ. Literature review

1. Climate change and water availability

1.1. Climate scenarios

Climate scenarios have been developed with various climate models to predict the impact of future climate change. The Intergovernmental Panel on Climate Change (IPCC) reports the projection of future climate around the world on a regular basis. The IPCC reports are based on the findings of peer reviewed reports, and climate change scenarios have been proposed for the future projections in this report. By inputting the anthropogenic factors on the global climate model (GCM), future greenhouse gas concentrations are calculated as a result of the impact of climate and projected future weather conditions. The Korea Meteorological Administration (KMA) introduced representative concentration pathways (RCP) as a greenhouse gas emission scenario in the IPCC Fifth Assessment Report in 2011 and has projects future climatic conditions based on the scenarios. In Table 1, the meaning of RCP scenarios[1)] has been described. The number assigned of RCP scenarios signifies the amount of energy absorbed additionally due to the greenhouse gas. The larger the number, the higher the greenhouse gas emissions. For active reduction of greenhouse gas emission, the RCP 2.6 scenario should be realized. RCP 4.5 is the scenario in which the greenhouse gas emission policy has been realized considerably.

1) http://sedac.ipcc-data.org/ddc/ar5_scenario_process/RCPs.html

The RCP 6.0 scenario assumes that the greenhouse gas reduction policies are barely applicable, and RCP 8.5 scenario is the business - as -usual scenario. Future climate projction and impact assessment based on the RCP scenarios reported in the IPCC Fifth Assessment Report.

Table 1 Description of RCP scenarios (Source: IPCC)

Scenario	Description
RCP 2.6	Peak in radiative forcing at ~ 3 W/m2 before 2100 and decline
RCP 4.5	Stabilization without overshoot pathway to 4.5 W/m2 at stabilization after 2100
RCP 6.0	Stabilization without overshoot pathway to 6 W/m2 at stabilization after 2100
RCP 8.5	Rising radiative forcing pathway leading to 8.5 W/m2 in 2100

Climate projections and scenarios are generated through the simulation process of GCM. GCM simulates climatic factors, such as temperature, humidity, radiation, precipitation, and air pressure, based on the laws of physics. GCM is one of the most effective tools to predict the future climate and is provided by various organizations and institutes all over the world (Table 2[2]). In order to estimate and assess the impact of future climate, a results from the various GCM climate simulations are widely used. Studies that project the future hydrological cycle are also progressing actively.

2) http://www.climate.go.kr/home/02_information/07_4.html

Table 2 Description of GCMs (Source: KMA)

GCM	Modeling center	Atmospheric resolution	Ocean resolution
BCC-CSM1.1	BCC	~2.8°, L26	0.3-1°, L40
CanESM2	CCCma	T63, L35	1.41°x0.94°, L40
GFDL-ESM2M	NOAA GFDL	2x2.5°, L24	1/3~1°, L63
HadGEM2-ES	MOHC	N96(~1.6°), L38	0.5~2°, L40
IPSL-CM5A-LR	IPSL	3.75x1.9, L39	0.5~2°, L31
MIROC-ESM	MIROC	T42, L80	0.5~1.7°, L43
MPI-ESM-LR	MPI-M	T63(~1.9°), L47	1.5°, L47
NorESM-ME	NCC	1.9x2.5°, L26	1°, L53

In case of regional climate change impact assessment, the spatial resolution of GCM is low because of a spatial scope of GCM is global. This is the reason why the process of downscaling of GCM is required. The regional climate model (RCM) is used in the downscaling process. In Korea, the KMA developed the RCM HadGEM3-RA based on HadGEM2-AO, which is developed by the Met Office Hadley Centre. KMA distributed the climate scenario, which has a spatial resolution of 12.5 km for the Korean Peninsula and 1 km for South Korea, and it has been used widely in the climate change research in Korea.

1.2. Concept of water availability

The meaning of water availability is the amount of available water resources. Water availability can be specifically defined in various ways. Cai and Rosegrant (2002) defined the available water resources as not only renewable water, such as surface water and groundwater

that can be supplied by natural hydrological circulation, but also artificial water transfer, desalinated water, and non-renewable groundwater. Vinay et al. (2013) defined the total water availability as the summation of river discharge of basin and stored water in aquifer and soil. Alcamo et al. (1997) defined the water availability of a basin as the amount of stored water in the reservoir of the basin. According to the Water Vision 2011-2020 of Water Resources Ministry of Land, Transport and Maritime Affairs, the total amount of water resources is obtained by multiplying the average annual precipitation and the land area. The total amount of water resources can be divided by the loss and runoff. Only runoff can be regarded as available water resources. The most available water resource is the runoff during floods. The remaining water resources, excluding the amount of water lost to the sea, and consisting of river water, water supplied by dams, and groundwater, is calculated as the actually available water resources (Ministry of Land, Transport and Maritime Affairs, 2011). Numerous studies have evaluated the available water resources by estimating the actually available water resources such as river discharge and the amount of stored groundwater (Lee et al., 2015). Many previous studies have assumed the water availability as the amount of discharge of the basin (Elliott et al., 2014; Hayashi et al., 2014; Collet et al., 2013; Oki et al., 2009; Haddeland et al., 2006; Alcamo et al., 2003; Doll et al., 1999). These studies on the estimation and evaluation of the water availability focus on estimating the river discharge and its changes with changing environmental conditions.

The estimation of water availability from on the grid-based hydrological model can provide an insight into the hydrological elements involved, such as surface runoff and available water resources, at all points of interest (Meigh et al., 1999). Therefore, many previous studies applied a grid-based model to estimate and evaluate of the hydrological impact and water availability. The available amount of surface water for a specific grid can be the river discharge of the grid (van Beek et al., 2011). Oki et al. (2009) presented the water availability of specific grid as shown in [Eq. 1] by accumulating the runoff from the upper grid cell. R refers to the runoff from a grid, and $\sum D_{up}$ is summation of the accumulated runoff from the upper grid, and α is the constant that represents factors such as water quality and water use affecting the amount of available water from the upper grid.

$$Q = R + \alpha \sum D_{up} \quad \text{[Eq. 1]}$$

When considering climate change, a variation in the flow regime of the river basin and sectoral water use of the basin can be constrained by a change in the water availability. Doll et al. (2003) projected vulnerable areas for water availability based on these future changes. In case of evaluating the water availability using the grid-based hydrological model for multiple catchments, the ratio between net water demand and available water in a grid can be an indicator of whether or not the amount of water can meet the net demand of the

grid (Wada et al., 2011; Falkenmark, 1989). Many previous studies have estimated the ratio of water demand and supply in order to determine the factors that can affect the amount of available water resource that the local community can directly use (Boulay et al., 2015). Reflecting a viewpoint in terms of water demand and supply balance, numerous studies have compared the ratio of water demand and supply (Hayashi et al., 2014; Collet et al., 2013; Hanasaki et al., 2013; Hanasaki et al., 2008; Alcamo et al., 2003). Lee et al. (2015) evaluated water availability in the Asian monsoon region by calculating the surface runoff and evapotranspiration, using a hydrological model. Elliott et al. (2014) considered only renewable surface water to evaluate water availability in terms of irrigation water supply. They regarded runoff from the grid as water availability by using a grid-based hydrological model.

2. Hydrological model studies in the Korean Peninsula considering climate change scenarios

A hydrological model is a mathematical description of physical processes in the natural hydrological cycle of the real world and is used to understand and predict the hydrological processes. It is an important tool widely used to plan and manage the water resources of basins. A hydrological model can be categorized by a simulation process, temporal and spatial structure, and method of solution. According to the simulation process, a hydrological model can be categorized as a lumped model or a distributed model. A lumped model considers the whole basin as a single system, and then analyzes the relationship between rainfall and runoff. A distributed model divides the basin into homogeneous elements, and then analyzes respective hydrological factors to quantify the hydrological characteristics of watershed (Jang, 2003). A distributed hydrological model can be further categorized by its basic calculation unit and spatial structure used into either a grid-based model or a catchment based model. A grid-based hydrological model has difficulty in calculation of larger basins. On the other hand, a subcatchment-based model has difficulties in calculating the overland flow simulation based on geographical elements and soil saturation (Jia et al., 2006). Preparing the input data for a distributed model is more difficult than the lumped model, but it is based on the physical theory and formula so it can reflect the spatial characteristics and circulation of hydrological elements (Jang et al, 2008). Moreover, a distributed model uses a digital elevation model

so the water balance elements can be calculated at any point of interest in a watershed. This indicates that the distributed hydrological model can calculate the spatial water balance and runoff reliably (Kim et al., 2010).

Water resources constitute an important sector that is expected to be directly affected by climate change and there are numerous studies on this. The analysis of the effect of climate change on water resources can be categorized by the approach to dealing with the climate data. The first approach is to analyze the trends using observation data. The second approach is divided into two methods, one using a climate model, and the second using a combination of a climate model and a deterministic hydrological model. Most of the previous studies have used GCM. Future climate scenarios generated from GCM can be inputted on the hydrological model to analyze the effects of climate change on water resources (Bae and Jeong, 2005). Changes in air temperature and precipitation cause changes in the hydrological elements, such as runoff and evapotranspiration, and water availability. A number of studies focusing on runoff changes have been undertaken in Korea since the climate change scenario were introduced. The majority of study sites for domestic research include watersheds in South Korea, which has provided for most of the runoff estimates of the basins. In addition, the evaluation of supply ability of available water resources by estimating the water flows of reservoirs and dams have also been conducted.

Previous studies related to the runoff estimation are described as

follows. Park et al. (2011) projected future discharge of Yongdam and Daecheong dam watersheds based on A1B scenario and SWAT hydrological model. Lee et al. (2012) evaluated the changes in runoff caused by climate change using SWAT model. Kim et al. (2010) considered the land use changes as well as climate change. They simulated the changes in water balance as well as the discharge of Han River basin using the SLURP model and land use change scenario based on the SRES A2 scenario and the CA-Markov Chain method. Park et al. (2010) simulated the water resources and hydrological changes in the Soyanggang basin considering climate change based on the A2, A1B, B1 scenarios and land use change using CA-Markov Chain method and regression equation considering the relationship between temperature and leaf area index (LAI). Many studies consider the uncertainty in climate change. Bae et al. (2011) assessed the impact of climate change on water resources by simulating the river discharge considering the uncertainties that may occur in a process of selecting GCM and the hydrological model. In order to take into account the uncertainty and present a range of uncertainty in the projected hydrological changes, they used the A2, A1B, B1 scenarios, and 13 GCMs, and 3 hydrological models named PRMS, SWAT, and SLURP.

Studies assessing the climate change impact of the actual amount of water supply capacity of the reservoirs have been actively conducted in recent years. Kim et al. (2010) simulated the river discharge using SLURP model and A2 scenario, and then analyzed the water scarcity

of Han River basin using the K-WEAP model based on the simulated discharge. Kim et al. (2013) analyzed the water scarcity in South Korea based on the water supply network using K-WEAP model for the simulated discharge using TANK model. Jeong et al. (2011) analyzed inflow, storage, and outflow of 5 reservoirs in Han River basin using a fuzzy inference mechanism based on the precipitation changes of A1B scenario. Nam et al. (2014) assessed the agricultural water availability at a local scale by using an irrigation vulnerability assessment model based on the simulated inflow using TANK model and the amount of water supply and demand of reservoirs under RCP scenarios.

3. Regional application of H08 in previous studies

H08 was originally developed as a global hydrological model with a spatial resolution of 1° × 1°. However, it is also applicable for the simulation of the hydrological cycle and river discharge at a regional scale. H08 can not only simulate natural hydrological processes, but also the impact of anthropogenic activities, such as reservoir operation and water withdrawal. The spatial resolution of H08 for global application can be 1° × 1° or 0.5° × 0.5°. In case of regional application of H08, 5′ × 5′ (approximately 9 km × 9 km) of the spatial resolution can be applicable (Hanasaki and Yamamoto, 2010).

Khajuria et al. (2013) applied H08 in India to estimate the present and future water availability on a spatial resolution of 0.5° × 0.5°. They used the land surface module and river routing module in the H08 model to simulate the annual flow and divided it with the total population, and then estimated the annual per capita water availability. Future water withdrawal and availability with changing climate and population was estimated for India.

Mateo et al. (2014) modeled the coupled H08 and CaMa-Flood model to assess the impact of reservoir operation on the inundation in the Chao Phraya River basin in Thailand. H08 was used to simulate land surface hydrological process and reservoir operation rules. Additionally, the applied spatial resolution of H08 was 5′ × 5′.

Okada et al. (2014) developed the CROVER model, which consists of H08 and crop model PRYSBI-2, to assess the integrated impact of

climate change on the hydrological processes and the crop yield in the Songhua River basin in China. H08 was used to simulate the runoff, evapotranspiration, and soil moisture.

Masood et al. (2014) used H08 to simulate the impact of climate change on the hydrological processes in the Ganges - Brahmaputra - Meghna (GBM) River basin in a spatial resolution of 5′ × 5′ based on the RCP scenarios.

Agricultural activities in the Upper Chao Phraya river basin is directly related to surface water and groundwater resources affected by flood and drought conditions. Pratoomchai et al. (2015) investigated the impact of drought and flood conditions on the agricultural productivity related to the surface water and groundwater. H08 was used to simulate changes in surface runoff, discharge, and evapotranspiration along with the soil moisture deficit method and Penman-Monteith method for calculating groundwater storage and crop water demand.

Table 3 presents previous studies on the regional application of H08 for regional impact assessment of environmental changes on the hydrological process and water availability. H08 has been successfully applied to a part of the catchment area spread over 100,000 km^2. Therefore, it is considered that H08 is appropriate for application in a scale of the Korean Peninsula.

Table 3 Study sites and spatial resolution of previous studies for regional application of H08

Author	Year	Study site	Area(km^2)	Spatial resolution
Khajuria et al.	2013	India	3,287,263	0.5°×0.5°
Mateo et al.	2014	Chao Phraya river basin, Thailand	160,400	5′×5′
Masood et al.	2014	Ganges-Brahmaputra-Meghna(GBM) river basin	1,712,700	5′×5′
Okada et al.	2014	Songhua river basin, Northeast China	212,000	5′×5′
Pratoomchai et al.	2015	Upper Chao Phraya river basin, Thailand	109,973	5′×5′

Ⅲ. Methodology

1. Scope of the study

Since water resources are widely involved in fields such as natural hydrology, energy circulation, and human activity, it is necessary to limit the scope of the study. Especially, a study to assess the impact of future conditions on water resources along with climate change, water use changes, and human activities should also be considered. In order to assess the impacts of climate change, socio-economic changes were excluded from the scope of this study. Thus, the estimation of water availability in future has been studied for climate change impact assessment. Climate change leads to changes in land use and in the distribution of crop species. However, this study does not cover the impact of land use changes or crop species changes on water resources. Therefore, this study only estimates water balance and river discharge on land surfaces caused by climatic phenomena.

The location of this study is the Korean Peninsula. However, major rivers are located near in the national border with China, which were included in the simulation. To limit the spatial scope to latitudinal and longitudinal extents for convenience in simulation, the areas within the Korean Peninsula (124°E - 131°E, 33°N - 44°N) was included in the simulation.

The period for model calibration and validation was set to 10 years (from 1986 to 1995). For the first 5 years, the model was calibrated;

then the model was validated for the next 5 years. After the completion of model validation, a reference period and objective periods were set to assess the impact of climate change as shown in Table 4.

Table 4 Temporal scope of this study

Classification	Period
Calibration, validation period	1986-1995
Reference(baseline) period	1971-2000
Objective period 1 (2020s)	2010-2039
Objective period 2 (2050s)	2040-2069
Objective period 3 (2080s)	2070-2099

2. Materials and method

2.1. Study flow

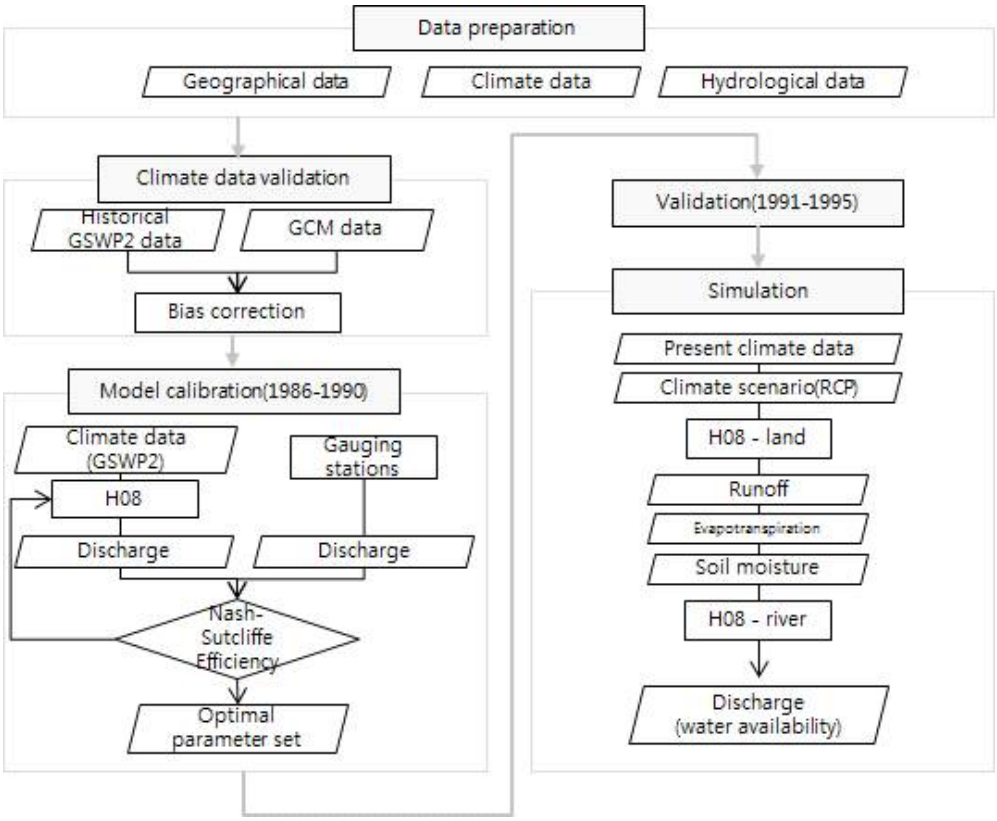

Figure 1 Flow chart of this study

Figure 1 presents the flow chart of this study. First of all, an input data for model simulation including meteorological data, geographical data and hydrological data was prepared. Then a process of verifying the input climate data by comparing with the observed climate data is required to correct the bias of the climate data for model simulation. The bias-corrected meteorological data is used as the input data for

hydrological simulation for calibration period in order to optimize the model parameters to Korean Peninsula. The model calibration is carried out by tuning the parameters based on NSE value, which can evaluate the model performance on the river discharge simulation compared with the observed discharge. After the calibration, validation is carried out to evaluate the adaptability of the model. After the validation of the model, climate change impact assessment simulation is carried out. Finally, the simulated river discharge is regarded as water availability.

2.2. Introduction to hydrological model H08

H08 was developed by Hanasaki et al. (2008) to estimate water availability in a global scale. This model can simulate representative anthropogenic activities that affect the hydrological cycle such as reservoir operation, water withdrawal, crop growth as well as natural hydrological process (Hanasaki et al., 2008). H08 model is consisted with 6 modules – Land surface hydrology module, river routing module, crop growth module, reservoir operation module, water withdrawal module, environmental flow module.

Land surface module of H08 can be classified as land surface model (LSM) that can solve both the surface energy and water balances (Haddeland et al., 2011).

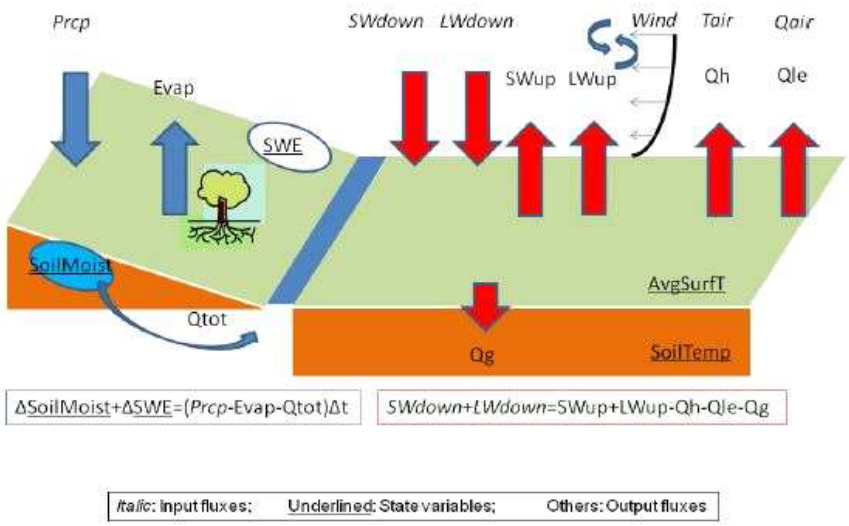

Figure 2 Schematic diagram of land surface process module of H08 (Hanasaki and Yamamoto, 2010)

FIgure 2 shows schematic diagram of land surface process in H08. Land surface module calculates water and energy balance based on bucket model (Manabe, 1969). In H08, one grid is conceptually one bucket. When the bucket is empty, the soil moisture of bucket is at wilting point. When the bucket is full, soil moisture is at field capacity. The definition of field capacity is maximum capacity of soil water contents that can be exist against the gravity force. Evapotranspiration is expressed as a function of potential evapotranspiration and soil moisture. In the original bucket model, runoff is generated only when the bucket is full. But H08 applied leaky bucket (Robock et al., 1995) so that subsurface runoff is calculated. Total runoff can be divided into surface runoff and subsurface runoff.

LSMs have differences in their choice of evapotranspiration and runoff schemes. There are many formulas for calculating evapotranspiration, such as Penman-Monteith, Pristley-Taylor, and Hamon. In this leaky bucket model, evapotranspiration is estimated by using bulk formula which uses bulk transfer coefficient to calculate turbulent heat fluxes. Potential evapotranspiration $E_P[kg/m^2/s]$ can be estimated by [Eq. 2].

$$E_P(T_S) = \rho C_D U(q_{SAT}(T_S) - q_a) \quad \text{[Eq. 2]}$$

$\rho[kg/m^3]$ is density of air, C_D is bulk transfer coefficient, $U[m/s]$ is wind speed, $q_{SAT}(T_S)[kg/kg]$ is saturated specific humidity of a given surface temperature. Actual evapotranspiration can be calculated by [Eq.3] by multiplying a function of soil moisture W to potential evapotranspiration.

$$E = \beta E_P(T_S) \quad \text{[Eq. 3]}$$

$$\beta = \begin{cases} 1 & 0.75\,W_f \leq W \\ W/0.75\,W_f & W < 0.75\,W_f \end{cases} \quad \text{[Eq. 4]}$$

$W[kg/m^2]$is soil moisture, W_f is fixed with $150kg/m^2$ as a soil moisture at field capacity. Actual evapotranspiration is proportional to the soil moisture W.

Water balance equation of soil is represented as [Eq. 5]

$$\frac{dW}{dt} = Rainf + Q_{sm} - E - Q_s - Q_{sb} \quad \text{[Eq. 5]}$$

$Q_s[kg/m^2/s]$is surface runoff, $Q_{sm}[kg/m^2/s]$is snow melt rate, Q_{sb} $[kg/m^2/s]$is subsurface runoff. surface runoff Q_s take place based on [Eq. 6]. Runoff scheme of this model is based on saturation excess and beta function which defines runoff as a nonlinear function of soil moisture (Haddeland et al., 2011). Surface runoff is generated if the soil water content exceeded the field capacity.

$$Q_s = \begin{cases} W - W_f & W_f < W \\ 0 & W \leq W_f \end{cases} \quad \text{[Eq. 6]}$$

In case of subsurface runoff Q_{sb}, it is newly added scheme for leaky bucket module compared with original bucket model. Subsurface runoff is generated based on [Eq. 7]. τ and γ are globally uniform as a constant parameter.

$$Q_{sb} = \frac{W_f}{\tau}\left(\frac{W}{W_f}\right)^{\gamma} \quad \text{[Eq. 7]}$$

River routing module of H08 is based on TRIP (Total Runoff Integrating Pathways) model (Oki and Sud, 1998). Land surface module calculates runoff on every grid, and then river routing module calculate river discharge accumulating runoff from upper grid based on flow direction.

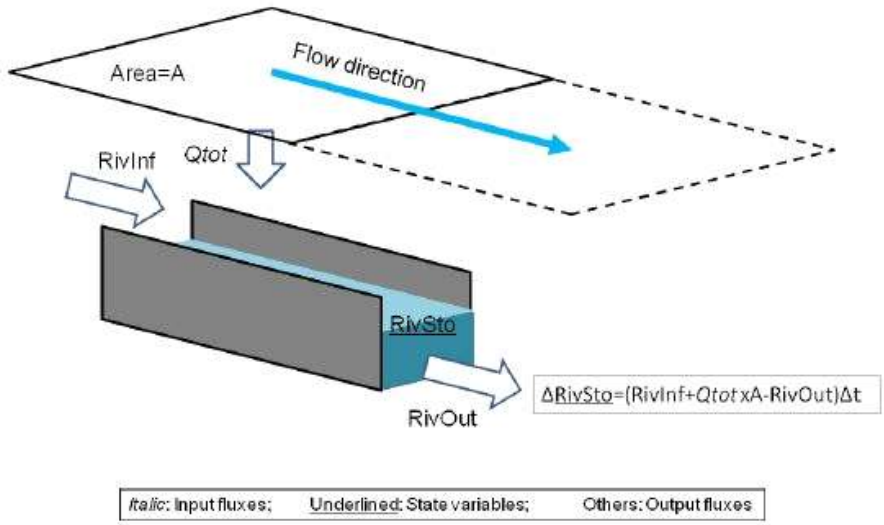

Figure 3 Schematic diagram of the river module of H08 (Hanasaki and Yamamoto, 2010)

There were two reasons for the selection of the H08 model in this study. First, this model can include multiple basins in one simulation to estimate water availability in the Korean Peninsula for the present and future climatic conditions. Second, the simulation results representing the water availability can be shown on a grid for spatial implications as a result, since H08 is a grid-based hydrological model. In this study, the land surface module and river routing module of H08 is applied.

For regional application of the global hydrological model H08, the applicable spatial resolution is 5′ × 5′ (approximately 9 km × 9 km) owing to the model structure. In case of Korean Peninsula, the spatial domain for simulation was set to be 124°E - 131°E, 33°N - 44°N.

Accordingly, in this mode, the Korean peninsula is configured by 84 grids on the horizontal axis, 123 grids on the vertical axis. It consists of a total number of 11088 grids.

2.3. Meteorological data

Eight meteorological variables (albedo, surface pressure, rainfall rate, wind speed, longwave downward radiation, specific humidity, shortwave downward radiation, air temperature) for H08 simulation is presented in Table 5. The input data for the past time period is provided by the Second Global Soil Wetness Project (GSWP2). In order to model surface - atmosphere system and provide the soil wetness data as a critically important component of the global energy and water balance (Dirmeyer et al., 2006), Global Soil Wetness Project (GSWP) was suggested. GSWP2 distributed the 3-hourly hydro-meteorological data, such as soil moisture, air temperature, water equivalent, and land surface fluxes. Some studies have carried out the validation of GSWP2 based on observed climate data (Hanasaki et al., 2008). The GSWP2 meteorological data can be easily obtained from the server of the H08 meteorological data[3].

3) http://h08.nies.go.jp/ddc/

Table 5 Meteorological variables

Meteorological variables	Unit
Albedo	-
Surface pressure	Pa
Rainfall rate	mm/s
Wind speed	m/s
Longwave downward radiation	W/m^2
Specific humidity	kg/kg
Shortwave downward radiation	W/m^2
Air temperature	K

H08 simulates the energy balance of the land surface as well as the water balance. The most principle meteorological variables to simulate hydrological process are air temperature and precipitation. Therefore, these 2 variables should be validated by comparing with the observed data from the Korea Meteorological Administration. The period of the available data of GSWP2 is 10 years (from 1986 to 1995). The model calibration and validation period was defined to be same as the period of the GSWP2 data.

Various GCMs generate future climate scenarios to assess the impact of climate change. The HadGEM2-AO model was downscaled by Korea Meteorological Administration to a spatial resolution of 1 km in South Korea. In Korean Peninsula, the spatial resolution of the downscaled HadGEM2-AO is 12.5 km. In this study, HadGEM2-AO was selected for climate change impact assessment on the water availability in Korean Peninsula because of its adaptability proved in many previous studies in Korea. HadGEM is known for its excellent performance, especially for East Asia and the Pacific Rim (Korea

Meteorological Administration, 2012). The RCP 8.5 scenario, which assumed current trends for future greenhouse gas emissions, is applied in this study. The climate change impacts based on the monthly climate data were estimated for the same period as Table 4. The climate scenario from the selected GCM is also obtained from the H08 meteorological data server.

Table 6 Classification of the climate data

Classification	Period	Source	Climate model
Observed	1961-1995	KMA (Korea Meteorological Administration)	Observed data
Calibration, validation	1986-1995	GSWP2 (Global Soil Wetness Project 2)	Observed data
Baseline	1971-2000	RCP 8.5 scenario	HadGEM2-AO
2020s	2010-2039		
2050s	2040-2069		
2080s	2070-2099		

The meteorological variables for future periods are same as the variables presented in Table 5. There are various methodologies for the projection and application of future scenarios to the hydrological models. In this study, the “shifting” and “scaling” methods (Lehner et al., 2006) were selected to apply to the future climate variables. This method is relatively simplified by adding, subtracting, or multiplying the amount that is expected to change in the future if present climatic conditions persist, and thus, predicts the impact of future climate change (Hanasaki et al., 2013). Meteorological variables to predict

changes in climate impacts are shown in Table 7. Variables for the future periods include rainfall, air temperature, and longwave downward radiation data. The remaining climate variables are fixed at the present condition.

Table 7 Meteorological variables and elements of the climate change scenario

Variables	Future projection method
Rainfall[$kg/m^2/s$]	Scaling
Air temperature[K]	Shifting
Longwave downward radiation[W/m^2]	Shifting
Shortwave downward radiation[W/m^2]	Fixed
Relative humidity[%]	Fixed
Wind speed[m/s]	Fixed
Air pressure[Pa]	Fixed

2.4. Geographical data

DEM data is provided by hydroSHEDS[4] and is resampled on ArcGIS to adjust the spatial resolution of 5′ × 5′. DEM is the principal geographical data input for the calculation of river discharge, since the flow direction map can be derived from the DEM data. Flow direction has a major influence on the hydrograph of the watershed by determining the length of flow from the starting point of the river to the observation point (Oki and Sud, 1998). The flow direction as a map data input of H08 is presented in Figure 4. Every grid has a specific number, which means the flow direction that is represented by the numbers from 0 to 9. Numbers from 1 to 8 represent various flow

4) http://hydrosheds.cr.usgs.gov/index.php

directions(Figure 4), 0 represents the sea, and 9 means the river outlet.

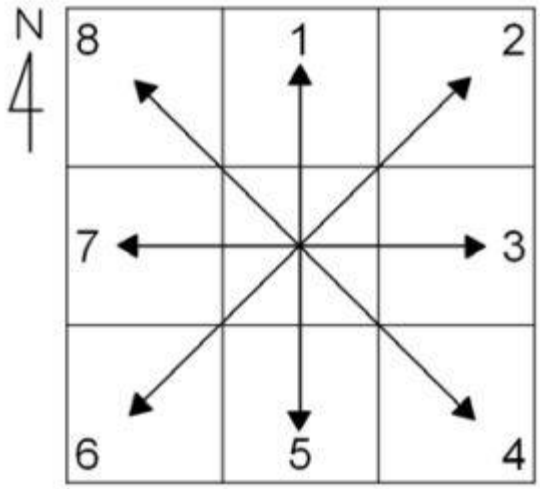

Figure 4 Flow direction for each cell (Hanasaki and Yamamoto(2010))

There are various methods to determine whether the modified flow direction can represent the true conditions. It is necessary to make a manual correction of points in the map (Oki and Sud, 1998), so that the catchment area delineated by the flow direction map could be matched with the actual catchment area. In this study, the comparison of the flow direction map of a spatial resolution of 9 km and the detailed flow direction map was carried out so that the original flow direction map can delineate the relevant catchment area when compared with the actual catchment area by manual correction of the flow direction map. Table 8 presents the catchment area delineated from the corrected flow direction map.

Table 8 Observed and simulated catchment area of the gauging stations from the corrected flow direction map

Watershed	Station	Location		Catchment area(km^2)		
		Lon.	Lat.	Observed	Simulated	Error(%)
Amnok	Supung reservoir	124.96	40.46	52,912	46,291	-14.3
	Unbong reseroir	126.51	41.38	24,168	19,911	-21.38
Taedong	Seohaegabmun reservoir	125.19	38.68	15,714	17,040	7.78
Han	Yeoju	127.65	37.3	11,095	8,673	-21.83
	Jingwan	127.15	37.65	202	203	0.5
	Hangang	126.96	37.52	24,753	21,470	-13.26
Geum	Gongju	127.14	36.46	7,150	7,180	0.42
	Gyuam	126.89	36.28	8,253	7,940	-3.79
Nakdong	Waegwan	128.39	36.18	11,074	11,309	2.12
	Goryeong	128.39	35.75	14,034	14,643	4.34
	Jeokpo	128.36	35.53	16,450	16,665	1.31
	Samrangjin	128.83	35.38	22,892	22,114	-3.4
Yeongsan	Naju	126.73	35.04	2,059	2,101	2.04

2.5. Hydrological data

Hydrological data is essentially required to calibrate and validate simulation results of the hydrological model and to evaluate the model performances. In case of South Korea, the Water Resources Management Information System (WAMIS)[5] provides the historical hydrological data. The observational hydrological data before 1995 can be obtained in terms of water level; so the confirmation and adjustment of the rating curve is required. In case of North Korea, the

5) www.wamis.go.kr

data distributed from the Global Runoff Distribution Center (GRDC)[6] was used. GRDC provides global river discharge data for the historical periods. It is reliable because it is widely used in a variety of previous studies and it is well validated with actual observational discharge data with the stations of the Korean Peninsula (Son et al., 2013). Therefore, the stations in North Korea can be calibrated and validated using the GRDC monthly average data. The stations in Korean Peninsula from the GRDC data are listed in Table 9.

Table 9 Information of stations in the Korean Peninsula from GRDC

Country [7]	Watershed	Station	Location		Area[km^2]
			Lon.	Lat	
KP	Duman	Yenam	128.83	41.73	720
KP	Amnok	Jonchon	126.45	40.67	2192
KP		Kumchang	127.13	41.53	18245
KP	Taedong	Mirim	125.78	39.02	12175
KP		Dokchon	126.3	39.75	3300
KP		Songchon	126.22	39.27	1878
KP		Samdung	126.18	38.98	2727
KR	Han	Indogyo	126.97	37.52	25046
KR		Yeoju	127.648	37.2961	11104.4
KR	Geum	Gongju	127.126	36.4636	7149.5
KR	Yeongsan	Naju	126.734	35.0333	2058.7
KR	Seomjin	Sing Jeon	127.57	35.18	4480
KR	Nakdong	Waegwan	128.394	36.0003	11074.4
KR		Jindong	128.48	35.38	20403
KR		Samrangjin	128.85	35.4	22916

The objective of this study is to estimate the impact of changes in the hydrological status and future water availability across the entire

6) http://www.bafg.de/GRDC/EN/03_dtprdcts/32_LTMM/longtermmonthly_node.html
7) KP : North Korea(Democratic People's Republic of Korea), KR : South Korea(Republic of Korea)

peninsula. Therefore, it is necessary to represent the simulation results for the main river basins in the peninsula. In case of North Korea, Amnok, Duman, Chongchon, and Taedong river basins were selected based on the major gauging stations. In case of South Korea, Han, Nakdong, Geum, and Yeongsan river basins were selected based on the major gauging stations. Table 10 provides the basic information on the major river basins and stations in Korean Peninsula.

Table 10 Observation period and references of hydrological data

Watershed	Station	Data period	Reference
Amnok	Kumchang	1976-1984	Global Runoff Data Center[8]
Duman	Yenam	1976-1979	
	Khasan	-	-
Chongchon	Pugwon	1923-1927	Lautensach, 1988
	Puksongri	1923-1927	
Taedong	Mirim	1976-1982	Global Runoff Data Center
	Dokchon	1976-1981	
Han	Yeoju	1986-1995, 1976-2009	Korea Water Resources Corporation[9], Global Runoff Data Center
	Hangang	1986-1995, 1947-1979	
Geum	Gongju	1986-1995, 1976-2009	
	Gyuam	1986-1995	
Nakdong	Waegwan	1986-1995, 1976-2009	
	Jeokpo	1986-1995	
	Samrangjin	1986-1995, 1953-1972	
Yeongsan	Naju	1986-1995, 1976-2009	

8) http://www.bafg.de/GRDC/EN/03_dtprdcts/32_LTMM/longtermmonthly_node.html
9) www.wamis.or.kr

Ⅳ. Results and discussion

1. Validation of meteorological data

1.1. Validation and bias correction of GSWP2 data

Meteorological data of GSWP2 is used for the period of model calibration and validation due to the accessibility of historical climate data for H08 simulation. The period of the data is 10 years from 1986 to 1995. Verification of the data is carried out by comparing observed 30-year climatological normals from 1981 to 2010 distributed by Korea Meteorological Administration[10]. Analyzed meteorological variables are air temperature and precipitation. Major weather stations used for validation of GSWP2 historical data are suggested on Table 11.

Table 11 Meteorological stations in the Korean peninsula

Watershed	Station	Location	
		Longitude	Latitude
Duman river	Sonbong	130.4	42.32
Amnok river	Hyesan	128.17	41.4
	Sinuiju	124.38	40.1
Chongchon river	Anju	125.65	39.62
Taedong river	Pyongyang	125.78	39.03
Ryesong river	Kaesong	126.57	37.97
Han river	Seoul	126.97	37.57
	Chuncheon	127.74	37.9
Geum river	Daejeon	127.39	36.37
Nakdong river	Busan	129.03	35.02
Yeongsan river	Gwangju	126.89	35.17
Seomjin river	Namwon	127.39	35.4

10) http://www.kma.go.kr/weather/climate/average_north.jsp

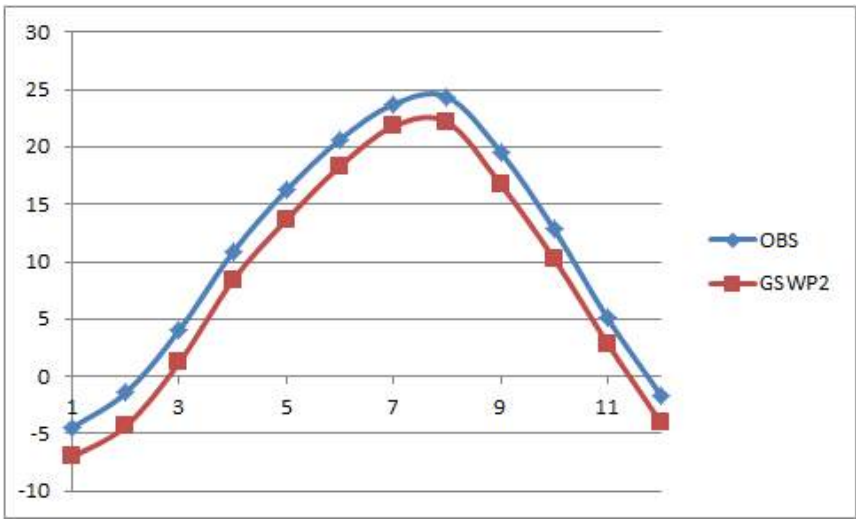

Figure 5 Comparison of monthly average temperature[℃] between observation and GSWP2

Figure 5 shows comparison of mean monthly air temperature of GSWP2 and observed data of the stations presented in Table 11. Mean monthly air temperature of GSWP2 is lower than observed value in a certain amount for the simulated period constantly. The original spatial resolution of GSWP2 meteorological data is 1 degree × 1 degree, so it is interpolated to a spatial resolution of 5 minutes × 5 minutes which was same as H08 simulation. In order to correct meteorological bias between observed data and simulated data, a ratio between observed value and simulated value can be defined as a bias correction factor (Bao et al., 2012). The bias of simulated GSWP2 meteorological data was corrected by multiplying monthly correction factor. Mean monthly temperature for observed data, GSWP2 data, and their correction factor are suggested on Table 12. As a result, calculated R^2 of corrected

GSWP2 mean annual temperature data and observed data for 10 years is 0.8879 (Figure 6).

Table 12 Comparison of observation and GSWP2 monthly temperature and correction factor

Month	OBS[℃]	GSWP2[℃]	Correction factor
1	-4.45	-7.02538	0.633418
2	-1.425	-4.32852	0.329212
3	4.05	1.225806	3.303948
4	10.84167	8.385971	1.292834
5	16.23333	13.65018	1.18924
6	20.64167	18.31283	1.12717
7	23.725	21.79436	1.088585
8	24.35833	22.16645	1.098883
9	19.55833	16.73821	1.168484
10	12.83333	10.24916	1.252136
11	5.058333	2.856155	1.771029
12	-1.68333	-4.07071	0.413523
average	10.81181	8.329541	

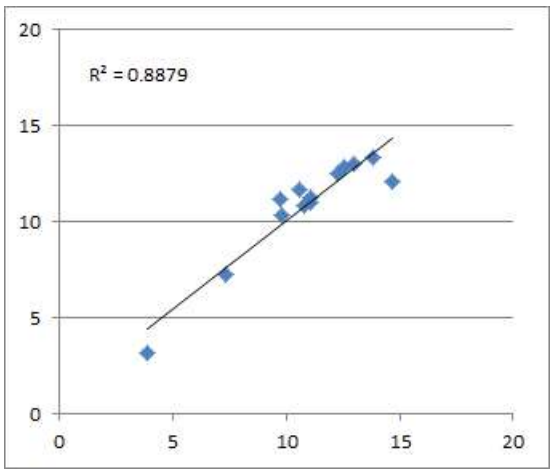

Figure 6 Comparison of annual average temperature[℃] between observation and GSWP2

Comparison of mean monthly precipitation between observation and GSWP2 data is also presented in Figure 7. In case of precipitation, GSWP2 data appeared similar to the observed data except for the small differences in winter period (Table 13).

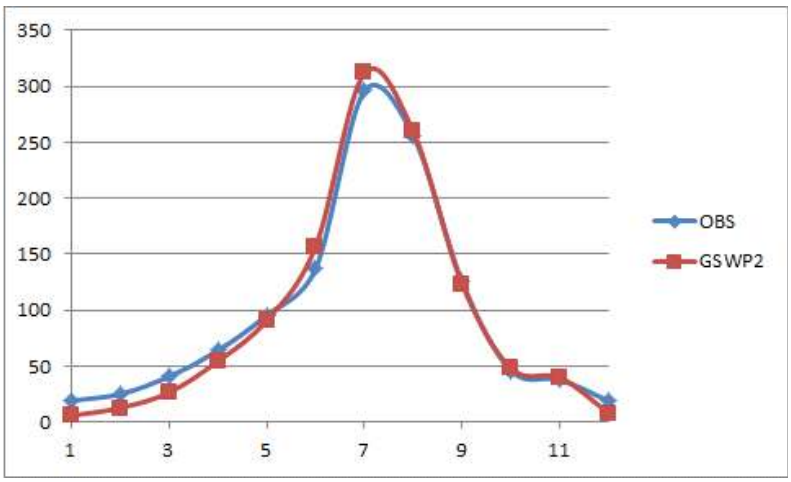

Figure 7 Comparison of monthly average precipitation[mm] between observation and GSWP2

Corrected mean annual precipitation data of GSWP2 compared with observed data for 10 years from 1986 to 1995 and calculated R^2 is presented in Figure 8.

As a result of bias correction of GSWP2 data, Figure 9 shows spatial variability of meteorological variables of GSWP2 used in this study for model calibration and validation period.

Table 13 Comparison of observation and GSWP2 monthly precipitation and correction factor

Month	OBS[mm]	GSWP2[mm]	Correction factor
1	19.01667	5.690204	3.342001
2	24.85833	12.46111	1.994874
3	40.45833	26.31819	1.537276
4	63.78333	54.21428	1.176504
5	95.41667	90.70703	1.051921
6	136.9	156.74	0.873421
7	295.7417	311.9215	0.948129
8	255.75	259.5222	0.985465
9	125.2917	123.2059	1.016929
10	45.83333	47.76976	0.959463
11	37.73333	39.66203	0.951372
12	18.85	7.829944	2.407425
sum	1159.633	1136.042	

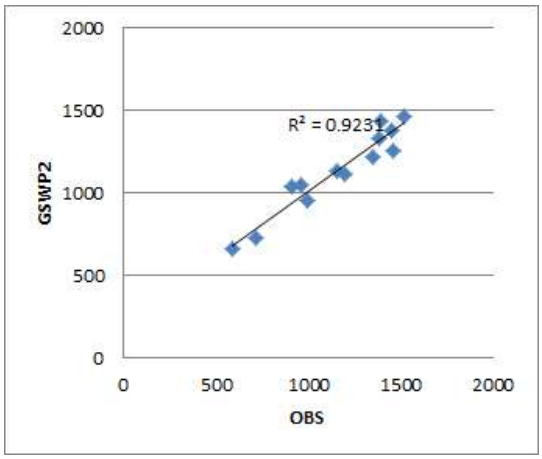

Figure 8 Comparison of annual precipitation[mm] between observation and GSWP2

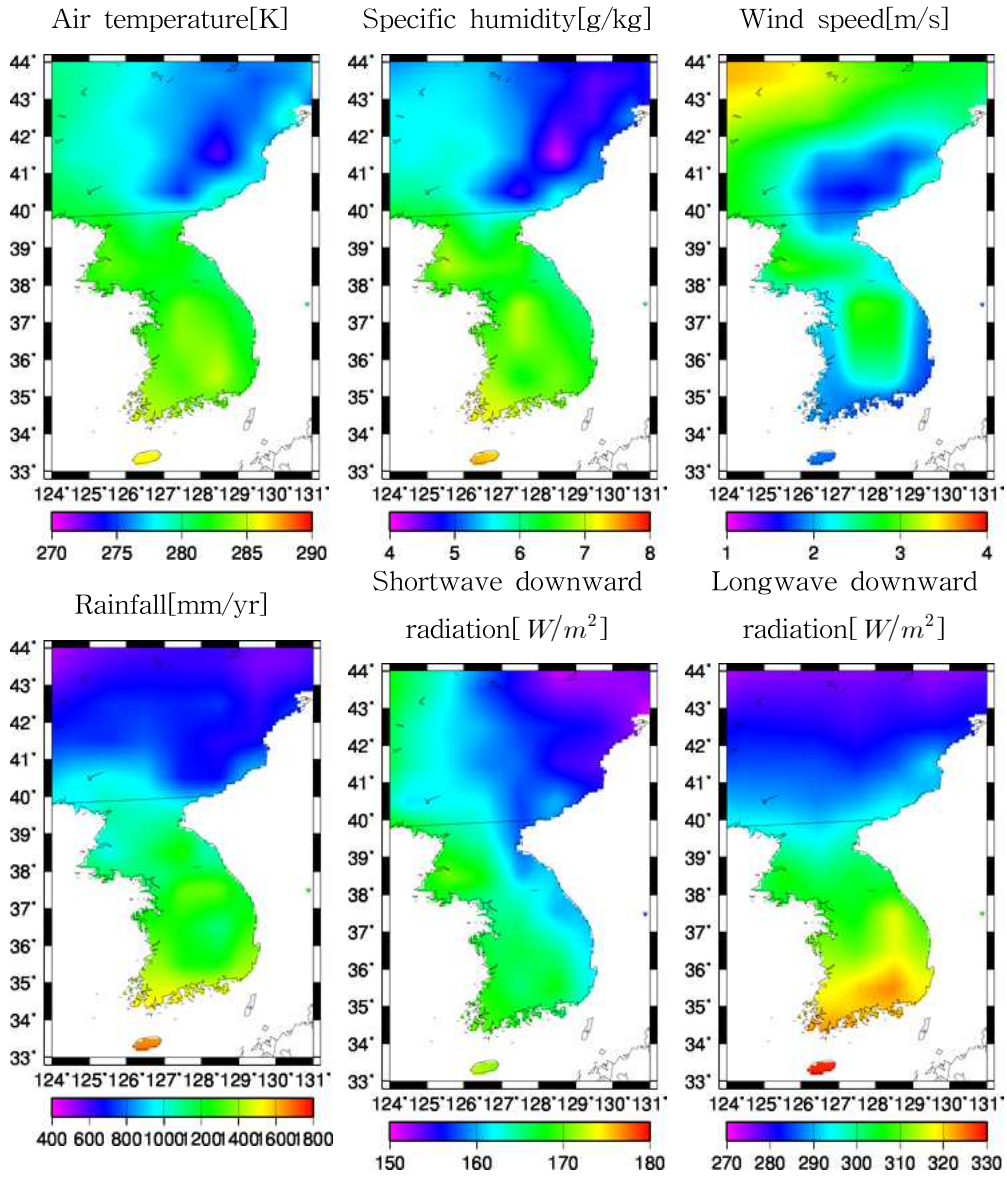

Figure 9 Meterological data from GSWP2 (average value from 1986 to 1995)

1.2. Validation and bias correction of GCM historical data

HadGEM2-AO is selected for climate change simulation as GCM in this study because most of previous studies in Korea selected this model for climate change impact assessment due to its adaptability to East Asia and the Pacific Rim (Korea Meteorological Administration, 2012). The validation and bias correction of air temperature and precipitation derived from the GCM is also carried out by using same method as the process of GSWP2 data based on 30-year climatological normals from 1981 to 2010.

Simulated mean monthly air temperature from the GCM is presented in Figure 10 compared with observed data. Same methodology used in the bias correction of GSWP2 data was applied for bias correction of climate data from GCM. Correction factor was defined as changed ratio from observed value to simulated value on a monthly basis (Table 14). Corrected temperature data of GCM on a annual basis is presented in Figure 11 compared with observed data for 10 years from 1986 to 1995.

Table 14 Comparison of observation and HadGEM2-AO monthly temperature and correction factor

Month	OBS[℃]	HadGEM2-AO[℃]	Correction factor
1	-4.45	-6.34092	0.701791
2	-1.425	-3.63876	0.391617
3	4.05	2.74544	1.475174
4	10.84167	9.510232	1.14
5	16.23333	15.05778	1.078069
6	20.64167	19.20608	1.074747
7	23.725	22.01859	1.077499
8	24.35833	22.39392	1.087721
9	19.55833	18.34633	1.066063
10	12.83333	12.13416	1.05762
11	5.058333	3.947176	1.281507
12	-1.68333	-2.95247	0.570144
average	10.81181	9.368963	

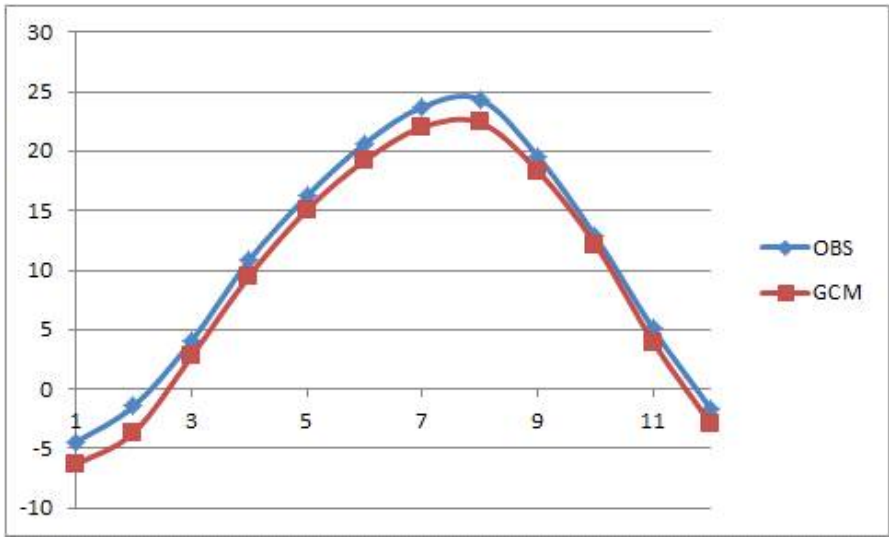

Figure 10 Comparison of monthly average temperature[℃] between observation and HadGEM2-AO

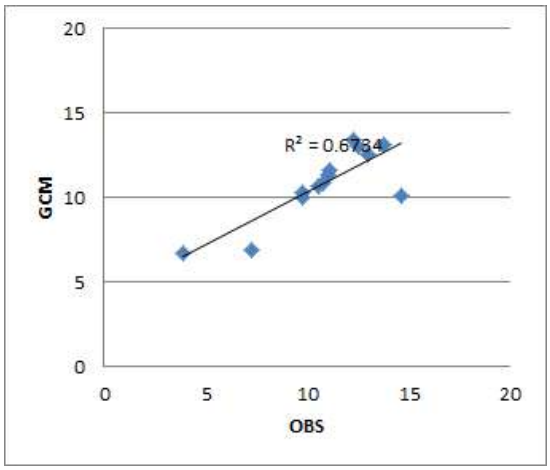

Figure 11 Comparison of annual temperature[℃] between observation and HadGEM2-AO

Figure 12 shows precipitation of GCM and observation. In case of precipitation data, GCM was evaluated that most GCMs could not simulate the peak rainfall events in summer so that the amount of summer rainfall is smaller than observed precipitation data. This is because GCM has low ability on simulating storm in summer and local rainfall events (Moon et al., 2013). Therefore, bias correction process was carried out in a same way as described above which is multiplying monthly correction factor. Figure 12 shows mean monthly precipitation of GCM and observation, and the value of correction factor is also presented in Table 15.

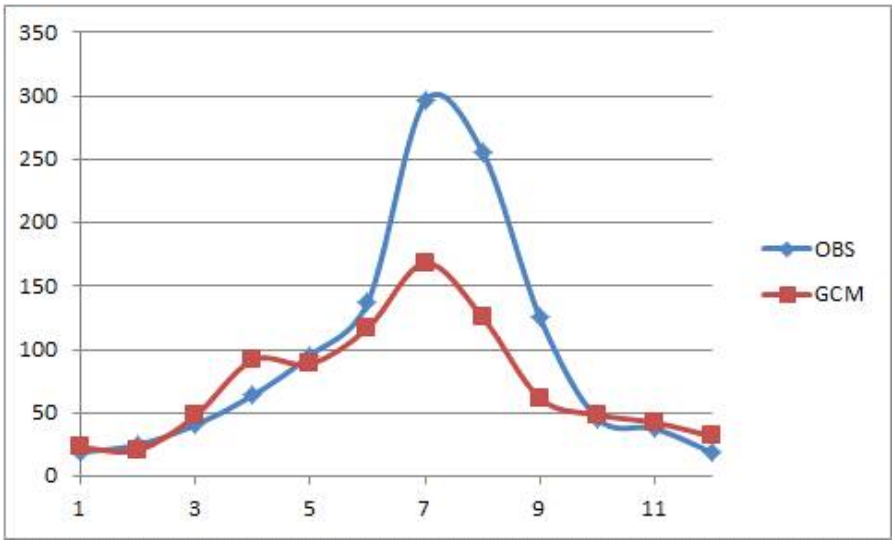

Figure 12 Comparison of monthly average precipitation[mm] between observation and HadGEM2-AO

Table 15 Comparison of observation and HadGEM2-AO monthly precipitation and correction factor

Month	OBS[mm]	HadGEM2-AO[mm]	Correction factor
1	19.01667	22.92972	0.829346
2	24.85833	20.69282	1.201302
3	40.45833	47.71821	0.847859
4	63.78333	91.64412	0.695989
5	95.41667	88.79413	1.074583
6	136.9	116.8833	1.171254
7	295.7417	168.1376	1.758926
8	255.75	125.4675	2.038376
9	125.2917	61.65168	2.032251
10	45.83333	48.55482	0.94395
11	37.73333	42.38216	0.890312
12	18.85	31.59677	0.59658
sum	1159.633	866.4529	

Corrected annual precipitation and observed data are plotted in Figure 13. Figure 14 and 15 present monthly precipitation of the stations

before versus after the bias correction of GCM. In case of North Korea, the precipitation is relatively low compared with regions of South Korea. The precipitation in northern region is slightly increased and southern region is slightly decreased in the process of multiplying uniform correction factor across the whole Korean Peninsula. It is because the amount of mean annual rainfall in southern region is larger than the northern region as shown in Figure 9

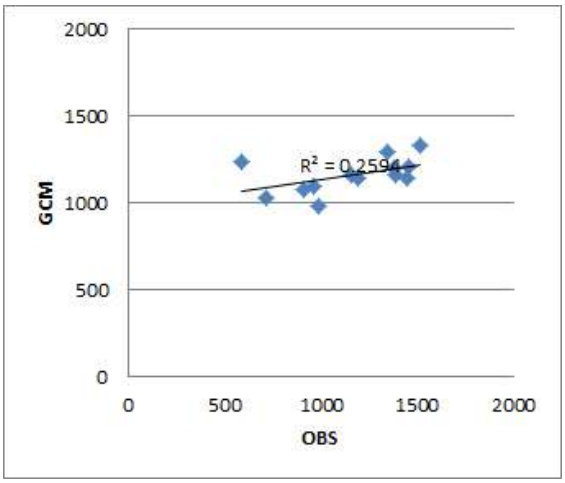

Figure 13 Comparison of annual precipitation[mm] between observation and HadGEM2-AO

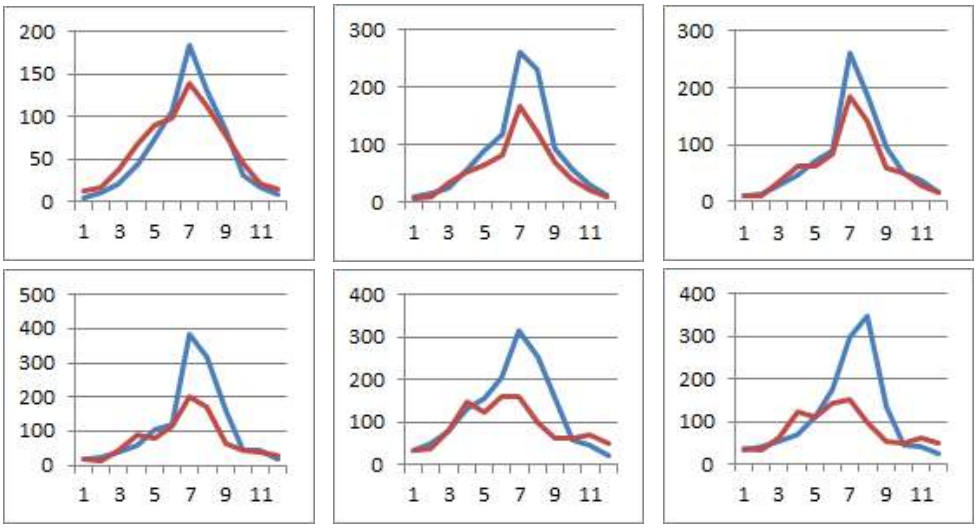

Figure 14 Monthly average precipitation from HadGEM2-AO for representative stations in Korean Peninsula before bias correction (from the top left: Sonbong, Sinuiju, Pyongyang, Chuncheon, Busan, Namwon).
Blue line : OBS, red line : HadGEM2-AO

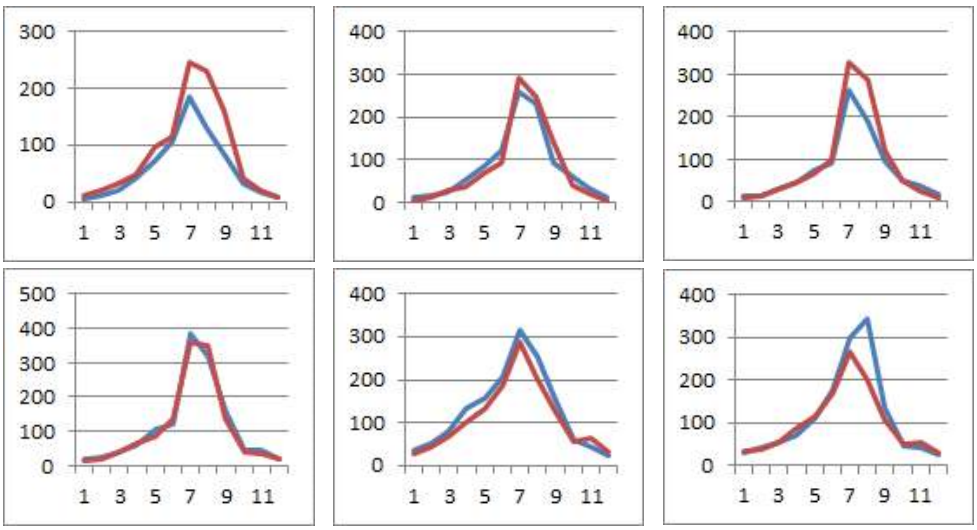

Figure 15 Monthly average precipitation from HadGEM2-AO for representative stations in Korean Peninsula after bias correction (from the top left: Sonbong, Sinuiju, Pyongyang, Chuncheon, Busan, Namwon)
Blue line : OBS, red line : HadGEM2-AO

2. Calibration and validation of H08

2.1. Parameter sensitivity analysis

The most sensitive parameters in H08 are soil depth SD, bulk transfer coefficient C_D that affects potential evapotranspiration, time constant τ that determines daily maximum subsurface runoff, and shape parameter γ related with a relationship between subsurface runoff and soil moisture (Masood et al., 2015; Hanasaki et al., 2014). Therefore, it is necessary to investigate the effects of these 4 variables on runoff hydrograph through a sensitivity analysis of the parameters.

Default values of 4 parameters in H08 are as follows: SD is 1m, C_D is 0.003, τ is 100, γ is 2. These default values were decided as a standard value for the turing of parameters. A lower bound of parameter is decided as a half of default value and an upper bound is decided as doubled default value (Table 16). The sensitivity analysis was carried out for 10 years from 1986 to 1995 which was set to the period of model calibration and validation for Hangang gauging station.

Table 16 Tested parameters for calibration

	SD	C_D	γ	τ
Lower bound	0.5	0.0015	1.0	50
H08 default value	1.0	0.003	2.0	100
Upper bound	2.0	0.006	4.0	200

In case of parameter SD, runoff hydrograph became gradual as the

soil depth increases (Figure 16) based on [Eq. 6] which calculates surface runoff from land surface module.

$$Q_s = \begin{cases} W - W_f & W_f < W \\ 0 & W \leq W_f \end{cases} \quad \text{[Eq. 6]}$$

Surface runoff Q_s is generated when the soil moisture W exceeds field capacity W_f. Figure 16 shows that runoff generation is delayed fluctuation of runoff hydrograph is decrease as SD increases because maximum capacity of soil moisture increases with soil depth. In a spring and winter season which recorded relatively low precipitation, generated runoff from the case of high value in SD is bigger than the case of low SD. On the other hand, it is simulated that generated runoff of high SD is smaller than the case of low SD.

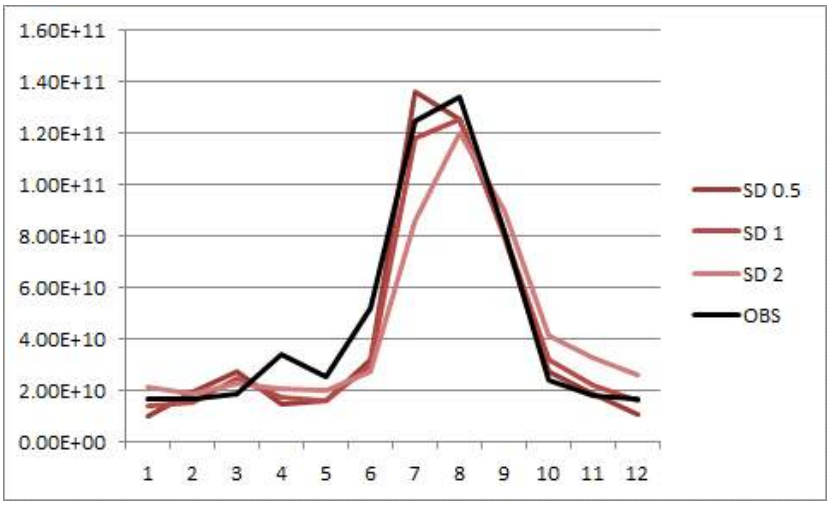

Figure 16 Discharge of Han River according to the changes in SD [mm/day]

Bulk transfer coefficient C_D is a parameter that directly affects to potential evapotranspiration E_P based on [Eq. 2].

$$E_P(T_S) = \rho C_D U(q_{SAT}(T_S) - q_a) \quad \text{[Eq. 2]}$$

When C_D increases, potential evapotranspiration increases according to [Eq. 2] and runoff decreases based on the water balance equation [Eq. 5]. Figure 17 presents the tendency of runoff generation according to the variation of C_D.

$$\frac{dW}{dt} = Rainf + Q_{sm} - E - Q_s - Q_{sb} \quad \text{[Eq. 5]}$$

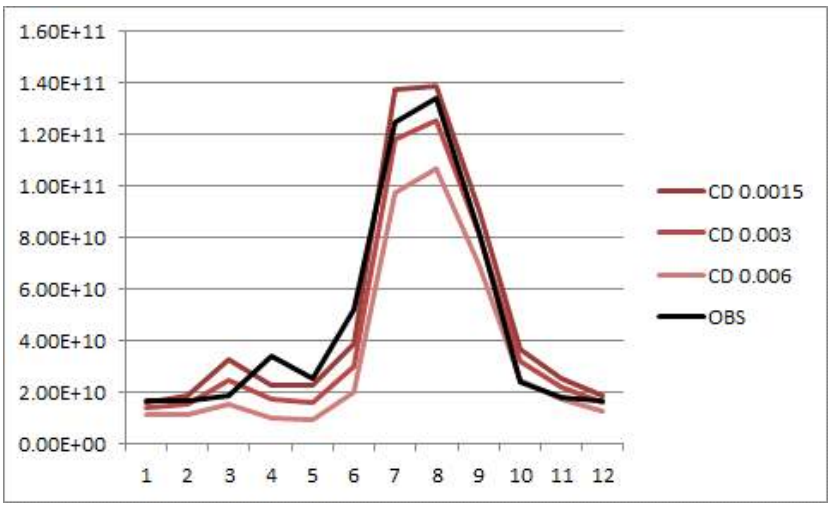

Figure 17 Discharge of Han River according to the changes in CD [mm/day]

Subsurface runoff Q_{sb} is calculated by [Eq. 7] that determines a relationship between soil moisture W and field capacity W_f.

$$Q_{sb} = \frac{W_f}{\tau}(\frac{W}{W_f})^{\gamma} \quad \text{[Eq. 7]}$$

As shown in Figure 18, runoff decreases with increasing γ except for summer that rainfall is concentrated. When the rainfall is concentrated, soil moisture increases to the field capacity, and then W/W_f approaches to 1. It means that the influence of γ on a runoff hydrograph decreases with increasing precipitation. The value of W/W_f is below 1 except for summer. Therefore, when γ increases, subsurface runoff Q_{sb} decreases and surface runoff Q_s increases based on a water balance equation [Eq. 3] under the condition precipitation and evapotranspiration is constant. τ is time constant which determines daily maximum subsurface runoff. When τ increases, subsurface runoff Q_{sb} decreases, and surface runoff Q_s increased based on [Eq. 7]. The parameter γ and τ affects the sensitivity of variation in Q_{sb} and Q_s. It should be noted that the sensitivity of these parameters to total runoff hydrograph which can be divided into a subsurface and surface runoff should be investigated (Mateo, 2012). In case of the parameter γ and τ, total runoff decrease with increasing values of the 2 parameters respectively (Figure 18, 19).

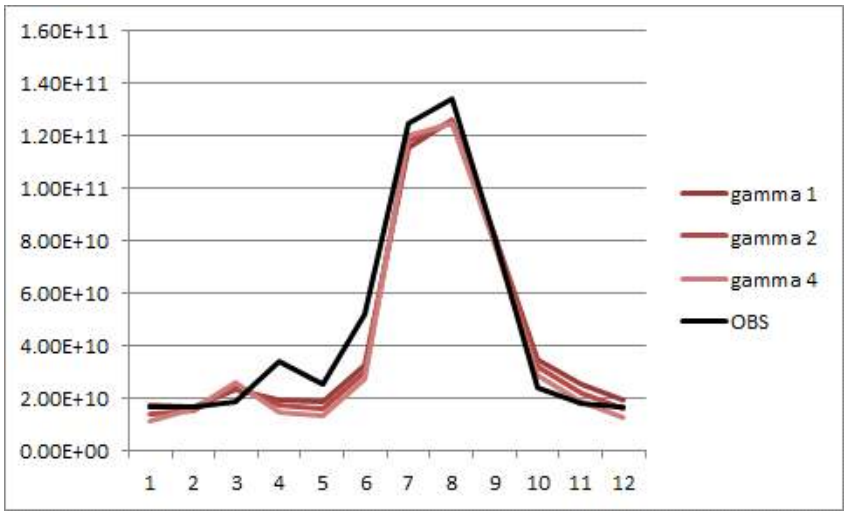

Figure 18 Discharge of Han River according to the changes in γ [mm/day]

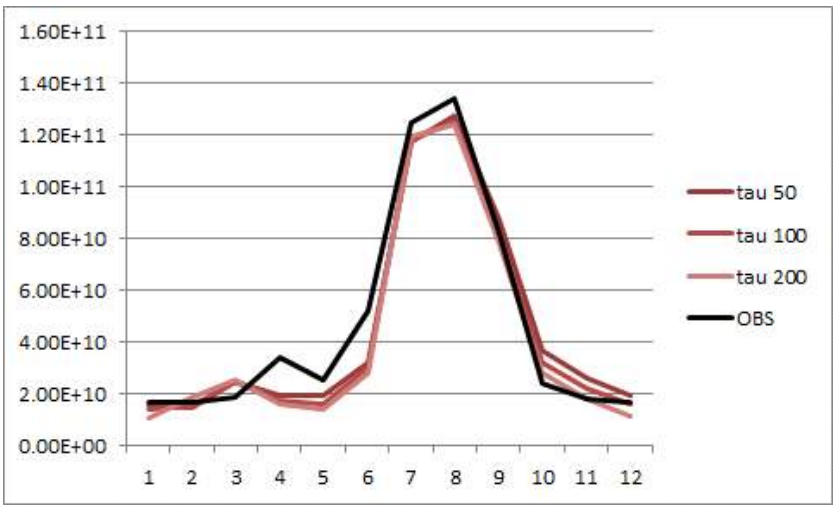

Figure 19 Discharge of Han River basin according to the changes in τ [mm/day]

2.2. Calibration of parameters

Model calibration and validation is carried out based on the GSWP2 meteorological data for 10 years of the period from 1986 to 1995. The

parameters were tuned for the first 5 years, and then simulated results based on the tuned parameters are validated for the last 5 years. Table 17 describes the list of gauging stations in the Korean Peninsula and types of available data used for calibration and validation. The code of the stations are temporarily assigned for convenience in the simulation process (Table 17). The observed discharge data of the GRDC which was used to calibrate the simulation results of the North Korea, only monthly data was available so that the interannual variations of simulated discharge did not considered for the calibration. In case of South Korea, WAMIS provide the interannual variability of river discharge as well as monthly discharge.

Table 17 Code of discharge stations and available types of observation data in this study

Watershed	Station	Code	Available OBS data[11)]
Amnok	Supung reservoir	N1	-
	Unbong reservoir	N2	-
	Kumchang	N3	M
Duman	Khasan	N4	-
	Yenam	N5	M
Chongchon	Puksongri	N6	-
Taedong	Seohaegabmun	N7	-
	Mirim	N8	M
	Dokchon	N9	M
Han	Yeoju	S1	M, Y
	Hangang	S2	M, Y
Geum	Gongju	S3	M, Y
	Gyuam	S4	M, Y
Nakdong	Waegwan	S5	M, Y
	Jeokpo	S6	M, Y
	Samrangjin	S7	M, Y
Yeongsan	Naju	S8	M, Y

The range of the parameters for calibration is same as shown in Table 16, and then the simulation was carried out for 81(=3^4) times for possible all the combinations of parameter set based on Table 16.

In order to derive optimal parameter set that can represent the hydrological process similar to real world, Nash-Sutcliffe model efficiency coefficient (NSE) is decided as an index to evaluate the applicability of model. NSE can be calculated by [Eq. 8]. Q_o^t is observed value at time t, $\overline{Q_o}$ is average total observed value, and Q_m^t is simulated value at time t (Nash and Sutcliffe, 1970). NSE has a value of range from $-\infty$ to 1. If the observed value and the simulated value is exactly same, NSE is represented to 1. Therefore, a simulated parameter set which has a value of NSE close to 1 is evaluated as a optimal parameter set that can simulates the real hydrologic phenomena reliably.

$$NSE = 1 - \frac{\sum_{t=1}^{T}(Q_o^t - Q_m^t)^2}{\sum_{t=1}^{T}(Q_o^t - \overline{Q_o})^2} \quad \text{[Eq. 8]}$$

Calculated NSE value is presented in Figure 20 based on simulated monthly discharge. Parameter sets are presented in Table 18 according to the value of NSE in highest order for the stations in Table 17

11) M : Only monthly average data for years of table10 is available, Y : Monthly average data and its interannual variation for years of table 10 is available

which have observed data for the simulated period, and then the parameter set which has the highest value of NSE is selected as an optimal parameter set that can represent the Korean Peninsula.

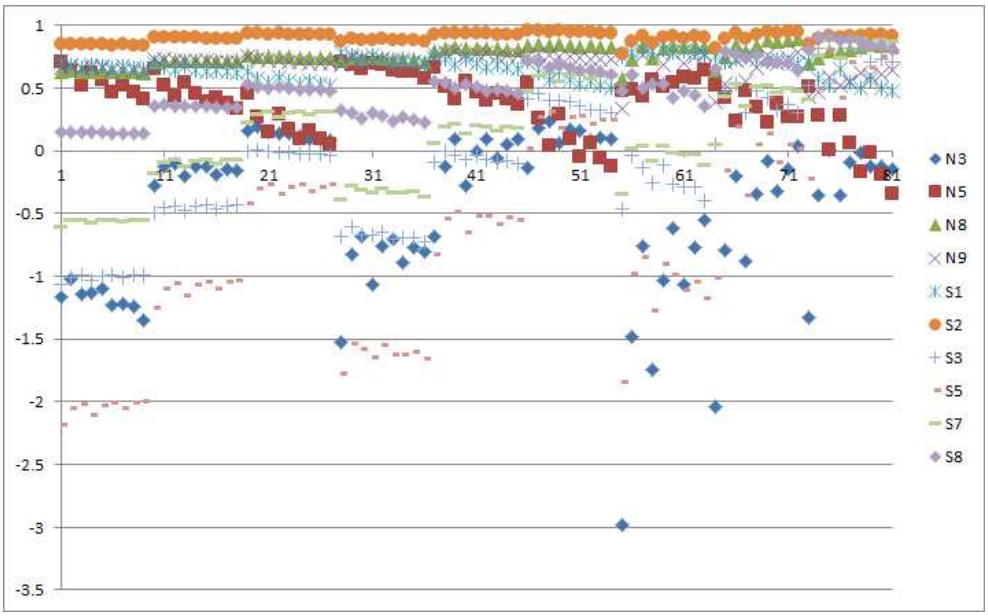

Figure 20 81 combinations of parameters and NSE for Kumchang, Yenam, Mirim, Dokchon, Yeoju, Hangang, Gongju, Waegwan, Samrangjin, Naju station for calibration period

Figure 20 shows all values of NSE based on the possible combinations of parameters. It is investigated that applicability of the parameter set which is represented as NSE value of the stations located in the South Korea is higher than the stations located in North Korea. Especially Kumchang station showed a lowest applicability with the low value of NSE. It is because the historical data of stations in South Korea is obtained in a same period with simulated period unlike

the stations located in North Korea. Table 18 shows 5 parameter sets which have the highest NSE value based on the simulated monthly discharge for 10 stations of the Korean Peninsula.

Table 18 Selected parameter set according to average NSE value

	SD	CD	γ	τ
Set 1	1.0	0.006	1.0	50
Set 2	1.0	0.006	1.0	100
Set 3	2.0	0.003	2.0	200
Set 4	2.0	0.003	4.0	200
Set 5	1.0	0.006	1.0	200

It was presented that top 5 combinations of parameters which have highest value of NSE among the 81 combinations in Table 19. The set 2 in Table 19 has the highest value in average NSE for the representative stations. Therefore, combination of parameters of set 2 is decided as an optimal parameter set for the Korean Peninsula.

Table 19 Order of parameter set according to ranking of respective NSE value of the stations and average NSE value of stations

Station	NSE				
	Set 1	Set 2	Set 3	Set 4	Set 5
N3	-0.1390209	0.1868466	-0.0760563	0.0377594	0.2333258
N5	0.5405963	0.2584994	0.2225441	0.2720746	0.0420492
N8	0.8434685	0.8494597	0.8846761	0.8932102	0.8424649
N9	0.7534607	0.7690814	0.7657216	0.7879039	0.7641413
S1	0.7064974	0.6210934	0.7216428	0.698029	0.5612036
S2	0.9601957	0.9593224	0.9471908	0.9496881	0.9508327
S3	0.4154237	0.4575716	0.4233243	0.3028412	0.4020997
S5	0.0143175	0.2668974	0.1356563	0.0198941	0.3088179
S7	0.473001	0.5987461	0.5199958	0.4737668	0.6193086
S8	0.7214605	0.7058833	0.7111296	0.6414967	0.6668549
average	0.52894	0.56734	0.525583	0.507666	0.53911

2.3. Validation of simulated discharge

A performance of the calibrated model was validated for the validation period based on the tuned parameters through the estimation of river discharge for major rivers in Korean Peninsula. An indicator for the evaluation of applicability of the calibrated model is NSE value which was used in the calibration process. Long-term historical discharge data for the calibration and validation period is obtained only for the stations in South Korea, such as Yeoju, Hangang station in Han River basin, Gongju, Gyuam station in Geum River basin, Waegwan, Jeokpo, Samrangjin station in Nakdong River basin, Naju station in Yeongsan River basin. The value of NSE derived from the river discharge simulation for the 10 years is presented in Table 20 based on the calibrated model. Simulated and observed hydrograph can be found in Figure 21 based on the calculated NSE in Table 20.

Table 20 NSE of calibrated H08 simulation result for calibration and validation period

Watershed	Station	NSE	
		Calibration period (1986-1990)	Validation period (1991-1995)
Han	Yeoju(S1)	0.279	0.643
	Hangang(S2)	0.756	0.732
Geum	Gongju(S3)	0.847	0.37
	Gyuam(S4)	0.852	0.806
Nakdong	Waegwan(S5)	0.702	0.397
	Jeokpo(S6)	0.848	0.777
	Samrangjin(S7)	0.56	0.725
Yeongsan	Naju(S8)	0.262	0.37

Yeoju station in Han River basin showed low applicability based on the selected parameter set for the calibration period, whereas the applicability for validation period is good. It is because a trend of the observed and simulated discharge appears to be different for the earlier period of calibration. Naju station in Yeongsan River basin also has low applicability due to the hydrologic phenomena in 1990 and missing data in 1992. In the year 1990, a trend of the hydrograph of all stations showed similar tendency except for observed data of Naju station. Simulated discharge of Naju in the year 1990 and 1992 has a similar tendency with other stations in Table 20. It is seemed that a regional hydro-meteorological phenomenon is not reflected in this model as shown in the hydrograph of the Figure 21(h).

Figure 22 shows mean monthly discharge of all the simulated and observed period for the stations. Kumchang station in Amnok River basin showed the strongest discrepancy between the observed and

simulated data. Thus the applicability based on NSE value of Kumchang station is evaluated as relatively poor. An applicability of the model for Taedong River basin is evaluated as appropriate based on NSE value over 0.7 for the correspondence of overall tendency of hydrograph despite the discrepancy of summer discharge for Mirim and Dokchon station located in a downstream area of Taedong River basin (Table 20). In case of the stations in South Korea, applicability of the calibrated model is evaluated as high based on the NSE value over 0.5 for the most part of the stations with similar tendency of simulated and observed discharge because of the consensus of the simulated and observed period.

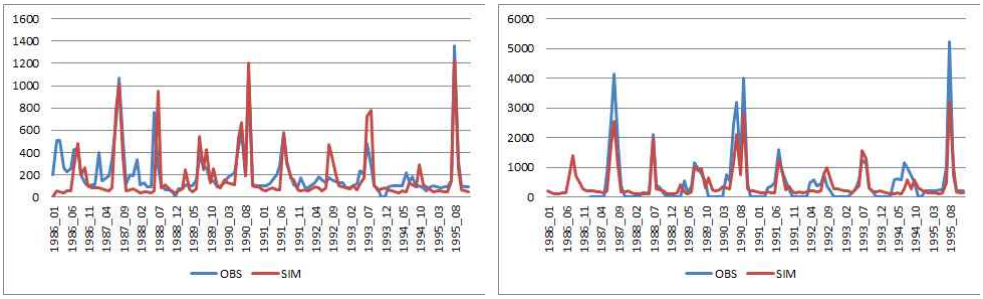

(a)

(b)

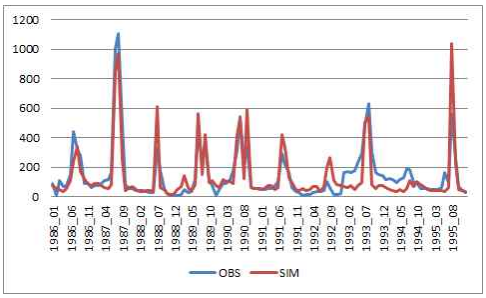

(c)

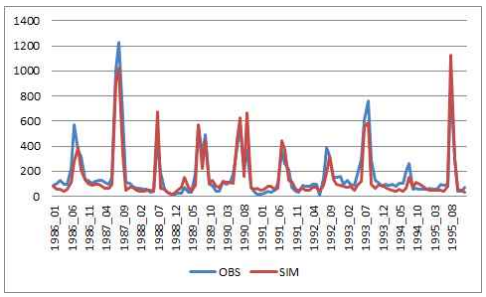

(d)

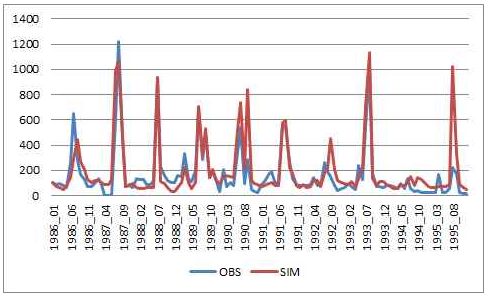

(e)

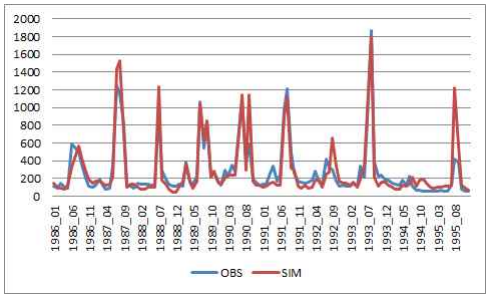

(f)

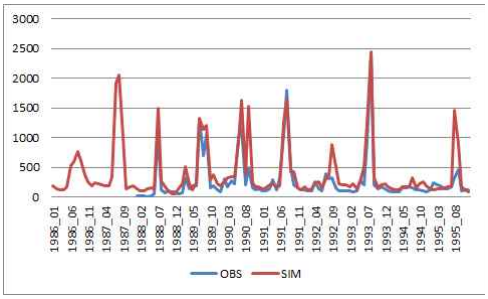

(g)

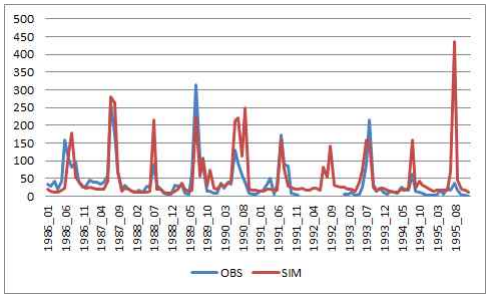

(h)

Figure 21 Observed and simulated discharge[m^3/s] for (a)Yeoju (b)Hangang (c)Gongju (d)Gyuam (e)Waegwan (f)Jeokpo (g)Samrangjin (h)Naju station

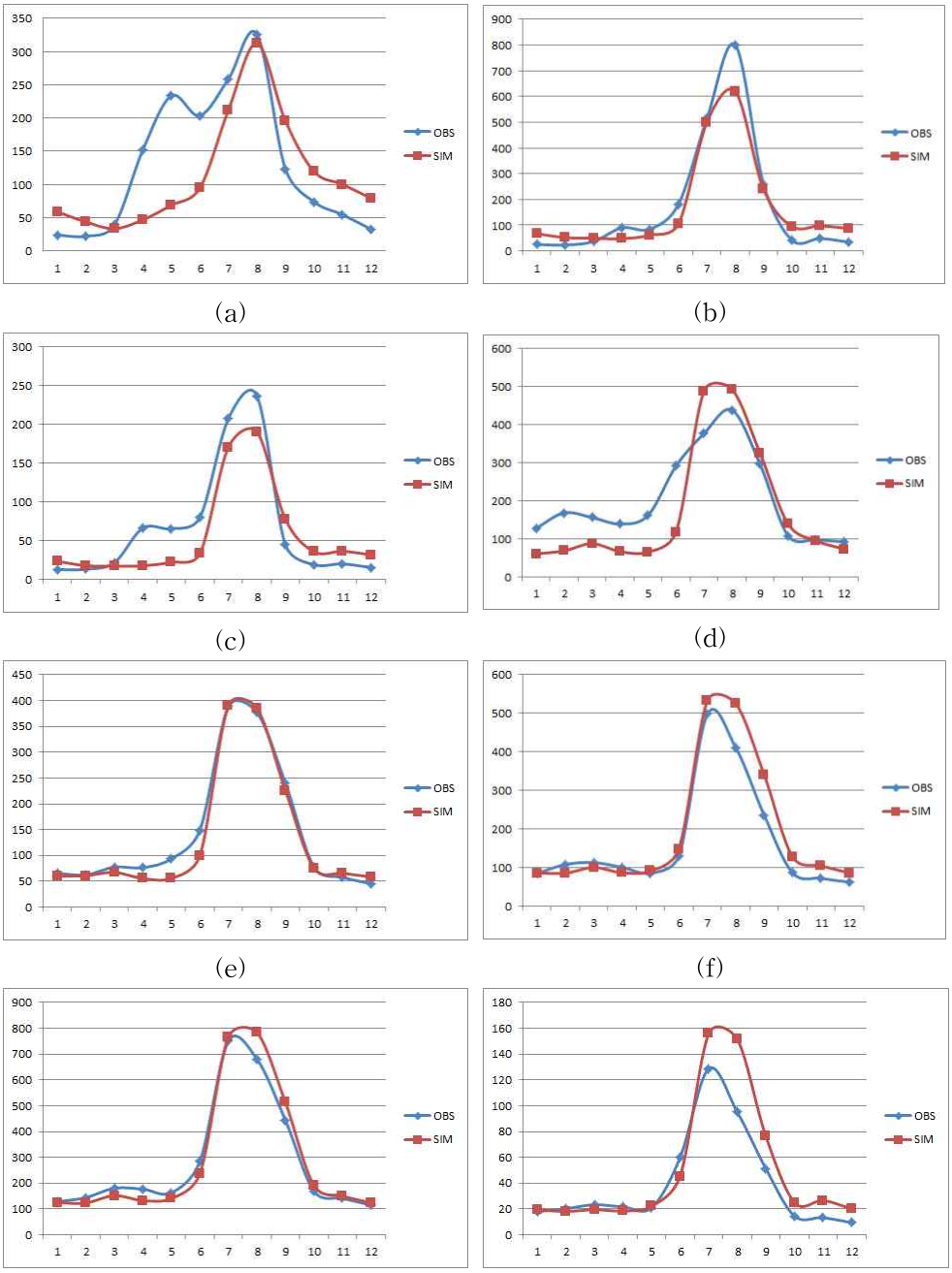

Figure 22 Observed and simulated average monthly discharge[m^3/s] for (a)Kumchang (b)Mirim (c)Dokchon (d)Yeoju (e)Gongju (f)Waegwan (g)Jeokpo (h)Naju station

3. Hydro-meteorological simulation

3.1. Meteorological characteristics and changes

In order to estimate the impact of climate change on water availability in the Korean Peninsula, it is investigated the spatial distribution of expected scenario-based meteorological changes across the Korean Peninsula. Air temperature and precipitation are the most important meteorological elements to assess the impact of climate change on water availability. Thus, it is necessary to investigate the spatio-temporal changes in air temperature and precipitation in advance of estimation of water availability.

3.1.1. Air temperature

Figure 23 shows spatial distribution of air temperature for the baseline period and its expected changes to the future period. Rising temperature with changing climate has investigated in numerous previous studies. The same trend was found in the climate change scenario used in this study. Projected changed ratio from the baseline period to the objective periods (2020s, 2050s and 2080s) is presented in Figure 24 along with its spatial distribution. Air temperature is projected to be increased by 1℃ in 2020s, 3℃ in 2050s, and 5~6℃ in 2080s. The rate of rising temperature in the northern region is larger than the southern region.

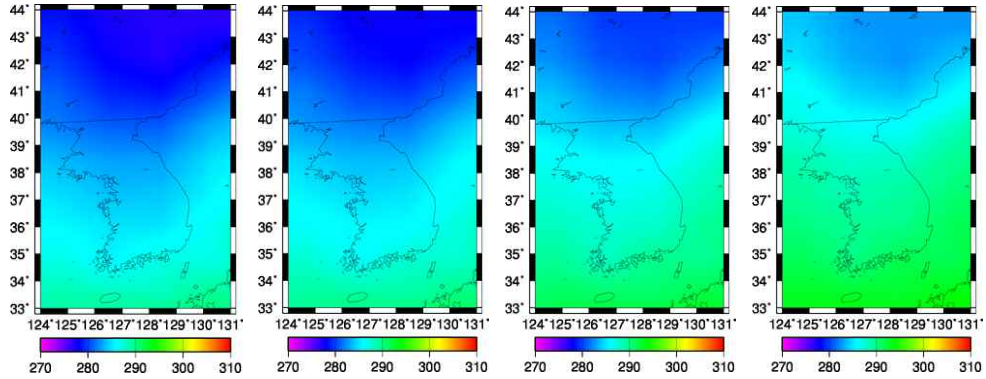

Figure 23 Spatial distribution of mean annual temperature[K] by climate change scenario for (a)baseline period, (b)2020s, (c)2050s, (d)2080s

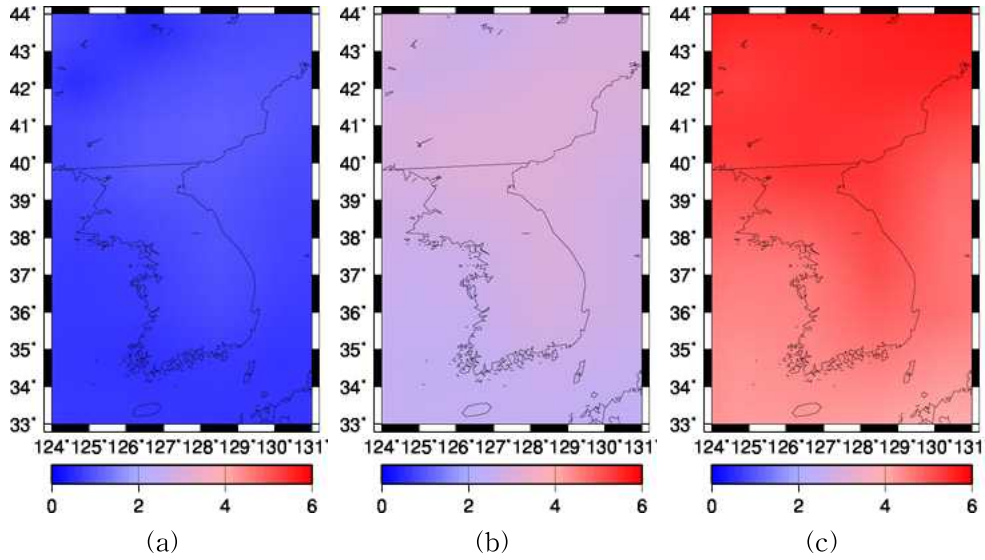

Figure 24 Spatial pattern of change of mean annual temperature[K] from the baseline period to (a)2020s, (b)2050s, (c)2080s

Air temperature of the reference and objective period is presented in Table 21 for the major gauging stations. There is slightly large

increase in temperature of some stations, such as Amnok, Duman, Chongchon in northern area which is located in the region under the impact of the continental climate compared with southern area as shown in Figure 24 (c). Mean annual temperature of baseline period was 11.127℃ across the Korean Peninsula. It is projected that the temperature will increase to 11.92℃ in 2020s, 13.92℃ in 2050s, and 16℃ in 2080s. Mean monthly air temperature of the stations for the baseline and objective periods is presented in Figure 25.

Table 21 Projected changes in average annual temperature [℃] in the Korean Peninsula

Watershed	Station	Period			
		Baseline	2020s	2050s	2080s
Amnok	Supung	9.663442	10.53238	12.63576	14.94317
Duman	Khasan	6.467678	7.442479	9.485969	11.98383
Chongchon	Puksongri	10.2459	11.12511	13.17418	15.40647
Taedong	Seohaegabmun	11.17551	11.96752	13.96217	16.11439
Han	Hangang	11.57132	12.35659	14.30385	16.29932
Geum	Gyuam	12.48789	13.21069	15.12924	17.07188
Nakdong	Samrangjin	14.26202	14.99234	17.00286	18.92391
Yeongsan	Naju	13.14125	13.76179	15.67227	17.60266
Average		11.12688	11.92361	13.92079	16.0432

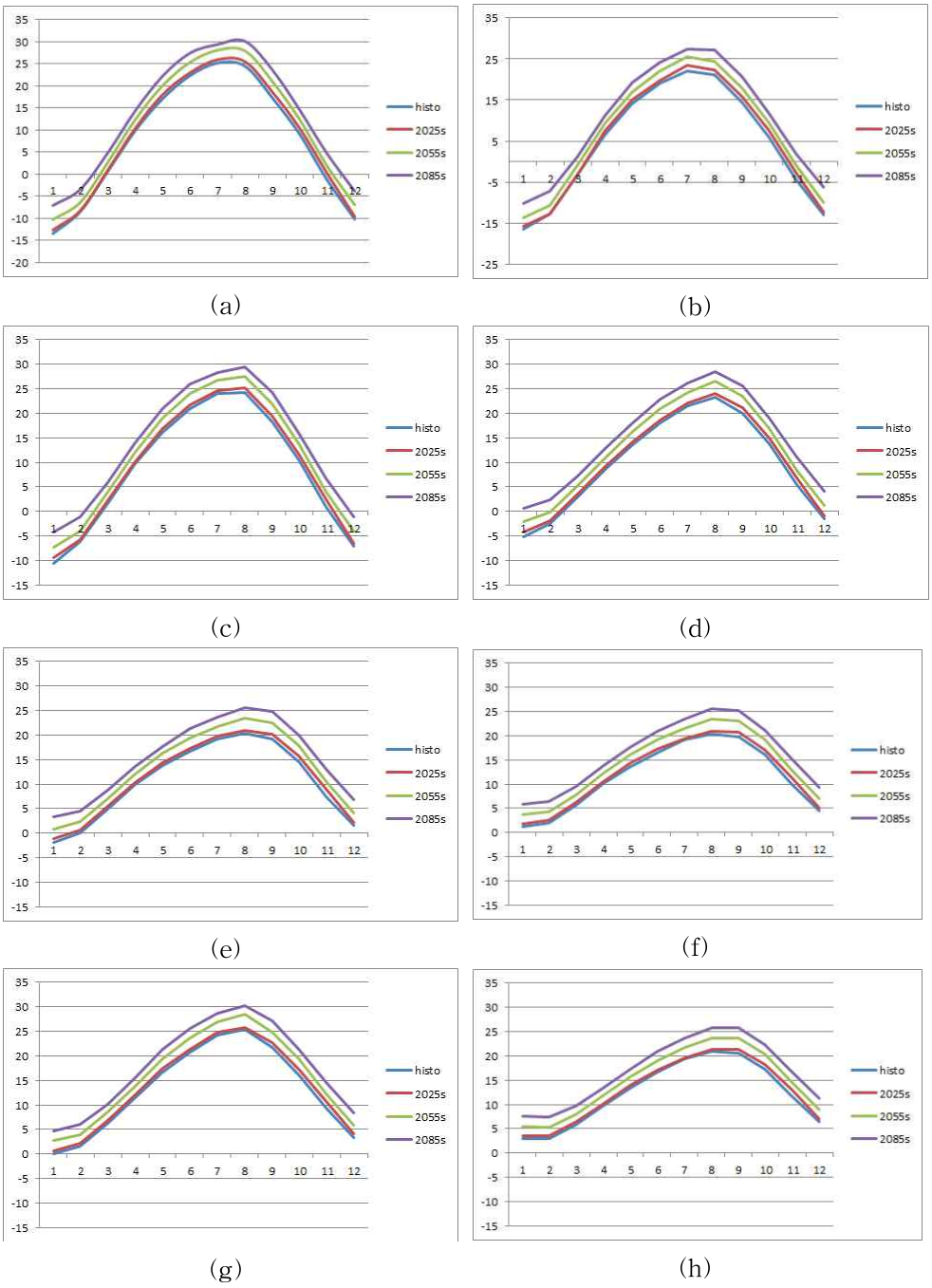

Figure 25 Monthly average temperature[℃] of baseline and future period by climate change scenario for (a)Supung, (b)Khasan, (c)Puksongri, (d)Seohaegabmun, (e)Hangang, (f)Gyuam, (g)Samrangjin, (h)Naju station

3.1.2. Precipitation

Precipitation is projected to be increased in the future as shown in Figure 26 and 27. In case of precipitation, increased ratio is calculated from the baseline period to the objective periods. Changed ratio of precipitation is different depending on the region. The tendency of larger increase in precipitation is presented in the middle and northwestern region of the peninsula and Nakdong River basin in the southeast area. The precipitation of these regions is gradually increased to 2020s, 2050s, and 2080s. Relatively small increases in precipitation is projected for the regions of south coast in South Korea and northeastern region which downstream of Duman river basin is located in North Korea. The difference of changed ratio in precipitation is projected to increase gradually for the objective periods.

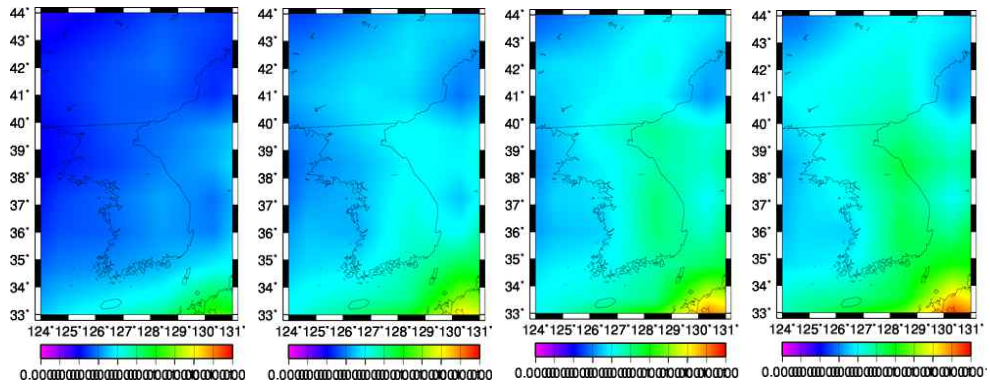

Figure 26 Spatial distribution of annual precipitation[mm/s] by climate change scenario for (a)baseline period, (b)2020s, (c)2050s, (d)2080s

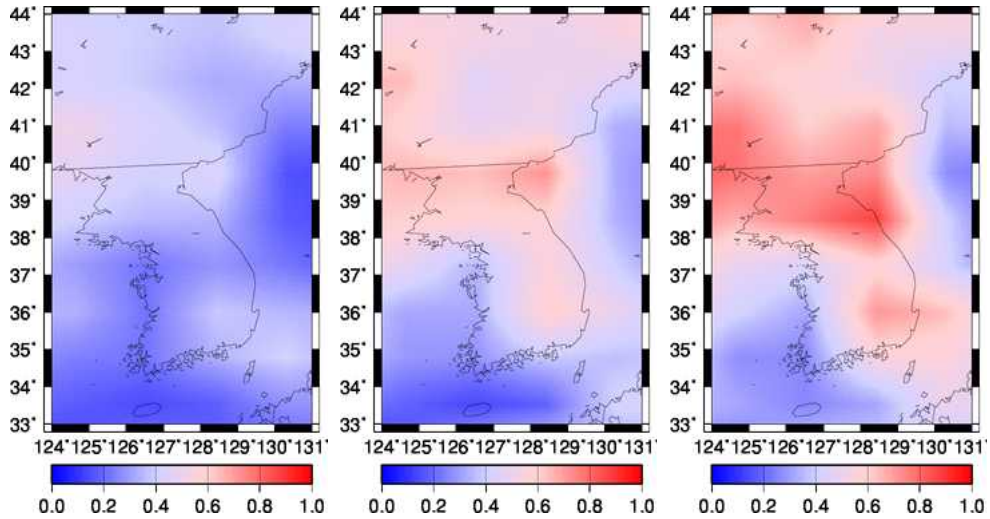

(a) (b) (c)

Figure 27 Spatial pattern of changed ratio of annual precipitation from the baseline period to (a)2020s, (b)2050s, (c)2080s

Precipitation of the major stations for the baseline and objective periods is presented in Table 22. The precipitation in 2020s is projected to be decreased at the stations in downstream of Duman, Chongchon, Taedong, Geum, and Han River basin. Average precipitation in the Korean Peninsula in 2020s is projected to be decreased from 1126.876 mm in baseline to 1124.744 mm. In some regions, the highest precipitation is projected in the 2050s amongst all the objective periods at the stations in Han, Geum, Nakdong, Yeongsan River basin. However, precipitation is projected to be increased in most regions as shown in Figure 28 based on the general trend in the late 21th century gradually after 2050s. Precipitation is projected to be increased to 15.78% as the average increased rate across the whole study area (Table 22). According to the report of

National Institute of Meteorological Research (NIMR), precipitation of Korea is going to be increased to 20.4% by the end of 21th century based on the RCP 8.5 scenario in spite of regional differences (NIMR, 2011). As shown in Table 22, increased ratio of the stations in North Korea is bigger than the stations in South Korea. When considering the uncertainties in GCMs, average projected increased ratio of precipitation using multiple GCM is 6.1% for the Korean Peninsula, and 18% for the North Korea (Shin and Jung, 2015).

Table 22 Projected changes in annual precipitation [mm/yr] in the Korean Peninsula

Watershed	Station	Period			
		Baseline	2020s	2050s	2080s
Amnok	Supung	1068.456	1074.358	1153.34	1267.566
Duman	Khasan	1063.463	1041.608	1128.536	1103.78
Chongchon	Puksongri	1056.035	1033.257	1184.475	1256.932
Taedong	Seohaegabmun	1011.831	991.6913	1142.399	1215.514
Han	Hangang	1209.04	1115.15	1264.637	1358.807
Geum	Gyuam	1126.187	1113.919	1229.364	1258.923
Nakdong	Samrangjin	1314.133	1433.001	1537.259	1702.797
Yeongsan	Naju	1165.865	1194.965	1265.829	1273.505
Average		1126.876	1124.744	1238.23	1304.728

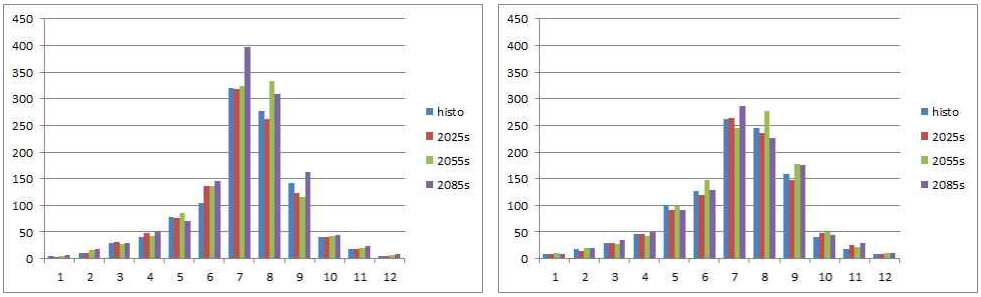

(a)

(b)

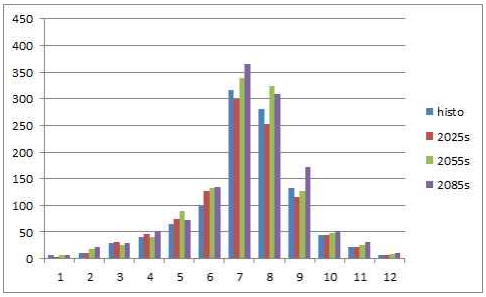

(c)

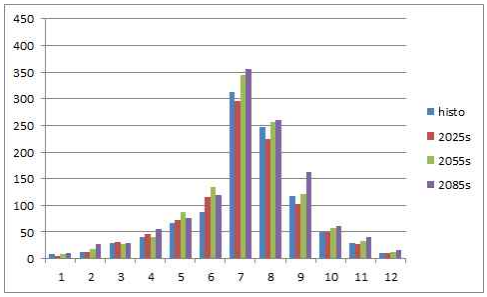

(d)

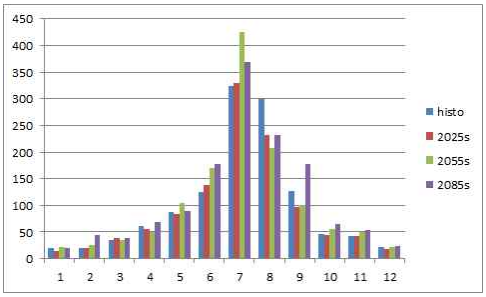

(e)

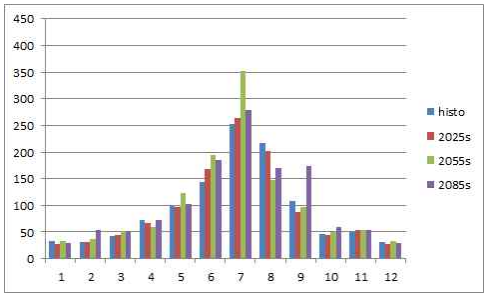

(f)

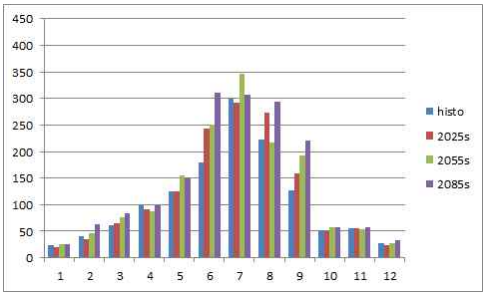

(g)

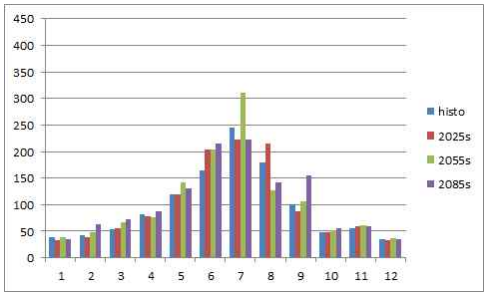

(h)

Figure 28 Monthly precipitation[mm] of baseline and future period by climate change scenario for (a)Supung, (b)Khasan, (c)Puksongri, (d)Seohaegabmun, (e)Hangang, (f)Gyuam, (g)Samrangjin, (h)Naju station

3.2. Hydrological characteristics and changes

In order to estimate the impact of scenario of climate change on water availability in the Korean Peninsula, it is necessary to investigate the regional variability of hydrological elements affected by air temperature and precipitation. H08 can simulate water balance as well as energy balance. However, this study considered only hydrological attributes because it directly affects to the concept of water availability defined above. The hydrological elements simulated in H08 are potential evapotranspiration, actual evapotranspiration, surface runoff, subsurface runoff, and total runoff. These attributes contributes to assess the water availability based on river discharge. Water availability is affected by spatio-temporal variability of hydrological attributes, and it is required to investigate its spatial distribution, as well as climatic variables across varying time series.

In order to investigate hydrological characteristics of the major river basins, historical simulation was carried out for the baseline period on the preferential basis. Simulated hydrological elements are evapotranspiration, subsurface, surface and total runoff, as well as precipitation on a monthly basis (Figure 29). The changes in hydrological attributes as described in Figure 29 are presented in Table 23 for the objective periods.

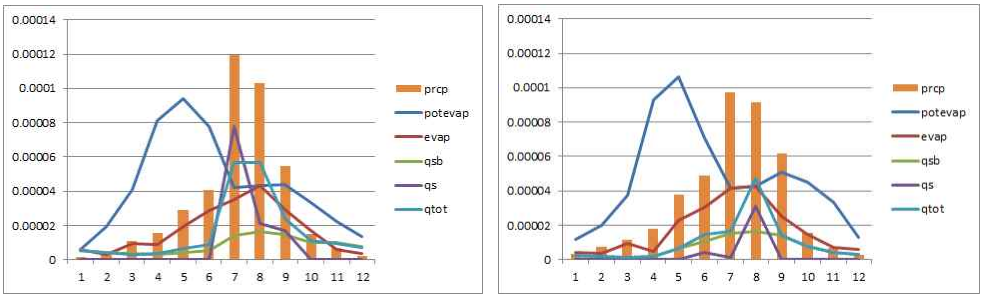

(a) Supung (b) Khasan

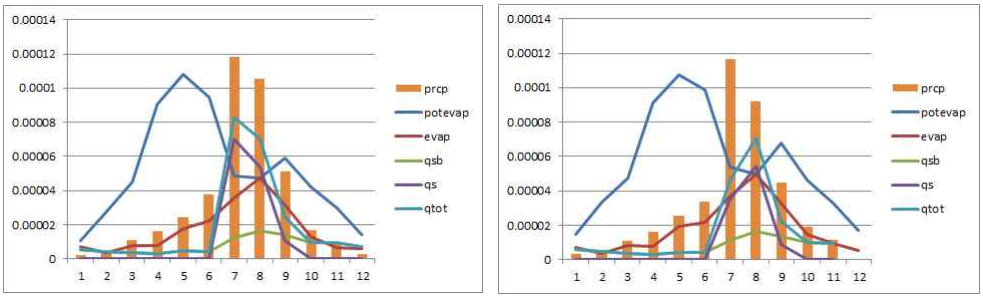

(c) Puksongri (d) Seohaegabmun

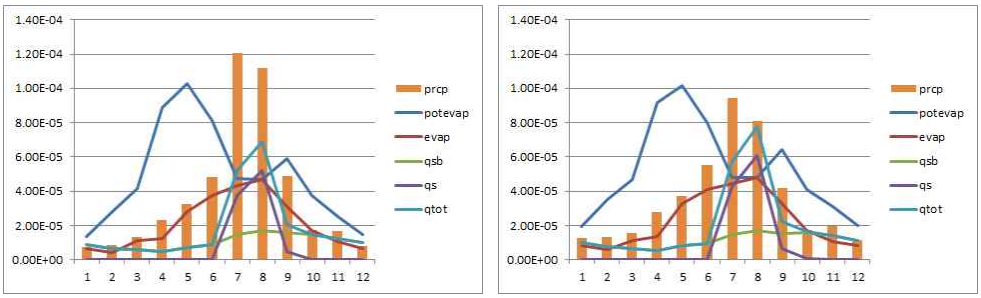

(e) Hangang (f) Gyuam

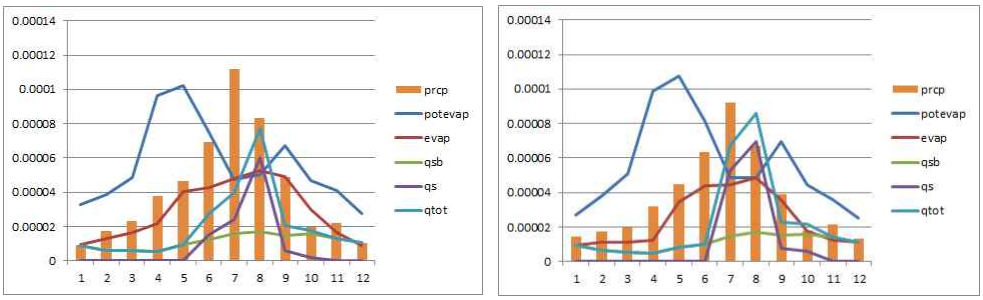

(g) Samrangjin (h) Naju

Figure 29 Monthly average hydrological elements in historical period for major stations (prcp : precipitation, potevap : potential evapotranspiration, evap : evapotranspiration, qsb : subsurface runoff, qs : surface runoff, qtot : total runoff [mm/s])

Table 23 Projected hydrological changes for the baseline and future period

Watershed	Station	Period	Hydrological variables[12]			
			PotEvap	Evap	Qtot	SoilMois
Amnok	Supung	baseline	1358.8	554.5	569.4	828.5
		2020s	1292.8	649.6	600.9	941.1
		2050s	1393.3	639.04	566.9	735.9
		2080s	1506.2	696.5	952.3	738.8
Duman	Khasan	baseline	1490.7	558.7	323.4	753.5
		2020s	1329.3	642.6	344.06	856.6
		2050s	1419.9	636.9	304.3	635.9
		2080s	1560.9	656.4	238.4	629.2
Chongchon	Puksongri	baseline	1623.4	543.3	606.9	790.2
		2020s	1418.5	663.06	577.3	840.3
		2050s	1508.7	654.7	627.9	660.8
		2080s	1610.6	703.3	645.8	653.7
Taedong	Seohaegabmun	baseline	1734.4	571.8	510.8	806.7
		2020s	1512.8	684.5	484.3	840.6
		2050s	1594.1	703.5	514.1	685.05
		2080s	1706.4	756.4	531.3	692.4
Han	Hangang	baseline	1540.1	672.8	585.2	1060.8
		2020s	1353.9	764.2	498.6	980.2
		2050s	1432.3	807.2	526.4	873.3
		2080s	1509.7	896.6	533.9	939.3
Geum	Gyuam	baseline	1647	720.7	650.1	1126.7
		2020s	1428.5	834.06	606.8	1002.5
		2050s	1505.7	882.3	602.5	895.3
		2080s	1589.9	945.9	575.2	917.6
Nakdong	Samrangjin	baseline	1770.1	770.8	639.04	1122.02
		2020s	1535.4	918.5	749.9	1030.7
		2050s	1639.06	965.6	692.7	933.5
		2080s	1723.7	1036.8	842.4	911.1
Yeongsan	Naju	baseline	1772.6	771.2	708.2	1091.2
		2020s	1526.6	909.4	709.1	1000.4
		2050s	1598.2	949.8	614.4	894.1
		2080s	1691.3	1012.5	555.9	910.5

12) PotEvap : potentail evapotranspiration[mm/yr], Evap : evapotranspiration[mm/yr], Qtot : total runoff[mm/yr], SoilMois : soil moisture[mm]

3.2.1. Evapotranspiration

Amount of evapotranspiration is affected by various reasons, such as differences in elevation, amounts of surface water to evaporate, air temperature, wind, and solar radiance (Masood et al., 2015). Potential evapotranspiration is affected by bulk transfer coefficient, wind speed, and a difference between specific humidity and saturated specific humidity based on [Eq. 2].

Bulk transfer coefficient C_D was calibrated because it is a principal parameter that affects runoff hydrograph. Wind speed is low in coastal areas in South Korea and plateau area in North Korea as shown in Figure 9. This can be the reason of spatial distribution of wind speed value in Figure 30. Potential evapotranspiration in 2020s is projected to be decreased compared with baseline period and gradually increased to 2080s. The potential evapotranspiration is going to be increased in 2080s while the amount of 2020s and 2050s is smaller than the baseline period. The increased amount of potential evapotranspiration in northern plateau region is larger than other areas.

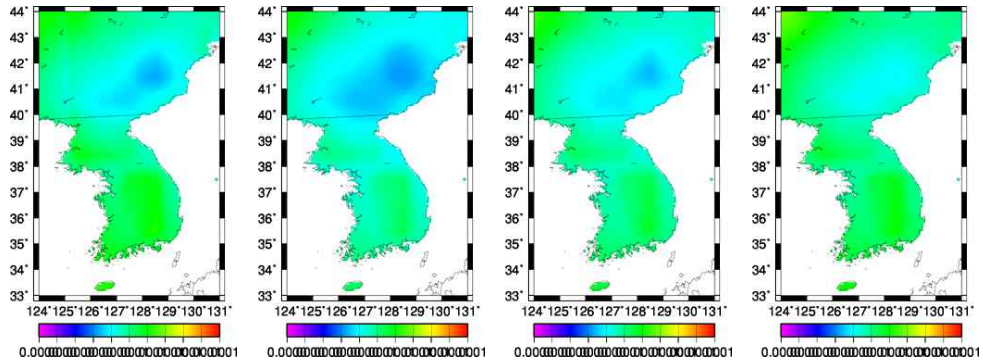

Figure 30 Spatial distribution of potential evapotranspiration[mm/s] by climate change scenario for (a)baseline period, (b)2020s, (c)2050s, (d)2080s

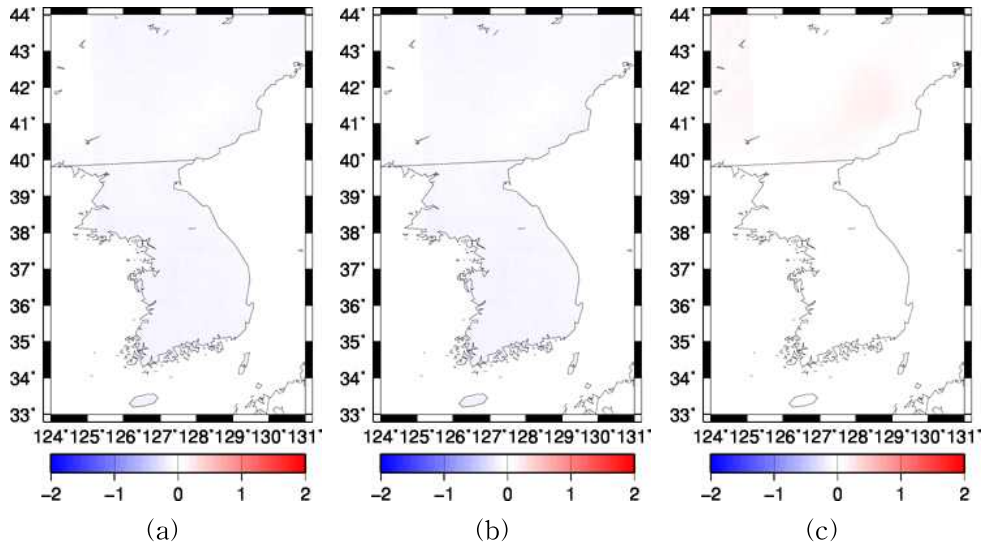

Figure 31 Spatial pattern of changed ratio(%) of potential evapotranspiration from the baseline period to (a)2020s, (b)2050s, (c)2080s

Actual evapotranspiration can be estimated by [Eq. 3] and [Eq. 4] by multiplying a function of soil moisture to potential evapotranspiration. It is projected to be continuously increased for all the objective periods. The amount of evapotranspiration increases as precipitation

increases because soil become saturated with increasing rainfall according to [Eq. 3]. Potential evapotranspiration is same with actual evapotranspiration when the soil moisture is larger than 75% of field capacity based on [Eq. 4].

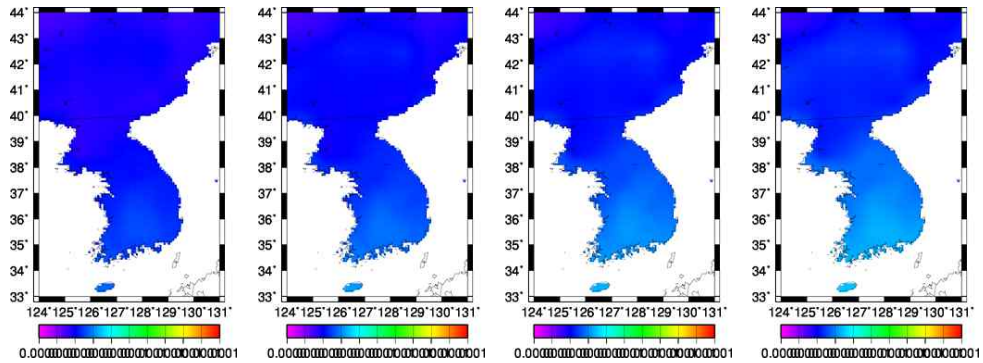

(a) (b) (c) (d)

Figure 32 Spatial distribution of evapotranspiration[mm/s] by climate change scenario for (a)baseline period, (b)2020s, (c)2050s, (d)2080s

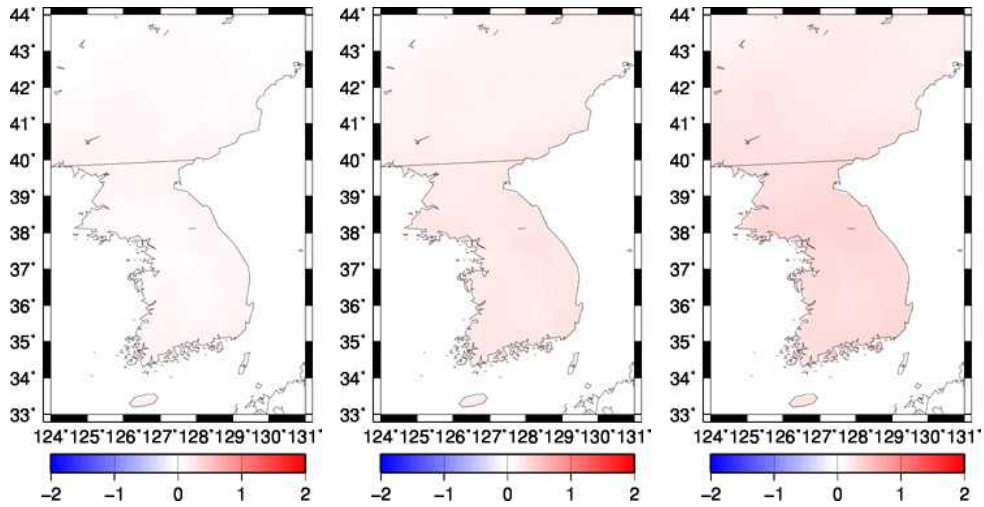

(a) (b) (c)

Figure 33 Spatial pattern of changed ratio(%) of evapotranspiration from the baseline period to (a)2020s, (b)2050s, (c)2080s

3.2.2. Runoff

Total runoff can be divided into surface runoff and subsurface runoff based on water balance equation [Eq. 6] in H08. Surface runoff occurs if the soil moisture exceed the field capacity, and does not occur if the soil moisture is smaller than the field capacity. Subsurface runoff is generated in proportion to the ratio between soil moisture and field capacity and is affected by the parameter τ and γ according to [Eq. 7] which was calibrated.

Subsurface runoff is a function of field capacity and soil moisture which tends to be maintained at a constant value throughout the year without significant change as shown in Figure 29. It is less sensitive to precipitation change than the surface runoff, as well as its spatial pattern of its distribution (Figure 34). Subsurface runoff is decreased in the period of 2020s compared with baseline period and projected to be slightly increased by 2080s (Figure 35).

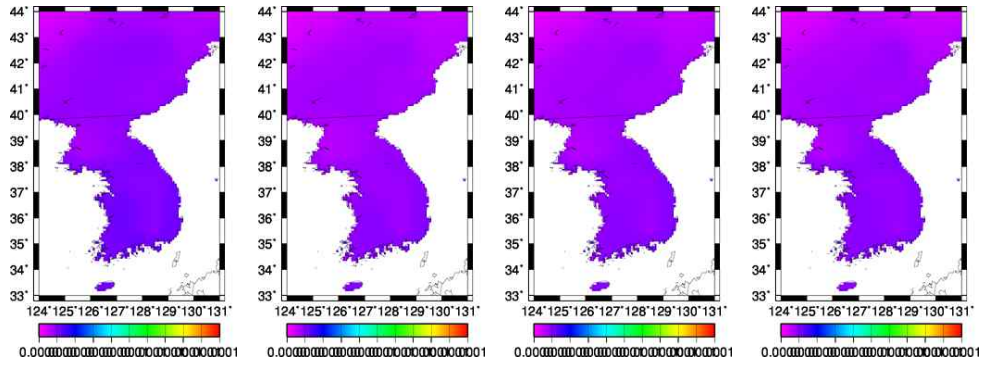

Figure 34 Spatial distribution of subsurface runoff[mm/s] by climate change scenario for (a)baseline period, (b)2020s, (c)2050s, (d)2080s

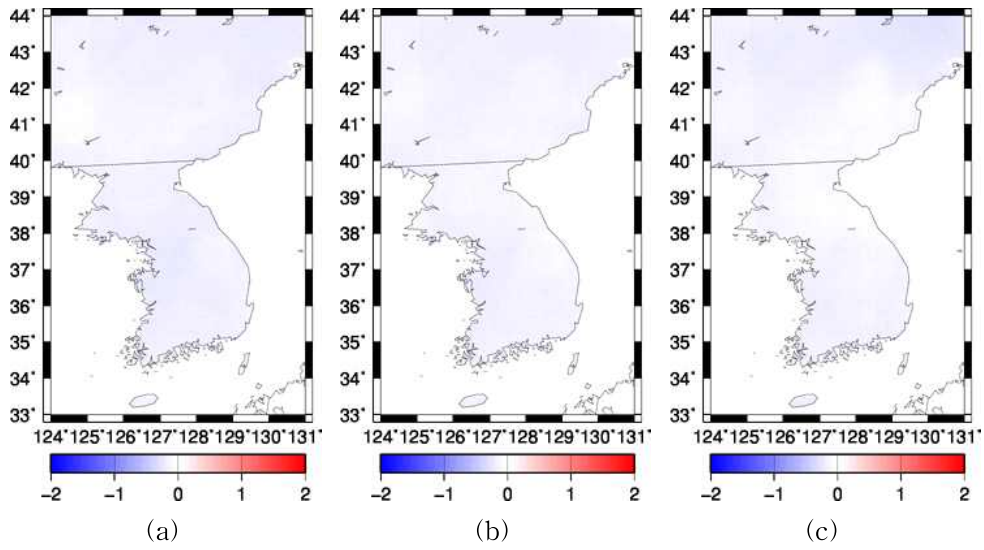

Figure 35 Spatial pattern of changed ratio(%) of subsurface runoff from the baseline period to (a)2020s, (b)2050s, (c)2080s

Surface runoff is generated due to the increase in soil moisture which is sensitive to changes in precipitation. Spatial pattern of surface runoff is presented in Figure 36. When it comes to changes in

precipitation based on climate scenario, spatial changes of surface runoff and precipitation is appeared similar. Surface runoff is decreased in 2020s in most parts of the country except for southern area, especially where the Nakdong River basin is located. Surface runoff is projected to be increased gradually by the 2080s in most parts of the Korean Peninsula. As shown in Figure 37, Nakdong River basin showed a significant increase in surface runoff compared with other areas. On the other hand, it is projected to be decreased compared with baseline period in northeast area where the Duman River basin located. The spatial pattern of changes in surface runoff is similar with the pattern of changes in precipitation.

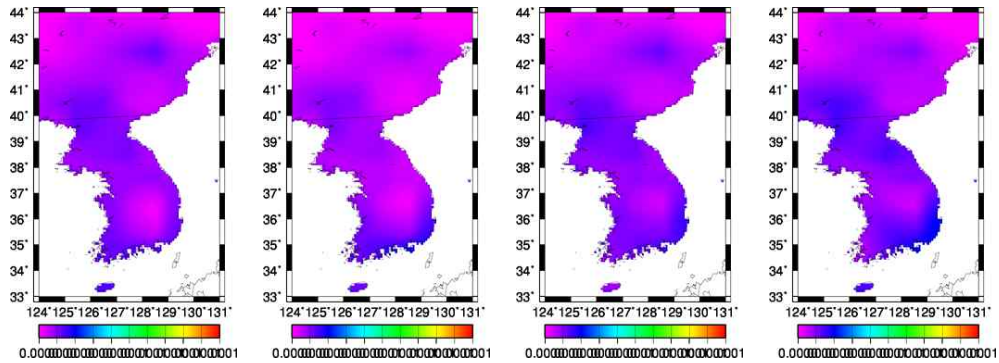

Figure 36 Spatial distribution of surface runoff[mm/s] by climate change scenario for (a)baseline period, (b)2020s, (c)2050s, (d)2080s

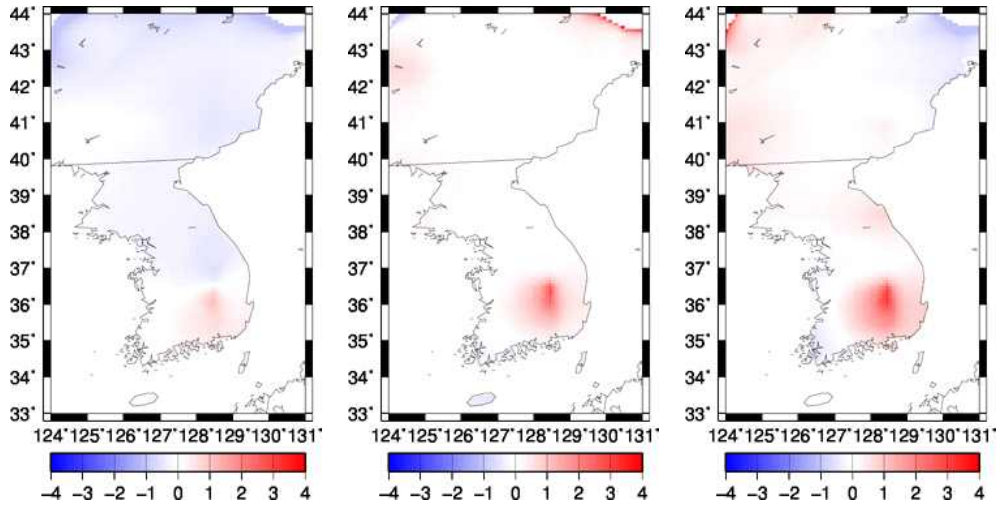

Figure 37 Spatial pattern of changed ratio of surface runoff from the baseline period to (a)2020s, (b)2050s, (c)2080s

Total runoff is sum of surface and subsurface runoff. However, sensitivity of runoff hydrograph to subsurface and surface runoff is different from each other according to Figure 29. Figure 38 shows spatial distribution of total runoff for the baseline and objective periods. Changed ratio from the baseline period to objective periods is presented in Figure 39. An overall tendency of spatial distribution and changed ratio of total runoff is similar to the trends of variability of changes in precipitation.

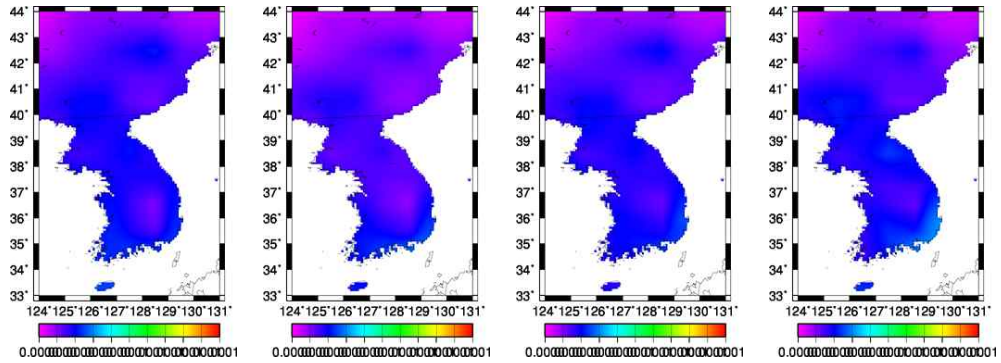

(a) (b) (c) (d)

Figure 38 Spatial distribution of total runoff[mm/s] by climate change scenario for (a)baseline period, (b)2020s, (c)2050s, (d)2080s

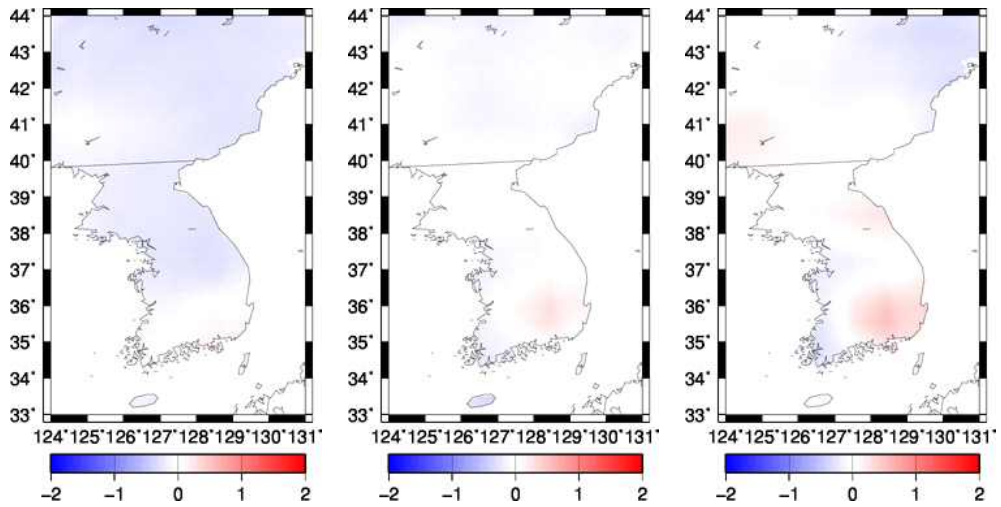

(a) (b) (c)

Figure 39 Spatial pattern of changed ratio of total runoff from the baseline period to (a)2020s, (b)2050s, (c)2080s

Figure 40 presents spatio-temporal variability of hydrological elements of the stations in major river basins in the Korean Peninsula for the baseline and objective periods based on Table 23. Potential

evapotranspiration of all stations is projected to be decreased in 2020s, and then gradually increased by the 2080s. Evapotranspiration is projected to be continuously increased by the 2080s in most parts of the region. The tendency of variations in total runoff is different from region to region. The amount of total runoff of each stations not equal to the river discharge. Simulated amount of runoff can represent one component of water balance of the region. Runoff is projected to be continuously decreased in Khasan, Gyuam, Naju station, and increased in Supung, Puksongri, Samrangjin station. Amount of the elements of water balance is related with the tendency of rainfall pattern, especially evapotranspiration and runoff which is directly affected by the amount of available water on surfaces. Thus, runoff, soil moisture, and evapotranspiration is large at the stations located in southern Korea, such as Hangang in Han River basin, Gyuam in Geum River basin, Samrangjin in Nakdong River basin, and Naju station in Yeongsan River basin.

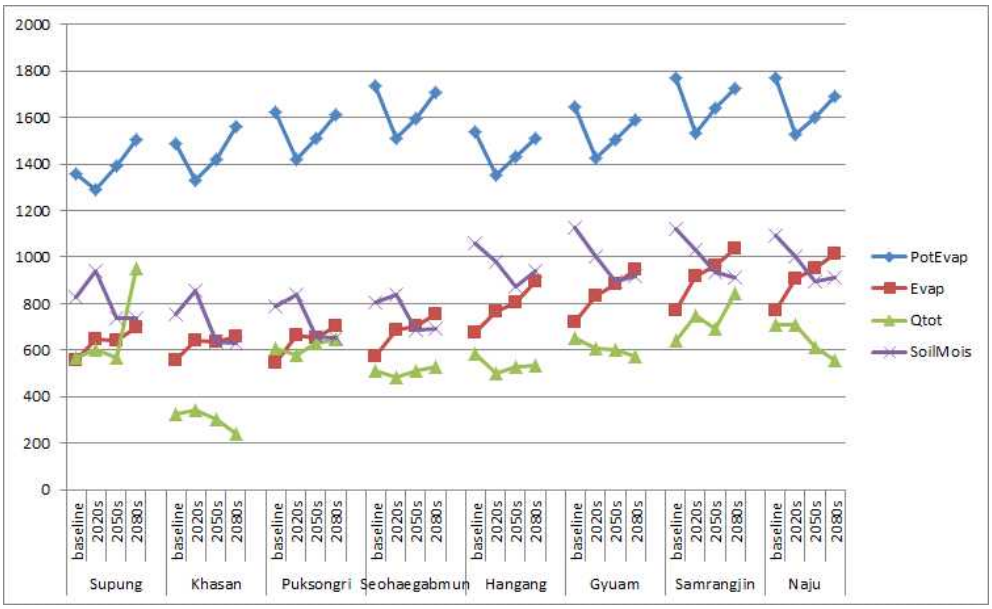

Figure 40 Comparison of simulated potential evapotranspiration[mm/yr], evapotranspiration[mm/yr], total runoff[mm/yr], soil moisture[mm]

3.3. Estimation of water availability

In this study, water availability is defined as a river discharge. River discharge of one grid is affected by various components from the meteorological variables to hydrological attributes investigated above. Water availability for major river basins is estimated based on changes in climate and hydrology. In order to estimate spatio-temporal variability in water availability, river discharge is projected and spatially presented for baseline and objective periods of Amnok, Duman, Chongchon, Taedong River in North Korea and Han, Nakdong, Geum, Yeongsan River in South Korea.

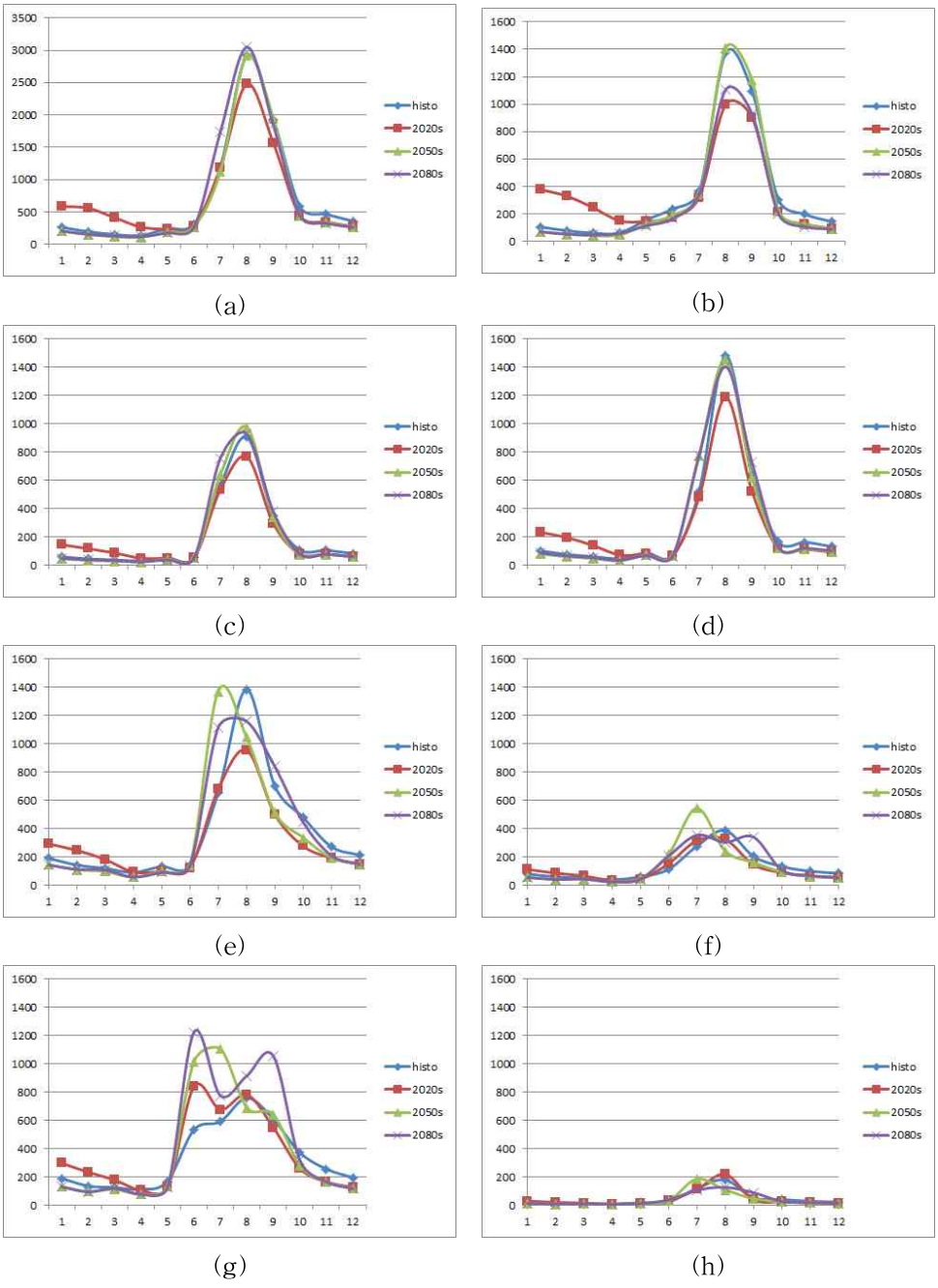

Figure 41 Monthly discharge[m^3/s] of baseline and future period by climate change scenario for (a)Supung, (b)Khasan, (c)Puksongri, (d)Seohaegabmun, (e)Hangang, (f)Gyuam, (g)Samrangjin, (h)Naju station

Simulated monthly river discharge is presented in Figure 41 for the principal 8 river basins. The majority of the stations are located in downstream region of the rivers. Amnok River basin where the Supung station located is the biggest river basin in the Korean Peninsula. This is the reason why a range of the value of y-axis of Supung station is different from other stations Figure 41 (a). In case of the basins in North Korea, month of peak discharge is same across all the objective periods. Mostly, discharge in 2020s is the lowest amongst all the periods, and tends to have a similar tendency of monthly discharge in the 2050s and 2080s. In case of the basins in South Korea, monthly variation in discharge is different from each objective period. River discharge of 2020s is decreased in Han River and Geum River, and increased in Nakdong River and Yeongsan River. In 2050s, month of peak discharge of all the basins changed to an earlier month. River discharge in 2080s of the stations in South Korea decreased for most stations and month of peak discharge is also changed in Han, Geum, Yeongsan River to the months similar with simulated results in the baseline and 2020s except for Samrangjin in Nakdong River basin. In case of Samrangjin station, total amount of discharge is projected to be increased with the course of time in climate scenario. However, monthly variation in discharge became intense as shown in Figure 41 (g).

Table 24 Projected mean annual discharge [m^3/s] in the Korean Peninsula

Watershed	Station	Period			
		Baseline	2020s	2050s	2080s
Amnok	Supung	728.508	719.1678	670.3311	724.4784
Duman	Khasan	369.451	335.8808	346.8199	290.9473
Chongchon	Puksongri	199.722	192.6889	199.6968	209.8714
Taedong	Seohaegabmun	295.8921	274.5976	294.7237	302.822
Han	Hangang	377.1458	316.1815	355.4432	381.3324
Geum	Gyuam	132.8693	124.2232	133.0489	137.3105
Nakdong	Samrangjin	338.3875	362.3996	381.9661	427.396
Yeongsan	Naju	45.78367	46.25489	41.15759	39.96073

Table 24 describes total annual amount of river discharge for the baseline and objective periods as shown in Figure 42. Discharge of Supung station in Amnok River basin is projected to be decreased in 2050s, and then increased by 2080s. Discharge of Khasan station in Duman River basin is projected to be decreased continuously for all the objective periods by the 2080s. Discharge of Puksongri station in Chongchon River basin is projected to be decreased in 2020s, and then increased by the end of 21th century. Mean annual discharge of Seohaegabmun of Taedong River basin in 2020s is decreased and gradually increased by the 2080s similar with the tendency of changes in discharge of Chongchon River basin. Variability of discharge of Hangang station has also similar tendency with Chongchon River basin and Taedong River basin which shows decreased discharge in 2020s and increased discharge in 2050s and 2080s, as well as Gyuam station in Geum River basin. Only discharge of Samrangjin station in Nakdong River basin is continuously increased from the baseline to 2080s. Naju station in Yeongsan river basin shows increased discharge

in 2020s, and then continuously decreased by the 2080s.

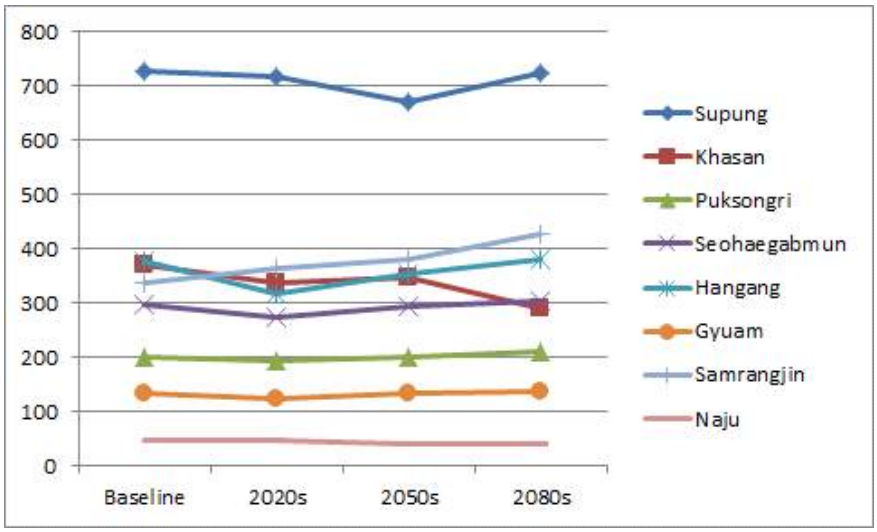

Figure 42 Mean annual discharge [m^3/s] of the stations

Simulated discharge for major river basins is regarded as water availability. When it comes to considering temporal variability of water availability, investigation of its seasonal variation is also required because rainfall is seasonally biased and concentrated in summer, especially in the Korean Peninsula. Mean seasonal discharge in spring and winter is projected to be increased in 2020s, while the discharge in summer and autumn is decreased at the same period (Figure 43). In 2050, discharge in spring and winter is going to be decreased below the amount of baseline, and then discharge in summer and autumn is increased. There is regional bias on the river discharge in 2080s. Summer discharge of Amnok, Han, Geum, and Nakdong River is projected to be increased, and autumn discharge of Taedong, Han,

Geum, and Nakdong River is going to be increased. In case of spring and winter discharge, temporal variation from baseline to 2080s is simulated to have a low variability except for 2020s. On the other hand, summer and autumn discharge have different spatial variability depending on a regional characteristics.

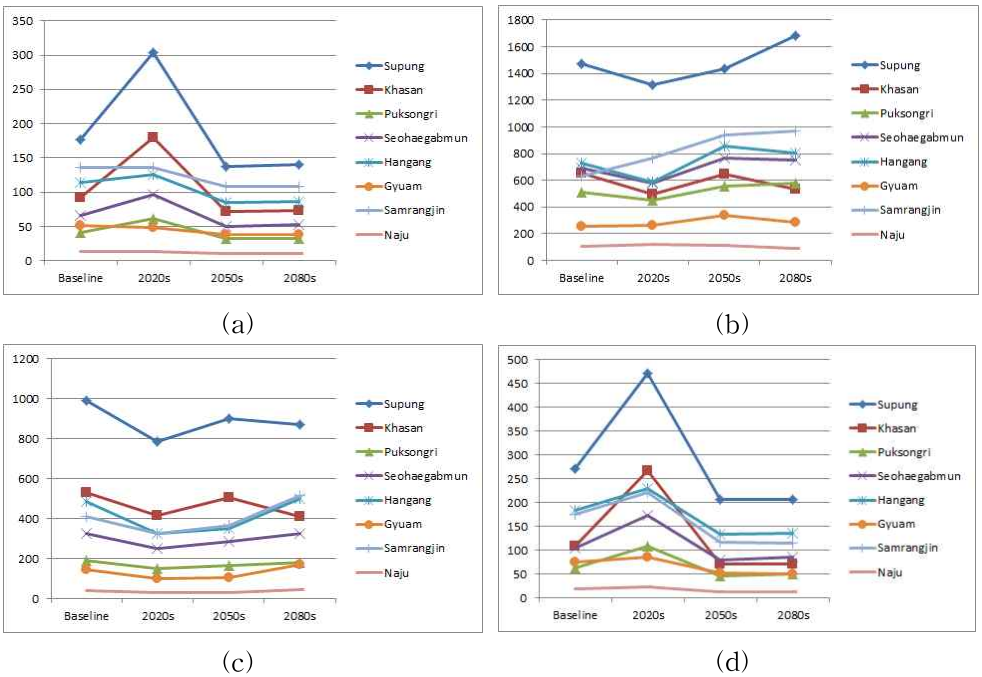

FIgure 43 Mean seasonal discharge[m^3/s] of the stations for (a)spring(MAM), (b)summer(JJA), (c)autumn(SON), (d)winter(JJA)

Spatial distribution and variations of the simulated river discharge is presented in Figure 44. Spatial variability of water availability based on river discharge also can be represented spatially from baseline to the objective periods. Water availability defined as river discharge of a

grid is affected by hydrological attributes, such as runoff and evapotranspiration which was investigated above. Water availability of white colored region is same with baseline period. Blue colored region and Red colored region has decrease and increase in water availability, respectively. Spatial variation of water availability tends to be similar with spatial distribution of total runoff and precipitation. Because river discharge is accumulated runoff from upper grid based on flow direction.

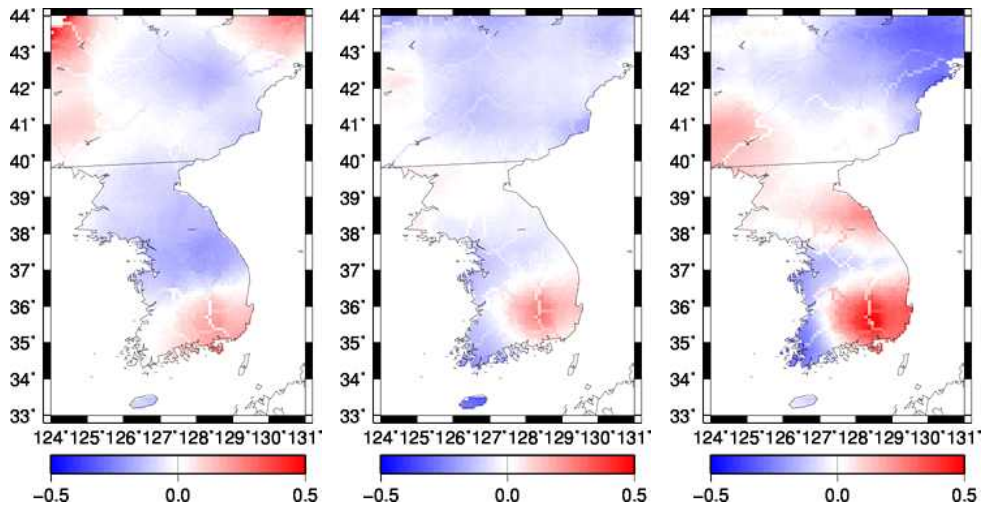

(a) (b) (c)

Figure 44 Spatial pattern of changed ratio(%) of water availability from the baseline period to (a)2020s, (b)2050s, (c)2080s

4. Implication for spatial planning

Water resources and its availability of region are being considered as an essential component to establish a spatial plan such as land use planning in consideration of its spatio-temporal variability. This study applied grid-based hydrological model to estimate a water availability by calculating water balance and river discharge under changing climate in the future. Input data of the model for calculation is also grid-based. One grid of hydrological simulation can represent geographical characteristics, climate condition, water balance, and river discharge. The regional characteristics as a input of hydrological model in this study focused on geographical aspects, such as flow direction derived from DEM. Therefore, regional implication of this study is focused on geographical and meteorological characteristics, as well as hydrological characteristics in order to estimate and assess the impact of climate change on water availability.

Figure 45 shows spatial pattern of changed ratio of water availability in Amnok River outlet region from the baseline to the objective periods. In case of Amnok River basin, water availability is projected to be increased in 2020s, and decreased in 2050s especially main river stream. River stream also can be represented on this simulated results because the river stream is representation of accumulated runoff from upper grid. Discharge of downstream of Amnok River is decreased on 2050s compared with baseline. However, overall river discharge of downstream area in Amnok River is going to be increased while the

accumulated river discharge of Amnok River is projected to be decreased. One example of spatial application of the simulation result can be introduction of facilities related with water resources management such as reservoir. There will be a region projected to be in the conditions of decrease in water availability while river discharge of main stream is going to be increased compared with nearby areas. In this case, reservoir can be introduced in this river to enhance the water availability in the projected future hydrological condition of the region.

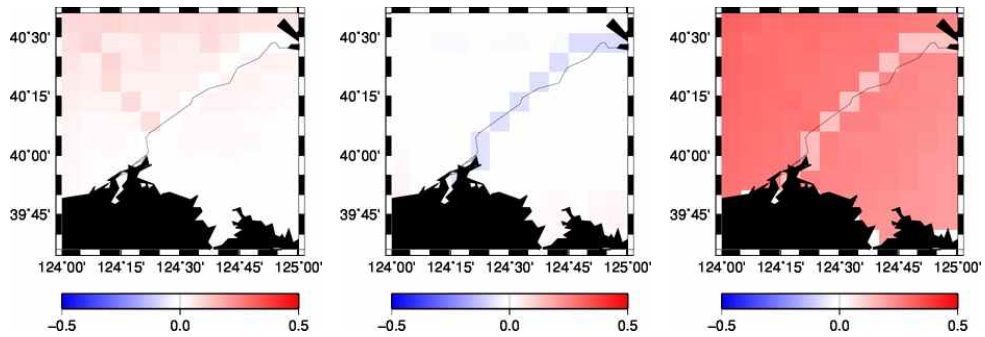

Figure 45 Spatial pattern of changed ratio(%) of water availability in Amnok River outlet region from the baseline period to (a)2020s, (b)2050s, (c)2080s

In case of the downstream region of Duman River, the discharge is projected to be decreased continuously by the 2080s. On the other hand, river discharge of nearby northeast area will be increased on 2020s. However, water availability of this region generally tends to be decreased. Decreased ratio of 2080s in nearby region is much larger than main stream of Duman River (Figure 46). In this case, reservoir

or weir can be installed in the main stream of the river to enhance the water availability of the region against to the expected changes in water availability. Spatio-temporal variation of water availability of nearby area of river junction of Namhan and Bukhan River is presented in Figure 47 and Nakdong River outlet region is presented in Figure 48.

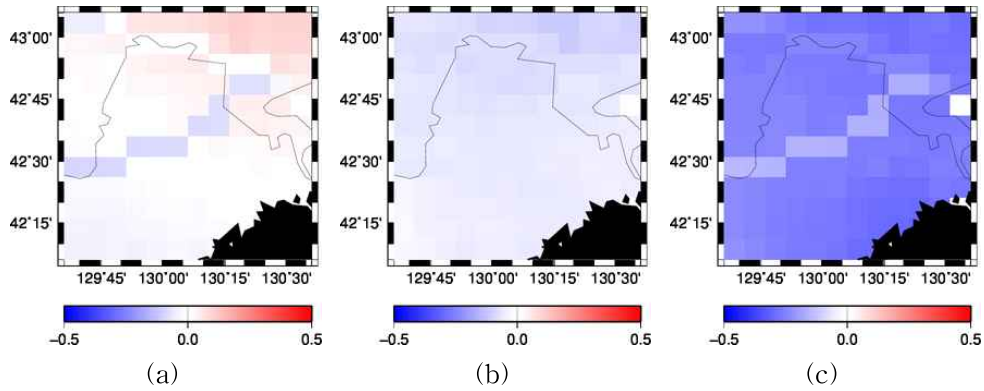

Figure 46 Spatial pattern of changed ratio(%) of water availability in Duman River outlet region from the baseline period to (a)2020s, (b)2050s, (c)2080s

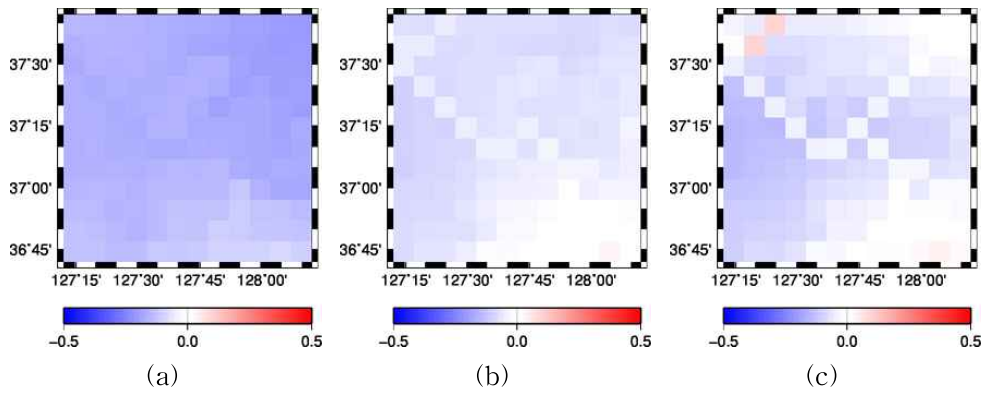

Figure 47 Spatial pattern of changed ratio(%) of water availability in Han River basin region from the baseline period to (a)2020s, (b)2050s, (c)2080s

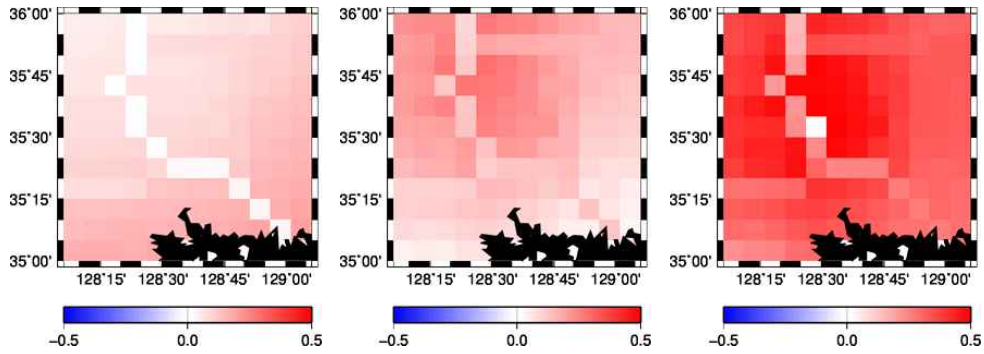

Figure 48 Spatial pattern of changed ratio(%) of water availability in Nakdong River outlet region from the baseline period to (a)2020s, (b)2050s, (c)2080s

Ⅴ. Conclusion

Amount of available water resources of region has been important issues for establishing various land management plan in dealing with climate change. It is necessary to estimate and assess an impact of climate change on water availability to establish an effective management plan and draw an implication for future spatial planning, global hydrological model H08 is regionally applied for simulating hydrological cycle and water availability in this study. The model was calibrated and validated based on 10-year data of GSWP2 from 1986 to 1995. Input meteorological data for the hydrological simulation was also validated. In order to estimate future water availability, future climate scenario from the GCM is used after the correction of bias in air temperature and precipitation. Model calibration was conducted by tuning 4 parameters based on historical discharge data for major river basins in the Korean Peninsula. There were many differences in changes of meteorological and hydrological characteristics as well as river discharge defined as water availability from region to region.

Naturalized flow is assumed for the simulation of river discharge in this study. However, major rivers in the Korean Peninsula has various reservoirs, so that assuming naturalized flow is only reliable in the stations located in upstream area. This study did not considered reservoir operation rules and water supply capacity of the reservoirs. As a result, this study projected water availability based on the naturalized river discharge in the Korean Peninsula on a macroscale using regionalized global hydrological model. When considering climate

change scenario generated from the GCM and future hydrological simulation, an uncertainty of the process of selecting GCM and hydrological model should be considered. Limitation of this study in terms of future projection is mainly caused by this process. This study considered one climate change scenario, which is based on the HadGEM2-AO and RCP 8.5. Hydrological simulation results also should be compared with performance of other models which is successfully applied in the Korean Peninsula.

This study estimated water availability based on projection of river discharge and water balance simulation and derived spatial implication introducing a hydraulic structure such as reservoir for effective management of available water resources against climate change in a scale of the Korean Peninsula and this results could be used as a preliminary information for establishing spatial planning under climatic changes across the Korean Peninsula considering water availability.

Ⅵ. References

Alcamo, J., Döll, P., Henrichs, T., Kaspar, F., Lehner, B., Rösch, T., & Siebert, S. (2003). Development and testing of the WaterGAP 2 global model of water use and availability. Hydrological Sciences Journal, 48(3), 317 – 337. doi:10.1623/hysj.48.3.317.45290

Alcamo, J., Döll, P., Henrichs, T., Kaspar, F., Lehner, B., Rösch, T., & Siebert, S. (2003). Global estimates of water withdrawals and availability under current and future "business-as-usual" conditions. Hydrological Sciences Journal, 48(3), 339 – 348. doi:10.1623/hysj.48.3.339.45278

Alcamo, J., Doll, P., Kaspar, F., Siebert, S. (1997). Global change and global scenarios of water use and availability : An application of WaterGAP1.0. Report A9701, Center for Environmental Systems Research, University of Kassel, Germany

Bae, D.-H. & Jeong, I.-W. (2005). Impact assessment of climate change on water resources, Disaster Prevention Review, 21, 16-22

Bae, D.-H., Jeong, I.-W., Lee, B.-J., & Lee, M.-H. (2011). Future Korean water resources projection considering uncertainty of GCMs and hydrological models, Journal of Korea Water Resources Association, 44(5), 389-406

Bao, Z., Fu, G., Wang, G., Jin, J., He, R., Yan, X., & Liu, C. (2012). Hydrological projection for the Miyun Reservoir basin with the impact of climate change and human activity. Quaternary International, 282, 96 – 103. doi:10.1016/j.quaint.2012.07.012

Bates, B.C., Z.W. Kundzewicz, S. Wu and J.P. Palutikof, Eds. (2008). Climate Change and Water. Technical Paper of the Intergovernmental Panel on Climate Change, IPCC Secretariat, Geneva, 210 pp.

Boulay, A.-M., Bare, J., De Camillis, C., Döll, P., Gassert, F., Gerten, D., … Pfister, S. (2015). Consensus building on the development of a stress-based indicator for LCA-based impact assessment of water consumption: outcome of the expert workshops. The International Journal of Life Cycle Assessment, 577 - 583. doi:10.1007/s11367-015-0869-8

Cai, X., & Rosegrant, M. W. (2002). Global Water Demand and Supply Projections. Water International, 27(2), 159 - 169. doi:10.1080/02508060208686989

Collet, L., Ruelland, D., Borrell-Estupina, V., Dezetter, A., & Servat, E. (2013). Integrated modelling to assess long-term water supply capacity of a meso-scale Mediterranean catchment. Science of the Total Environment, 461-462, 528 - 540. doi:10.1016/j.scitotenv.2013.05.036

Dirmeyer, P. a., Gao, X., Zhao, M., Guo, Z., Oki, T., & Hanasaki, N. (2006). GSWP-2: Multimodel analysis and implications for our perception of the land surface. Bulletin of the American Meteorological Society, 87(10), 1381 - 1397. doi:10.1175/BAMS-87-10-1381

Döll P, Kaspar F, Alcamo J. (1999). Computation of global water availability and water use at the scale of large drainage basins.

Math Geol 4:111 – 118

Döll, P., Kaspar, F., & Lehner, B. (2003). A global hydrological model for deriving water availability indicators: Model tuning and validation. Journal of Hydrology, 270(1-2), 105 – 134. doi:10.1016/S0022-1694(02)00283-4

Elliott, J., Deryng, D., Müller, C., Frieler, K., Konzmann, M., Gerten, D., … Wisser, D. (2014). Constraints and potentials of future irrigation water availability on agricultural production under climate change. Proceedings of the National Academy of Sciences of the United States of America, 111(9), 3239 – 44. doi:10.1073/pnas.1222474110

Falkenmark, M. (1989). The massive water scarcity now threatening Africa-why isn't it being addressed?, Ambio, 18, 112 – 118

GRDC, (2015), Long-Term Mean Monthly Discharges and Annual Characteristics of GRDC Stations / Online provided by the Global Runoff Data Centre of WMO. 2015 ed. Koblenz: Federal Institute of Hydrology (BfG)

Haddeland, I., Clark, D. B., Franssen, W., Ludwig, F., Voß, F., Arnell, N. W., … Yeh, P. (2011). Multimodel estimate of the global terrestrial water balance: setup and first results, 869 – 884. doi:10.1175/2011JHM1324.1

Haddeland, I., Lettenmaier, D. P., & Skaugen, T. (2006). Effects of irrigation on the water and energy balances of the Colorado and Mekong river basins. Journal of Hydrology, 324(1-4), 210 – 223. doi:10.1016/j.jhydrol.2005.09.028

Hanasaki, N. & Yamamoto, T. (2010) H08 User's Manual, H08 Documentation.

Hanasaki, N., Fujimori, S., Yamamoto, T., Yoshikawa, S., Masaki, Y., Hijioka, Y., … Kanae, S. (2013). A global water scarcity assessment under Shared Socio-economic Pathways – Part 2: Water availability and scarcity. Hydrology and Earth System Sciences, 17(7), 2393 – 2413. doi:10.5194/hess-17-2393-2013

Hanasaki, N., Kanae, S., Oki, T., Masuda, K., Motoya, K., Shirakawa, N., … Tanaka, K. (2008). An integrated model for the assessment of global water resources – Part 1 : Model description and input meteorological forcing. Hydrol. Earth Syst. Sci., 12, 1007 – 1025. doi:10.5194/hess-12-1027-2008

Hanasaki, N., Kanae, S., Oki, T., Masuda, K., Motoya, K., Shirakawa, N., … Tanaka, K. (2008). An integrated model for the assessment of global water resources – Part 2: Applications and assessments. Hydrology and Earth System Sciences, 12(4), 1027 – 1037. doi:10.5194/hess-12-1027-2008

Hanasaki, N., Saito, Y., Chaiyasaen, C., Champathong, A., Ekkawatpanit, C., Saphaokham, S., … Thongduang, J. (2014). A quasi-real-time hydrological simulation of the Chao Phraya River using meteorological data from the Thai Meteorological Department Automatic Weather Stations. Hydrological Research Letters, 8(1), 9 – 14. doi:10.3178/hrl.8.9

Hayashi, A., Akimoto, K., Homma, T., Wada, K., & Tomoda, T. (2014). Change in the Annual Water Withdrawal-to-Availability Ratio

and Its Major Causes: An Evaluation for Asian River Basins Under Socioeconomic Development and Climate Change Scenarios. Energy and Environment Research, 4(2). doi:10.5539/eer.v4n2p34

Houghton-Carr, H.A., Boorman, D.B and Heuser, K. (2013). Land use, climate change and water availability: Phase 2a. Rapid Evidence Assessment: Results and synthesis. Centre for Ecology & Hydrology, Wallingford, UK.

IPCC. (2014). Summary for policymakers. In: Climate Change 2014: Impacts, Adaptation, and Vulnerability. Part A: Global and Sectoral Aspects. Contribution of Working Group II to the Fifth Assessment Report of the Intergovernmental Panel on Climate Change [Field, C.B., V.R. Barros, D.J. Dokken, K.J. Mach, M.D. Mastrandrea, T.E. Bilir, M. Chatterjee, K.L. Ebi, Y.O. Estrada, R.C. Genova, B. Girma, E.S. Kissel, A.N. Levy, S. MacCracken, P.R. Mastrandrea, and L.L.White (eds.)]. Cambridge University Press, Cambridge, United Kingdom and New York, NY, USA, pp. 1-32.

Jang, C.-H., Kim, H.-J., Noh, S.-J., & Kim, C.-G. (2008). Analysis of the hydrologic cycle in Pangyo watershed using distributed hydrologic model, Journal of Korea Water Resources Association, 1315-1319 pp.

Jang, J.-S. (2003). Introduction of hydrologic models and parameters, Korean National Committee on Irrigation and Drainage, 10:1, 99-102

Jeong, G.-H., Jeon, M.-H., Kim, H.-S., & Kim, T.-W. (2011). Adaptation capability of reservoirs considering climate change in the Han river basin, South Korea, Journal of the Korean Society of Civil Engineers, 31(5B), 439-447

Jia, Y., Wang, H., Zhou, Z., Qiu, Y., Luo, X., Wang, J., Yan, D. & Qin, D. (2006). Development of the WEP-L distributed hydrological model and dynamic assessment of water resources in the Yellow River basin, Journal of Hydrology, 331, 606-629

Khajuria, A., Yoshikawa, S., & Kanae, S. (2013). Estimation and prediction of water availability and water withdrawal in India. Journal of Japan Society of Civil Engineers, 69(4), 145 - 150.

Kim, B.-S., Kim, S.-J., Kim, H.-S., & Jun, H.-D. (2010). An impact assessment of climate and landuse change on water resources in the Han river, Journal of Korea Water Resources Association, 43(3), 309-323

Kim, B.-S., Yoon, S.-G., Yang, D.-M., & Kwon, H.-H. (2010). Development of grid-based conceptual hydrologic model, Journal of Korea Water Resources Association, 43:7, 667-679

Kim, C.-R., Kim, Y.-O., Seo, S.-B., & Choi, S.-W. (2013). Water balance projection using climate change scenarios in the Korean Peninsula, Journal of Korea Water Resources Association, 46(8), 807-819

Kim, S.-J., Kim, B.-S., Jun, H.-D., & Kim, H.-S. (2010). The evaluation of climate change impacts on the water scarcity of the Han river basin in South Korea using high resolution RCM

data, Journal of Korea Water Resources Association, 43(3), 295-308

Kondo, J. (1994). Meteorology of Hydrological Environment, Asakura Shoten, Tokyo, Japan, 368 pp.

Korea Meteorological Administration. (2012). Climate change projection report in Korea, pp. 19

Lautensach, H. (1988). Korea: A geography based on the author's travels and literature, Springer-Verlag.

Lee, J.-M., Kim, Y.-D., Kang, B.-S., & Lee, H.-S. (2012). Impact of climate change on runoff in Namgang dam watershed, Journal of Korea Water Resources Association, 45(6), 517-529.

Lee, M.-H. & Bae, D.-H. (2015). Climate Change Impact Assessment on Green and Blue Water over Asian Monsoon Region. Water Resources Management, 29(7), 2407 - 2427. doi:10.1007/s11269-015-0949-3

Lehner, B., P. Doll, J. Alcamo, T. Henrichs, and F. Kaspar. (2006). Estimating the Impact of Global Change on Flood and Drought Risks in Europe: A Continental, Integrated Analysis, Climatic Change, 75, 273-299

Manabe, S. (1969). Climate and the ocean circulation - 1: The atmospheric circulation and the hydrology of the Earth's surface, Mon.Weather Rev., 97, 739 - 774.

Martin, N. and Giesen, N. (2009). Spatial distribution of groundwater production and development potential in the Volta River basin of Ghana and Burkina Faso, Water International, 30:2, 239-249.

Masood, M., Yeh, P. J.-F., Hanasaki, N., & Takeuchi, K. (2014). Model study of the impacts of future climate change on the hydrology of Ganges – Brahmaputra – Meghna (GBM) basin. Hydrology and Earth System Sciences Discussions, 11(6), 5747 – 5791. doi:10.5194/hessd-11-5747-2014

Mateo, C. M. (2012) Hydrological modeling with reservoir operation in the Chao Phraya River Basin for flood mitigation, Master's thesis documentation, Graduate School of Engineering, the University of Tokyo.

Mateo, C. M., Hanasaki, N., Komori, D., Tanaka, K., Kiguchi, M., Champathong, a., … Oki, T. (2014). Assessing the impacts of reservoir operation to floodplain inundation by combining hydrological, reservoirmanagement, and hydrodynamicmodels, 7245 – 7266. doi:10.1002/2013WR014845.

Meigh, J., McKenzie, A., & Sene, K. (1999). A grid-based approach to water scarcity estimates for eastern and southern Africa. Water Resources Management, (13), 85 – 115.

Milly, P.C.D., Dunne, K.A., Vecchia, A.V. (2005). Global pattern of trends in streamflow and water availability in a changing climate, Nature, 148, 347-350.

Ministry of Land, Infrastructure and Transport. (2013). Water and sustainable development 2015 – Water for the future, 22 pp.

Ministry of Land, Transport and Maritime Affairs. (2011). Water Vision 2020.

Moon, S.-J., Kim, J.-J., & Kang, B.-S. (2013). Bias correction fof

GCM long-term prediction using nonstationary quantile mapping, Journal of Korea Water Resources Association, 46:8, 833-842.

Nam, W.-H., Hong, E.-M., Kim, T.-G., & Choi, J.-Y. (2014). Projection of future water supply sustainability in agricultural reservoirs under RCP climate change scenarios, Journal of the Korean Society of Agricultural Engineers, 56(4), 59 - 68.

Nash, J. E. and J. V. Sutcliffe. (1970). River flow forecasting through conceptual models part I — A discussion of principles, Journal of Hydrology, 10 (3), 282 - 290.

NIMR. (2011). Climate change scenario report 2011 to respond to the IPCC 5th Assessment Report. National Institute of Meteorological Research, Korea

Okada, M., Iizumi, T., Sakurai, G., Hanasaki, N., Sakai, T., Okamoto, K., & Yokozawa, M. (2014). Modeling irrigation based climate change adaptation in agriculture: Model development and evaluation in Northeast China. Journal of Advances in Modeling Earth Systems, 6, 513 - 526. doi:10.1002/2013MS000282.

Oki, T. and Sud, Y. C. (1998). Design of Total Runoff Integrating Pathways (TRIP)-A Global River Channel Network, Earth Inter., 2, EI013.

Oki, T., Agata, Y., Kanae, S., Saruhashi, T., Yang, D., & Musiake, K. (2001). Global assessment of current water resources using total runoff integrating pathways. Hydrological Sciences Journal, 46(6), 983 - 995. doi:10.1080/02626660109492890

Park, J.-H., Kwon, H.-H., & Noh, S.-H. (2011). Outlook of discharge

for Daecheong and Yongdam dam watershed using A1B climate change scenario based RCM and SWAT model, Journal of Korea Water Resources Association, 44(12), 929-940.

Park, M.-J., Shin, H.-J., Park, G.-A., & Kim, S.-J. (2010). Assessment of future hydrological behavior of Soyanggang Dam watershed using SWAT, Journal of the Korean Society of Civil Engineers, 30(4B), 337-346.

Pratoomchai, W., Kazama, S., Ekkawatpanit, C., & Komori, D. (2015). Opportunities and constraints in adapting to flood and drought conditions in the Upper Chao Phraya River basin in Thailand. International Journal of River Basin Management, (April), 1 - 15. doi:10.1080/15715124.2015.1013036

Robock, A., K. Vinnikov, C. Schlosser, N. Speranskaya, & Y. Xue. (1995). Use of midlatitude soil moisture and meteoro- logical observations to validate soil moisture simulations with biosphere and bucket models. J. Climate, 8, 15 - 35.

Shin, Y. & Jung, H. (2015). Assessing uncertainty in future climate change in Northeast Asia using multiple CMIP5 GCMs with four RCP scenarios, Journal of Environmental Impact Assessment, 24(3), 205-216.

Son, K.-H., Lee, M.-H., & Bae, D.-H. (2012). Runoff analysis and assessment using land surface model on East Asia, Journal of Korea Water Resources Association, 15(2), 165-178.

UN World Water Assessment Programme(UN-Water WWAP). (2006). The United Nations World Water Development Report

Van Beek, L. P. H., Wada, Y., & Bierkens, M. F. P. (2011). Global monthly water stress: 1. Water balance and water availability. Water Resources Research, 47(7). doi:10.1029/2010WR009791

Vinay, S., Bharath, S., Bharath, H. A., & Ramachandra, T. V. (2013). Hydrologic model with landscape dynamics for drought monitoring, Joint International Workshop of ISPRS VIII/1 and WG IV/4 on Geospatial Data for Disaster and Risk Reduction, 67 - 72.

Vorosmarth, C.J., Green, P., Salisbury, J., Lammers, R.B. (2000). Global water resources: Vulnerability from climate change and population growth, Science 289:5477, 284-288.

Wada, Y., van Beek, L. P. H. (2011). and Bierkens, M. F. P.: Modelling global water stress of the recent past: on the relative importance of trends in water demand and climate variability, Hydrol. Earth Syst. Sci., 15, 3785-3808, doi:10.5194/hess-15-3785-2011

국문초록

기후변화를 고려한 한반도의 가용 수자원 추정

지도교수 : 이 동 근
서울대학교 대학원
조경·지역지스템공학부 생태조경학 전공
유 소 현

기온과 강수량의 변화로 나타나는 기후변화 현상은 전 지구적으로 일어나고 있으며 이는 가용 수자원에 직접적으로 영향을 끼칠 것으로 예측되고 있다. 한반도 지역의 경우, 강우가 여름철에 집중되므로 가용 수자원의 시간적, 공간적 편중이 주요하게 다루어져 왔다. 기후변화로 인하여 이러한 한반도 가용수자원의 시·공간적 편중이 심화될 것으로 예상되며 이는 수자원 안정성의 문제를 악화시키는 요인이 될 것으로 예상되고 있다. 가용 수자원의 변동은 도시지역, 작물 재배지, 산림 등 수자원을 직접적으로 이용하게 되는 토지이용과도 밀접하게 관련되어 있기 때문에 그 공간적 변동에 대한 파악은 필수적이다.

가용 수자원은 유역 내에서 사용할 수 있는 물의 양을 의미하며, 연구 범위에 따라서 댐의 저수량, 하천 유량 등 다양하게 정의될 수 있다. 본 연구에서는 문헌 고찰을 통해 가용 수자원을 하천의 유량으로 정의하였다. 이에 근거하여 기후변화 영향에 따른 한반도 가용 수자원의 변동을 추정하기 위해 북한을 포함한 한반도 전 지역을 연구 대상지로 하여 RCP 기후변화 시나리오를 입력 자료로 하여 수문 모형을 활용하여 모의된 유

량을 가용 수자원으로 추정하였다. 향후 공간 계획적 시사점을 제공하기 위하여 격자 기반의 수문 모형 중 한반도 스케일에서 적용하기 적합한 모형으로 H08 모형을 선정하였다. H08은 1° × 1° 해상도의 전 지구적인 수자원 가용성을 평가하기 위해 개발된 모형으로 5′ × 5′ 해상도로 지역적으로도 적용이 가능하다. 입력자료로 과거 기간에 대해서는 GSWP2에서 제공하는 기상자료를 활용하였으며 기후변화 시뮬레이션을 위해서 HadGEM2-AO 모형에서 생산되는 RCP 8.5 시나리오를 사용하였다. GCM으로부터 제공되는 미래 기온, 강수량 자료는 과거 관측 자료에 근거하여 편차를 보정하였다. 과거 기간의 기후자료를 바탕으로 모형의 매개변수를 검·보정하여 적용성을 검증하였으며, 보정된 모형에 기후변화 시나리오를 적용하여 한반도의 미래 수문 변동 및 가용 수자원의 변화를 추정하였다.

한반도의 가용 수자원과 수문 변동을 파악하기 위하여 한반도 전 범위를 대상으로 각 요소들의 시·공간적 변동을 표현하는 동시에 대표적인 관측소 지점을 선정하여 정량적인 모의를 진행하였다. 북한 지역의 경우는 압록강, 두만강, 청천강, 대동강 유역, 남한 지역의 경우는 한강, 낙동강, 금강, 영산강 유역의 관측소를 선정하여 총 8개 관측소에 대해 기온, 강수량의 기후 요소와 더불어 유출량, 증발산량의 수문 요소의 변동을 파악하였으며 최종적으로 유량을 추정하여 RCP 8.5시나리오에 근거한 한반도의 수문 요소 및 유량 변동을 추정하였다. 수문 모의 결과를 공간적으로 제시하여 최종적으로 이를 공간 계획적으로 활용할 수 있는 시사점을 제공하였다. 하지만 미래 현상을 모의하는 과정에 있어서 1가지 GCM만을 적용하여 미래 기후 시나리오가 가지는 불확실성을 고려하지 못하였다는 점과, 댐의 유량 조절 효과와 시설물의 물 공급 능력을 반영하지 못했다는 한계점을 지니고 있다. 본 연구는 전 지구적 수문 모형을 한반도를 대상

으로 지역적으로 적용하여 격자 단위로 주요 하천 유량에 근거하여 가용 수자원을 전망하였으며 본 연구의 결과는 향후 미래 전망 기간에 유황 변동에 대비한 시설물 도입 등의 공간 계획 시 기초자료로 활용될 수 있을 것이다.

▫ 주요어: 수자원 가용성, 기후변화, RCP 시나리오, GCM, 수문 모형, H08

▫ 학번: 2014-20049